*sustainability*

MDPI

*Article*

# Stronger Hurricanes and Climate Change in the Caribbean Sea: Threats to the Sustainability of Endangered Coral Species

**Edwin A. Hernández-Delgado [1,2,3,*], Pedro Alejandro-Camis [3], Gerardo Cabrera-Beauchamp [3], Jaime S. Fonseca-Miranda [3], Nicolás X. Gómez-Andújar [3], Pedro Gómez [3], Roger Guzmán-Rodríguez [3], Iván Olivo-Maldonado [3] and Samuel E. Suleimán-Ramos [3]**

[1] Interdisciplinary Studies Program, Faculty of Natural Sciences, University of Puerto Rico, San Juan 00931, Puerto Rico
[2] Center for Applied Tropical Ecology and Conservation, University of Puerto Rico, San Juan 00925, Puerto Rico
[3] Sociedad Ambiente Marino, San Juan 00931-2158, Puerto Rico; pedro.alejandro@upr.edu (P.A.-C.); gerardocabrera@sampr.org (G.C.-B.); jaimefonseca@sampr.org (J.S.F.-M.); hnicolasgomez@sampr.org (N.X.G.-A.); nicolas.x.gomez@gmail.com (P.G.); rogerguzman@sampr.org (R.G.-R.); ivanolivo@sampr.org (I.O.-M.); samuelsuleiman@sampr.org (S.E.S.-R.)
* Correspondence: edwinhernandez@sampr.org; Tel.: +1-939-642-7264

**Abstract:** An increasing sea surface temperature as a result of climate change has led to a higher frequency and strengthening of hurricanes across the northeastern Caribbean in recent decades, with increasing risks of impacts to endangered corals and to the sustainability of coral reefs. Category five Hurricanes Irma and María during 2017 caused unprecedented damage to coral reef ecosystems across northeastern Puerto Rico, including mechanical destruction, localized sediment bedload (horizontal sediment transport and abrasion), and burial by hurricane-generated rubble fields. Hurricanes inflicted significant site-, depth-, and life history trait-specific impacts to endangered corals, with substantial and widespread mechanical damage to branching species, moderate mechanical damage to foliose species, and moderate to high localized damage to small-sized encrusting and massive morphotypes due to sediment bedload and burial by rubble. There was a mean 35% decline in *Acropora palmata* live cover, 79% in *A. cervicornis*, 12% in *Orbicella annularis*, 7% in *O. faveolata*, 12% in *O. franksi*, and 96% in *Dendrogyra cylindrus*. Hurricane disturbances resulted in a major regime shift favoring dominance by macroalgae, algal turf, and cyanobacteria. Recovery from coral recruitment or fragment reattachment in *A. palmata* was significantly higher on more distant coral reefs, but there was none for massive endangered species. Stronger hurricanes under projected climate change may represent a major threat to the conservation of endangered coral species and reef sustainability which will require enhancing coral propagation and restoration strategies, and the integration of adaptive, ecosystem-based management approaches. Recommendations are discussed to enhance redundancy, rapid restoration responses, and conservation-oriented strategies.

**Keywords:** Caribbean Sea; climate change; coral reefs; disturbance; ecological restoration; endangered species; hurricanes; Puerto Rico; recovery; sustainability



**Citation:** Hernández-Delgado, E.A.; Alejandro-Camis, P.; Cabrera-Beauchamp, G.; Fonseca-Miranda, J.S.; Gómez-Andújar, N.X.; Gómez, P.; Guzmán-Rodríguez, R.; Olivo-Maldonado, I.; Suleimán-Ramos, S.E. Stronger Hurricanes and Climate Change in the Caribbean Sea: Threats to the Sustainability of Endangered Coral Species. *Sustainability* **2024**, *16*, 1506. https://doi.org/10.3390/su16041506

Academic Editor: Gioele Capillo

Received: 2 December 2023
Revised: 27 January 2024
Accepted: 5 February 2024
Published: 9 February 2024



## 1. Introduction

Coral reefs in the Anthropocene are rapidly declining on a global scale due to a combination of local-scale anthropogenic factors and large-scale climate change-related impacts, threatening the ecosystem's persistence, resilience, and the sustainability of their ecological functions, services, and benefits. During recent decades, coral reefs have been increasingly impacted by a gradual decline associated to regime shifts in microbial diversity and algal dominance [1], and by numerous ecological surprises including mass bleaching events [2–7], and widespread mortality from diseases such as the white pox [8] and the stony coral tissue loss disease (STCLD), with significant alterations in coral species composition and reef accretion [9,10]. Climate change is also driving coral reefs to a generalized state of

hypoxia, threatening numerous species on a global scale [11,12]. There has also been an increase in the frequency and magnitude of hurricanes across the western Atlantic that have been associated with increased sea surface temperatures (SST) [13–16] and have resulted in substantial social–ecological impacts [17]. These factors have had widespread impacts on coral reefs species composition and sustainability across the wider Caribbean region, including Puerto Rico (PR).

There is evidence of unparalleled coral mortality in recent decades [18,19], a long-term decline in coral growth rates [20], and no net signs of significant natural recovery ability for many species across the wider Caribbean region [21–23]. In contrast, most reefs are showing limited recovery ability [24–26], and permanent regime shifts in community structure and trajectory [27–29], leading to dominance by ephemeral coral species and non-reef builders [30], and to major population declines in important reef-building species, such as *Orbicella* spp. [31–33]. This often results in a long-term loss in an ecosystem's resilience, socio-economic value, and net functions, goods, benefits, and services [34–36]. Such changes have also resulted in the evolution of novel ecosystems [37,38], characterized by altered coral reef benthic assemblages and ecological functions [39–41]. Such altered community trajectories are concerning and represent a major challenge for managers and decision-makers [5,42–45] as they may jeopardize the sustainability of biodiversity, its persistence, resilience, and the services a coral reef provides [46]. The magnitude of such impacts is becoming increasingly stronger in small island developing states (SIDS) impacted by climate change and declining community-based livelihoods [47].

Observed coral reef declining trends over the last decades have prompted the designation of several Caribbean coral species as endangered under the International Union of the Conservation of Nature (IUCN) Red List (https://www.iucnredlist.org/en (accessed on 1 December 2023)). It has also led to the designation of seven Caribbean coral species as threatened under the U.S. Endangered Species Act (ESA) across the U.S. Caribbean, including PR [48]. However, little is still known about the spatial distribution and actual population status and trends of most ESA-listed species across several important remote locations through PR, such as the Northeast Reserves System Habitat Focus Area (NER-HFA) and Culebra Island, PR. The northeastern PR wide shelf sustains important coral reefs of regional importance [49–53]. PR coral reefs play a fundamental role for corals' genetic connectivity and region-wide natural reef recovery ability. However, the northeastern Caribbean region has been significantly impacted by increasing tropical storms and hurricanes over recent decades (https://coast.noaa.gov/hurricanes/ (accessed on 1 December 2023)). For instance, a total of 168 different storms passed within a radius of 300 km or less from northeastern PR between 1851 and 2022 (https://coast.noaa.gov/hurricanes/#map=4/32/-80 (accessed on 1 December 2023)) (Figure 1), which suggests that storms play a vital role in shaping coral reef communities across the northeastern Caribbean.

PR was significantly impacted by rapidly intensifying category five hurricanes Irma (6 September 2017) and María (20 September 2017). Hurricane María resulted in the greatest 24 h rain intensities among all storms recorded in PR, causing hundreds of casualties, extensive damage to agriculture and infrastructure, and numerous landslides [54]. Both hurricanes caused extensive and unprecedented damage across northeastern PR coral reefs (see Appendix A). These hurricanes sustained winds over 270 $kmh^{-1}$ [55,56], leading to strong swells and wave action and causing extensive mechanical impacts to coral reefs [57]. At its closest point to Culebra, the eyewall of Hurricane Irma passed just 20 km off the north coast of Culebra with sustained winds of 276 $km{\cdot}h^{-1}$. Hurricane María passed 32 km south of Culebra and crossed directly over PR with sustained winds of 276 $km{\cdot}h^{-1}$. Wave action exceeded 10 m around Culebra during both hurricanes, which resulted in severe impacts to exposed shallow coastal ecosystems [58]. Wave power was estimated by the Caribbean Coastal Ocean Observing System (CARICOOS) at 300 kW/m during Hurricane Irma and 230 kW/m during Hurricane María (Canals-Silander, unpublished data). Additionally, rainfall during Hurricane María was estimated to range from 250 to 750 mm across the eastern Puerto Rico region (Hernández-Delgado, unpublished data). The 2017 Atlantic

hurricane season was regarded as one of the most destructive on record [59]. These two consecutive major hurricanes represent a unique scenario throughout the northeastern Caribbean with unprecedented consequences to shallow endangered coral assemblages.

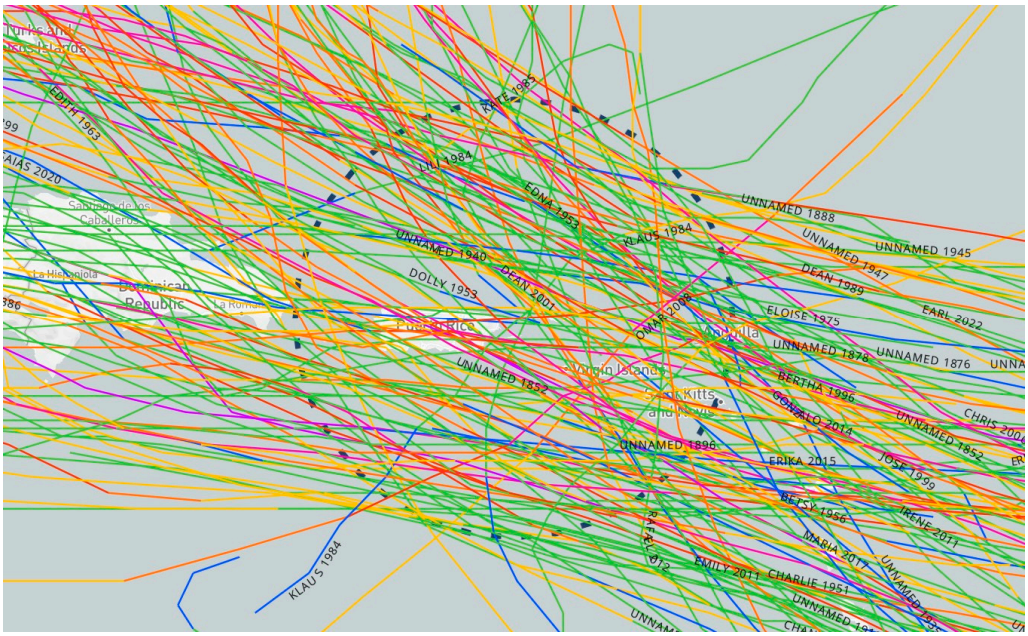


**Figure 1.** Storm trajectories within a radius of 300 km or less of northeastern Puerto Rico between 1851 and 2022 (Source: https://coast.noaa.gov/hurricanes/#map=4/32/-80 (accessed on 1 December 2023)).

This study quantified the status of endangered Elkhorn coral (*Acropora palmata*), Staghorn coral (*A. cervicornis*), Star corals (*Orbicella annularis*, *O. faveolata*, *O. franksi*), and Pillar coral (*Dendrogyra cylindrus*) across the NER-HFA and Culebra Island, PR, before and after the impacts of category five hurricanes Irma and María in 2017. This approach provides coral reef ecologists and managers with critical timely data regarding major hurricane impacts on endangered coral species across priority locations within the northeastern Caribbean. In addition, it contributes to the identification of conservation and restoration strategies targeted at the recovery and sustainability of impacted species.

## 2. Materials and Methods

### *2.1. Study Sites*

This study was conducted on 15 sites across the NER-HFA and Culebra Island in northeastern PR that were impacted by category five hurricanes Irma and María in 2017 (Figure 2, Table 1). Quantitative assessments of hurricane impacts on Elkhorn coral (*A. palmata*) assemblages were conducted at three sites across Arrecifes La Cordillera Natural Reserve (ALCNR), off Fajardo: Cayo Icacos (ICA), Audrey Rock (AUD), and Cayo Ratones (RAT), and three sites in Culebra Island, two of which were located within Canal Luis Peña Natural Reserve (CLPNR): Bahía Tamarindo (BTA), and Punta Tamarindo Chico (PTC), and another site outside the CLPNR: Arrecife Los Corchos-North (CON). Sampling for *A. palmata* was limited to depths < 5 m. Quantitative assessments of the remaining endangered coral species were conducted across three depth zones: <5 m, 5–10 m, and 10–15 m at 10 locations, one at ALCNR: PLM, and the remaining at Culebra Island, with one at CLPNR: PCR, and the remaining outside the reserve: DAK, CAR, AMA, GRO, COS, CRE, and CON (Figure 2, Table 1).

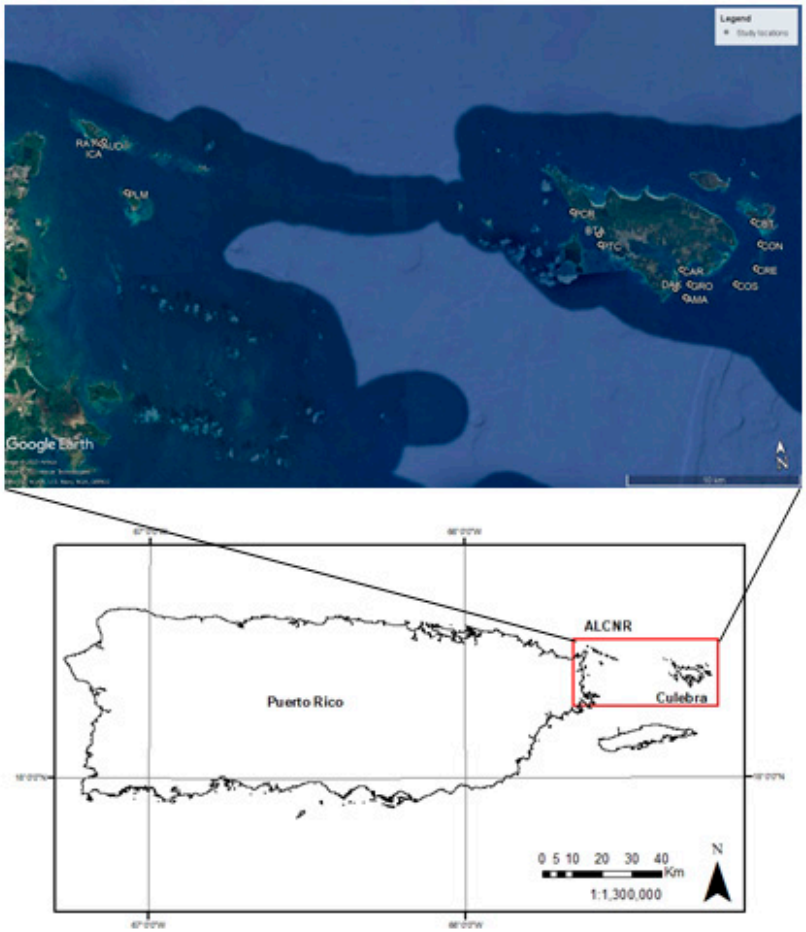


**Figure 2.** Study sites across northeastern Puerto Rico. Northeast Reserves System Habitat Focus Area (NER-HFA) within Arrecifes La Cordillera Natural Reserve (ALCNR): ICA, AUD, RAT, PLM; Culebra Island within Canal Luis Peña Natural Reserve (CLPNR): PCR, BTA, PTC; Culebra outside CLPNR: DAK, CAR, AMA, GRO, COS, CRE, CON, CBT. For acronyms, see Table 1. Aerial image source: Google Earth Pro v.7.3.6.9345. Tracks of category five hurricanes Irma and María are shown in Figures S1 and S2.

**Table 1.** Study site coordinates.

| Site | Acronym | Latitude | Longitude |
|---|---|---|---|
| Cayo Icacos | ICA | 18.379958° | −65.585074° |
| Audrey Rock | AUD | 18.379338° | −65.583138° |
| Cayo Ratones | RAT | 18.380443° | −65.581537° |
| Palominos Island | PLM | 18.353366° | −65.570911° |
| Bahía Tamarindo | BTA | 18.314467° | −65.317659° |
| Punta Tamarindo Chico | PTC | 18.309368° | −65.317045° |
| Playa Carlos Rosario | PCR | 18.327083° | −65.330703° |
| Cayo Dákity | DAK | 18.284020° | −65.278355° |
| Punta Carenero | CAR | 18.293450° | −65.274178° |
| Bajo Amarillo | AMA | 18.279045° | −65.273172° |
| Bajo Grouper | GRO | 18.285689° | −65.270431° |
| Los Corchos-South | COS | 18.283938° | −65.245307° |
| Cabezas Crespás | CRE | 18.291187° | −65.233909° |
| Los Corchos-North | CON | 18.303623° | −65.230626° |
| Culebrita Island | CBT | 18.315294° | −65.233359° |

### *2.2. Temporal Variation in Storm Frequency and Intensity across the Northeastern Caribbean*

Tropical storm and hurricane frequency and intensity across the northeastern Caribbean were analyzed to test the hypothesis of a recent increase in the frequency and in the intensification of storm events. The total number of storms passing directly or within a radius of 300 km off northeastern PR were quantified accessing historical hurricane track records at https://coast.noaa.gov/hurricanes/#map=4/32/-80 (accessed on 1 December 2023). A total of 168 storms were documented between 1851 and 2022. This included 34 tropical storms, and 134 hurricanes, including 23 category 1 (H1), 25 H2, 34 H3, 40 H4, and 12 H5 that at some point directly impacted or passed within 300 km off northeastern PR (Figure 1). The total number of storms by category was determined for the period of 1851 to 1980 and used to estimate the expected distribution of storms by decade (tropical storms = 1.69, H1 = 1.46, H2 = 1.69, H3 = 2.15, H4 = 2.23, H5 = 0.46, total storms = 9.68). A $X^2$ test was used to compare the observed to expected storm distributions per decade and determine if there has been a recent decadal increase in storminess for the period of 1981 to 2022.

Annual variation in global climate-related environmental variables for the period of 1981 to 2022 were obtained as follows: (a) atmospheric $CO_2$ concentration (https://scrippsco2.ucsd.edu/data/atmospheric_co2/mlo.html (accessed on 1 December 2023)); (b) annual increments in atmospheric $CO_2$ concentration (https://scrippsco2.ucsd.edu/data/atmospheric_co2/mlo.html (accessed on 1 December 2023)); (c) land–ocean temperature anomaly (https://data.giss.nasa.gov/gistemp/tabledata_v4/GLB.Ts+dSST.txt (accessed on 1 December 2023)); (d) ocean heat content (https://www.ncei.noaa.gov/access/global-ocean-heat-content/ (accessed on 1 December 2023)); (e) thermosteric component of sea level change (https://www.ncei.noaa.gov/access/global-ocean-heat-content/ (accessed on 1 December 2023)); and (f) North Atlantic Oscillation Index (https://www.ncei.noaa.gov/access/monitoring/nao/ (accessed on 1 December 2023)). Data were used to determine annual trends in each parameter though a combination of linear and quadratic regressions using Sigma Plot 11.0 (Systat Software, Inc., San Jose, CA, USA). Spearman rank correlations between storm intensity and climate parameters for the period of 1981 to 2022 across the northeastern Caribbean region were conducted using PRIMER v7.0.23 + PERMANOVA v.1.06 (PRIMER-e, Quest Research Laboratories, Inc., Auckland, NZ, USA) [60].

### *2.3. Status of Acropora palmata Populations*

A baseline large-scale assessment of the status of endangered Elkhorn coral (*Acropora palmata*) populations was carried out between 2016 and 2017 (before Hurricanes Irma and María) across six shallow-water (<5 m) coral reef locations, including ICA, AUD, and RAT, at ALCNR, and at Culebra Island at BTA, PTC, within CLPNR, and at CON, outside the reserve (Figure 1). This sampling effort was repeated between 2018 and 2019 (after the hurricanes). Field sampling was conducted using a GIS-based approach, with 6 to 20 randomly selected 100 $m^2$ circular transects per locality (N = 80 transects before hurricanes; N = 80 transects after hurricanes) using ArcMap. Sampling points were randomly selected and geo-referenced within polygons created from clipped GIS-based layers of reef substrates and a maximum depth contour of 5 m. Sampling points were subdivided between two depth zones (<2.5 m, 2.5–5.0 m), and classified by substrate type (i.e., linear reef, colonized pavement, rubble), and by reef zone (i.e., spur and groove, reef front, reef flat, backreef). Field surveys were conducted using standard methods by NOAA [61]. Each sampling station consisted of a geo-referenced 5.6 m radius circular transect (area = 100 $m^2$). Field data included: (a) Morphometrics (maximum length, width, height); (b) Colony condition (% live tissue cover, % old/recent mortality, live area index, disease, bleaching, bioerosion, predation, fragmentation, other condition); (c) Predator density per colony (i.e., gastropod *Coralliophila abbreviata*, fireworm *Hermodice carunculata*, damselfishes *Stegastes* spp., *Microspathodon chrysurus*). *Acropora palmata* data were summarized in box plots showing spatio-temporal variation in percent live coral cover across sites. 0 = before hurricanes, 1 = after hurricanes. Data for other coral species

were also summarized in box plots as above, but subdivided by depth zone: I = <5 m, II = 5–10 m, III = 10–15 m.

No significant differences were documented between any of the *A. palmata* depth zones, or among substrate types or reef zones (one-way permutational analysis of variance [PERMANOVA], $p > 0.0500$). Therefore, data per location were pooled prior to the before–after hurricane impact analysis. A three-way nested factorial design was used for data analysis, with Time (before, after hurricanes), Region (ALCNR, Culebra), and Site nested within Region ($n$ = 3 at ALCNR, $n$ = 3 at Culebra) as the main factors for 9999 random permutations. A balanced experimental design and the data's lack of normality suit the strengths and limitations of this test. PERMANOVAs yielded the traditional Fisher's F-value, yet without assuming normal distributions [62]. All tests were carried out in Bray Curtis dissimilarity space, a widely applied test for biological assemblages [63] to understand the interacting factors that most explained variances in the community structure. Analyses were carried out using PERMANOVA in PRIMER v. 7.0.23 + PERMANOVA v. 1.06 [64]. Multivariate RELATE routine, based on a Spearman rank correlation, was used to test correlations of the *A. palmata* parameters matrix with damselfish (Pomacentridae) and Long-spined urchin (*Diadema antillarum*) density, with red encrusting algae *Ramicrusta textilis* abundance, and with depth [60].

### *2.4. Status of Acropora cervicornis, Orbicella spp., and Dendrogyra cylindrus Populations*

A large-scale assessment of the status of endangered Staghorn coral (*A. cervicornis*), Columnar star coral (*Orbicella annularis*), Laminar star coral (*O. faveolata*), Boulder star coral (*O. franksi*), and Pillar coral (*Dendrogyra cylindrus*) populations was carried out between 2016 and 2017 (before Hurricanes Irma and María) across the following ten coral reef locations: PCR, within CLPNR, DAK, CAR, AMA, GRO, COS, CRE), CON, and CBT, all located in Culebra Island, and PLM at ALCNR. This sampling effort was repeated between 2018 and 2019 (after the hurricanes).

Sampling was randomly conducted using six replicate 10 × 1 m photo-transects per depth zone, across three depth zones (<5 m, 5–10 m, 10–15 m) (N = 18/site). A total of five haphazard digital images were obtained from each transect at 1, 3, 5, 7, and 9 m. A total of 20 digital sampling points were haphazardly projected on each image to calculate benthic components percent cover. Data obtained included percent cover of corals, macroalgae, algal turf, *R. textilis*, crustose coralline algae (CCA), cyanobacteria, and open substrate (sand, pavement, rubble). Percent cover data were also used to calculate species richness (S), Shannon–Weaver coral species diversity index (H'c), and Pielou's evenness (J'c). Octocorals were not included in this assessment. A three-way crossed factorial design was used, with Time (before, after hurricanes), Site ($n$ = 10), and *Depth* ($n$ = 3) as the main factors for 9999 random permutations. Analyses were carried out using PERMANOVA as described above. A similar procedure was used to test the spatio-temporal variation in S, H′c, and J′c. Permutational distance-based tests for homogeneity of multivariate dispersions (PERMDISP) were performed to measure the spatio-temporal variation in $\sqrt{}$-transformed β-diversity [65]. Principal component ordination (PCO) was used to identify which benthic community components influenced spatio-temporal patterns based on $\sqrt{}$-transformed species abundances. Similarity Percentages (SIMPER) analysis was also used to illustrate which taxa or benthic categories were indicators of spatio-temporal change among locations and after hurricane disturbance [60].

All counts data were $\log_{10}$-transformed. All percent cover data were $\sqrt{}$-transformed. Data on frequencies were P/A-transformed. Multivariate analyses were conducted using 9999 permutations.

## 3. Results

### *3.1. Hurricane Intensification across the Northeastern Caribbean*

Hurricanes have shown a general trend of intensification during recent decades across the northeastern Caribbean region. The frequency of storm events passing within a radius

of 300 km off northeastern PR has increased since the period of 1981–1990 (Figure 3). Overall, the frequency of tropical storms per decade for the period of 1981–2022 increased by 78% in comparison to the period of 1851–1980. The frequency of H1 hurricanes increased by 54%, H2 hurricanes declined by 56%, H3 hurricanes declined by 30%, H4 hurricanes increased by 23%, and H5 hurricanes increased by 226%. A $X^2$ analysis showed that overall storm frequency and intensity for the period of 2011–2022 was significantly higher in comparison to the expected historical mean of 1851–1980 ($X^2$ = 43.00; d.f. = 5; $p < 0.0001$). In contrast, the storm frequency and intensity for the period of 2001–2010 was not significantly higher in comparison to the expected historical mean of 1851–1980 ($X^2$ = 7.65; d.f. = 5; $p = 0.1767$). Similarly, storm frequency and intensity for the period of 1991–2000 was not significantly higher in comparison to the expected historical mean of 1851–1980 ($X^2$ = 2.76; d.f. = 5; $p = 0.7373$). Findings were similar when data from 1981–1990 were compared to the expected historical mean of 1851–1980 ($X^2$ = 10.77; d.f. = 5; $p = 0.0562$).

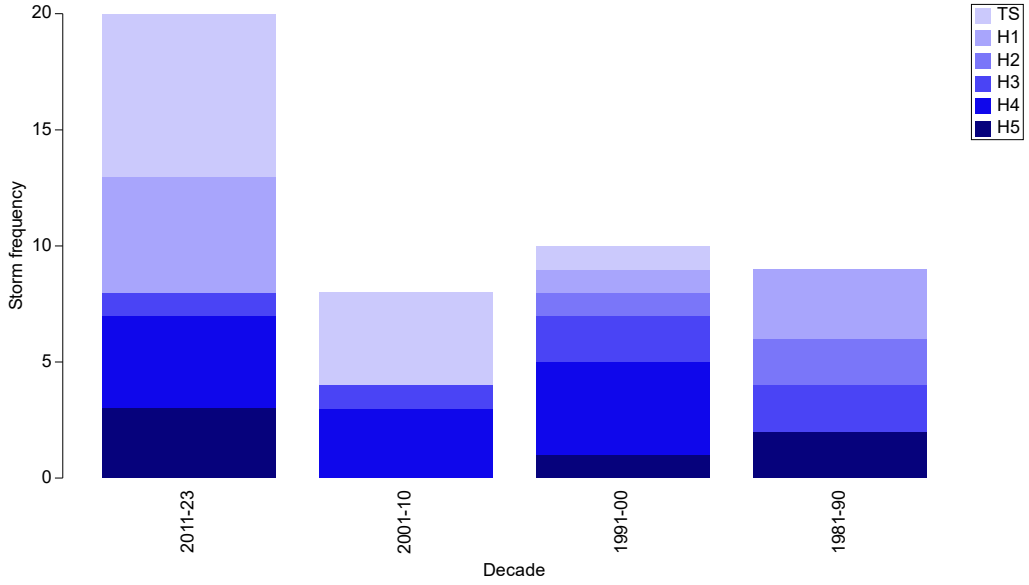


**Figure 3.** Increase in storm frequency and magnitude across the northeastern Caribbean for the period of 1981 to 2022.

Temporal variation in global climate-related environmental variables revealed a highly significant temporal increase in atmospheric $CO_2$ (ATM [$CO_2$]) concentration ($r^2$ = 0.9903; $p < 0.0001$) (Figure 4A), which showed a significant correlation with storm intensification for the period of 1981–2022 (Rho = 0.105; $p = 0.0187$) (Table 2). There was also a highly significant temporal increase in annual increments in ATM [$CO_2$] ($r^2$ = 0.3194; $p < 0.0001$) (Figure 4B). However, it was not correlated with storm intensification for the period of 1981–2022 (Rho = −0.042; $p = 0.7771$) (Table 2). A highly significant temporal increase in the land–ocean temperature anomaly was documented ($r^2$ = 0.8767; $p < 0.0001$) (Figure 4C). However, it was not correlated with storm intensification for the period of 1981–2022 (Rho = 0.053; $p = 0.1460$) (Table 2). Ocean heat content showed a highly significant temporal increase ($r^2$ = 0.9969; $p < 0.0001$) (Figure 4D), which significantly correlated with storm intensification for the period of 1981–2022 (Rho = 0.110; $p = 0.0181$) (Table 2). The thermosteric component of sea level change also exhibited a highly significant temporal increase ($r^2$ = 0.9949; $p < 0.0001$) (Figure 4E), which significantly correlated with storm intensification for the period of 1981–2022 (Rho = 0.104; $p = 0.0234$) (Table 2). There was a non-significant slight temporal decline in the North Atlantic Oscillation (NAO) index ($r^2$ = −0.0237; $p = 0.3308$) (Figure 4C), which neither showed correlation with storm intensification for the period of 1981–2022 (Rho = −0.027; $p = 0.6674$) (Table 2).

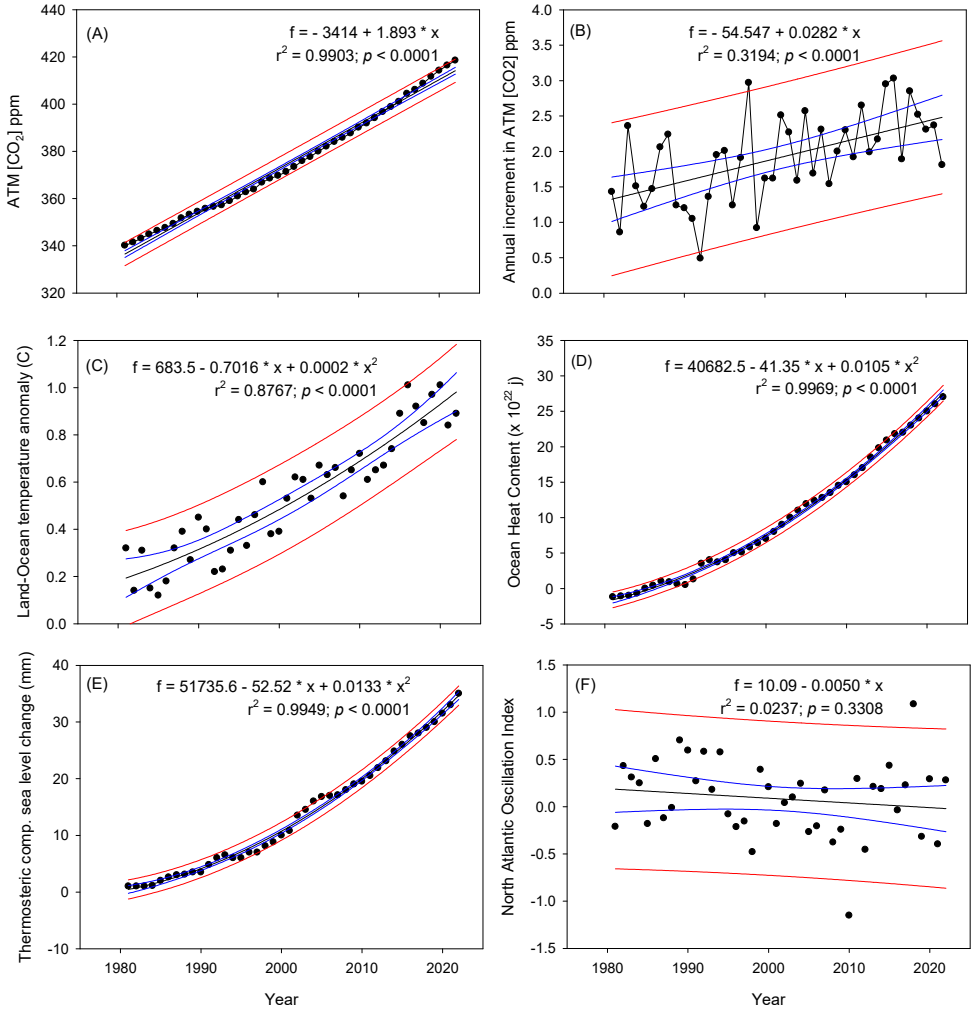


**Figure 4.** Temporal variation in global climate-related environmental variables: (**A**) atmospheric $CO_2$ concentration (ppm); (**B**) annual increments in atmospheric $CO_2$ concentration (ppm); (**C**) land–ocean temperature anomaly (°C); (**D**) Ocean heat content ($\times 10^{22}$ joules); (**E**) Thermosteric component of sea level change (mm); (**F**) North Atlantic Oscillation Index. Data are annual means for the period of 1981 to 2022. Black = regression line; blue = 95% confidence interval bands; red = prediction bands.

**Table 2.** Spearman rank correlations between storm intensity and climate parameters for the period of 1981 to 2022 across the northeastern Caribbean region.

| Source [1] | Rho | *p* |
|---|---|---|
| ATM [$CO_2$] | 0.105 | 0.0187 |
| Annual increment [$CO_2$] | −0.042 | 0.7771 |
| Temperature anomaly L-O | 0.053 | 0.1460 |
| NAO Index | −0.027 | 0.6674 |
| Ocean Heat Content | 0.110 | 0.0181 |
| Thermosteric component SLC | 0.104 | 0.0234 |

[1] Based on 9999 permutations; data = Pseudo-F statistic, *p* value.

The period of 1981 to 2022 shows further evidence of temporal changes in several important storm parameters. For example, total storm frequency around the northeastern Caribbean increased from seven during 1981–1990 to 10 in 1991–2000. It was eight during 2001–2010 but increased to 21 during 2011–2022 (Figure 5). The frequency of major hurricanes per decade also increased from one in 1981–1990 to three in 1991–2000 and 2001–2010, and to four during 2011–2022. Mean wind speed showed no significant fluctuations, with

64 kt during 1981–1990, 81 kt during 1991–2000, 74 kt during 2001–2010, and 62 kt during 2011–2022. However, maximum wind speed increased from 110 kt during 1981–1990 to 135 kt during 1991–2000, remained at 125 kt during 2001–2010, and increased to 155 kt during 2011–2022. Mean pressure showed no significant fluctuations, with 988 mb during 1981–1990, 976 mb during 1991–2000, 982 mb during 2001–2010, and 991 mb during 2011–2022. Observed variations point at the increasing threats to coral reefs across the northeastern Caribbean posed by increasingly stronger hurricane impacts.

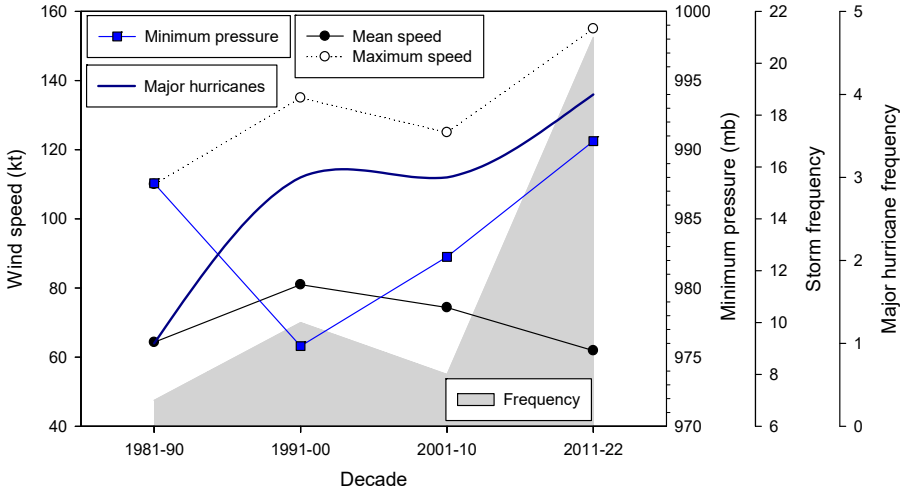


**Figure 5.** Temporal variation in the frequency and intensity of storms passing within a radius of 300 km off northeastern PR measured at the nearest point of each storm to the island: (1) Mean wind speed (kt); (2) Maximum wind speed (kt), (3) Minimum pressure (mb); (4) Total storm frequency per decade; and (5) Major hurricane frequency per decade. Data source: https://coast.noaa.gov/hurricanes/#map=4/32/-80 (accessed on 1 December 2023).

### *3.2. Spatio-Temporal Variation in Acropora palmata*

Hurricanes Irma and María had no significant temporal decline in the *A. palmata* colony surface area (Pseudo F = 4.09; $p = 0.1063$) (Figure 6a, Table 3). Colony surface area declined from a mean value of 0.42 $m^2$ to 0.12 $m^2$ (a net loss of 71%) following hurricanes, but with very high spatial variability. Colonies were not significantly different between regions (Pseudo F = 4.09; $p = 0.1525$). However, colonies from Culebra Island sites were significantly larger than those from ALCNR (Pseudo F = 11.00; $p < 0.0001$). There was no time × region interaction (Pseudo F = 0.60; $p = 0.5560$), but time × site (region) interaction was highly significant (Pseudo F = 16.62; $p < 0.0001$). Pairwise analysis showed that colony size distribution following both hurricanes declined significantly at ICA ($p = 0.0416$), AUD ($p = 0.0022$), PTC ($p = 0.0015$), and COR ($p < 0.0001$). These reefs were significantly exposed to strong southwestern swells during Hurricane Irma and southeastern swells during Hurricane María.

**Table 3.** Summary of a three-way nested PERMANOVA test of the spatio-temporal variation in *Acropora palmata* colony parameters area before and after Hurricanes Irma and María.

| Source [1] | df | Surface Area | Colony Volume | Colony Height | % Live Cover |
|---|---|---|---|---|---|
| Time | 1 | 4.09 | 3.43 | 8.15 | 7.26 |
| | | 0.1063 | 0.1291 | 0.0307 | 0.0369 |
| Region | 1 | 4.09 | 2.69 | 9.98 | 11.05 |
| | | 0.1525 | 0.177 | 0.0081 | 0.0044 |
| Site (Region) | 4 | 11 | 11.84 | 6.75 | 7 |
| | | <0.0001 | <0.0001 | <0.0001 | <0.0001 |
| Time × Region | 1 | 0.6 | 0.74 | 0.21 | 0.004 |
| | | 0.557 | 0.5149 | 0.8493 | 0.9711 |

**Table 3.** *Cont.*

| Source [1] | df | Surface Area | Colony Volume | Colony Height | % Live Cover |
|---|---|---|---|---|---|
| Time × Site (region) | 4 | 16.62 | 17.89 | 9.06 | 6.92 |
| | | <0.0001 | <0.0001 | <0.0001 | 0.0002 |
| Residual | 544 | | | | |

[1] Based on 9999 permutations; data = Pseudo-F statistic, $p$ value.

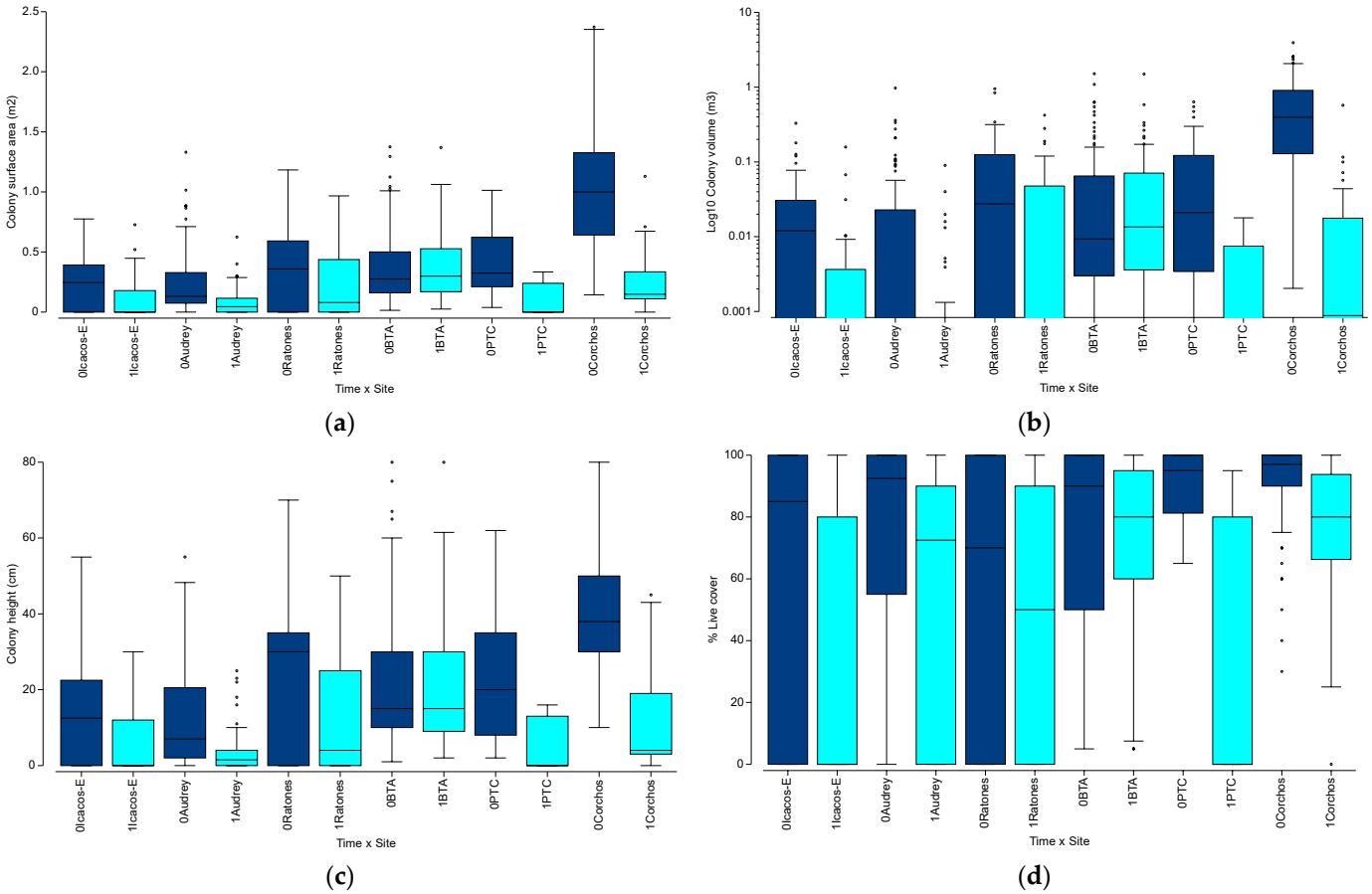


**Figure 6.** Box plot diagram of spatio-temporal variation in *Acropora palmata* population parameters before and after Hurricanes Irma and María: (**a**) Colony surface area ($m^2$); (**b**) Log10 Colony volume ($m^3$); (**c**) Colony height (cm); (**d**) Percent live cover. Each box plot is composed of a box and two whiskers. The box encloses the middle half of the data. The box is bisected by a line at the value for the median. The vertical lines at the top and the bottom of the box are the whiskers, and they indicate the range of "typical" data values. Whiskers always end at the value of an actual data point and cannot be longer than $1\frac{1}{2}$ times the size of the box. Extreme values are displayed as "○" for possible outliers and for probable outliers. Possible outliers are values that are outside the box boundaries by more than 1.5 times the size of the box. Probable outliers are values that are outside the box boundaries by more than 3 times the size of the box.

Hurricanes Irma and María had no significant temporal impact on *A. palmata* colony volume (Pseudo F = 3.43; $p$ = 0.1291), nor a significant regional difference (Pseudo F = 2.69; $p$ = 0.1770) (Figure 6b, Table 3). Colony volume declined from a mean value of 0.20 $m^3$ to 0.04 $m^3$ (a net loss of 78%) following the hurricanes, but with very high spatial variability. Differences in colony volume among sites (region) were highly significant (Pseudo F = 11.84; $p$ < 0.0001). Both hurricanes inflicted stronger damage to coral reefs at Culebra Island than at ALCNR. No significant time × region interaction was observed (Pseudo F = 0.74; $p$ = 0.5149). However, time × site (region) interaction was highly significant (Pseudo

F = 17.89; $p < 0.0001$). Pairwise analysis showed that colony volume distribution following both hurricanes declined significantly at ICA ($p = 0.0500$), AUD ($p = 0.0075$), PTC ($p = 0.0068$), and CON ($p < 0.0001$). Colony volume also showed a marginally significant post-hurricane decline at RAT ($p = 0.0524$). These reefs were significantly exposed to strong southwestern swells during Hurricane Irma and southeastern swells during Hurricane María.

There was a significant temporal decline in mean colony height following both hurricanes (Pseudo F = 8.15; $p = 0.0307$) and a significant regional reduction in colony height (Pseudo F = 9.98; $p = 0.0081$), with stronger hurricane impacts at Culebra Island (Figure 6c, Table 3). Colony height showed widespread decline from a mean value of 22.4 cm to 12.2 cm (a net loss of 46%) following the hurricanes. There was also a significant difference in *A. palmata* colony volume among sites (region) (Pseudo F = 6.75; $p < 0.0001$), but a non-significant time × region interaction (Pseudo F = 0.21; $p = 0.8493$). Time × site (region) interaction was highly significant (Pseudo F = 9.06; $p < 0.0001$). Pairwise analysis showed that colony height distribution following both hurricanes declined significantly at AUD ($p < 0.0001$), PTC ($p = 0.0002$), and CON ($p < 0.0001$). Colony height also showed a marginally significant post-hurricane decline at ICA ($p = 0.0587$). These reefs were significantly exposed to the strongest hurricane swells.

Both hurricanes also caused a significant temporal decline in *A. palmata* percent live cover (Pseudo F = 7.26; $p = 0.0369$) (Figure 6d, Table 3). Live tissue cover declined from a mean 75% before hurricanes to 58% following hurricanes (a 23% magnitude decline). There was also a significant regional difference in percent live cover (Pseudo F = 11.05; $p = 0.0044$). Impacts showed a significant variation among sites (region) (Pseudo F = 7.00; $p < 0.0001$), but there was no time × region interaction (Pseudo F = 0.004; $p = 0.9711$). Pairwise analysis showed that colony percent live tissue cover following both hurricanes declined significantly at AUD ($p = 0.0005$), PTC ($p < 0.0001$), and CON ($p = 0.0040$). Colony height also showed a marginally significant post-hurricane decline at ICA ($p = 0.0587$). These reefs were significantly exposed to the strongest hurricane swells.

There was a significant increase in the proportion of *A. palmata* fragmented colonies after the hurricanes (Pseudo F = 10.50; $p = 0.0396$) (Figure 7a, Table 4). The frequency of fragmented *A. palmata* colonies increased from a mean of 15% to 32% (a net increase of 113%) following the hurricanes, but with very high spatial variability. Regional differences were non-significant (Pseudo F = 5.63; $p = 0.1780$), but there was a significant difference in colony fragmentation among sites (Pseudo F = 3.09; $p = 0.0158$). Time × region interaction was non-significant (Pseudo F = 1.73; $p = 0.2870$). There was a significant time × site (region) interaction (Pseudo F = 2.76; $p = 0.0243$). The frequency of fragmented colonies at ICA increased from 3.6 to 18.2% (a 406% increase), from 17.4 to 29.4% at AUD (a 69% increase), from 2.5 to 12.9% at RAT (a 416% increase), from 30.6 to 39.4% at BTA (a 29% increase), from 13 to 50% at PTC (a 285% increase), and from 2.7 to 44.4% at CON (a 1544% increase). There was a significantly higher fragments abundance at the Culebra region following the hurricanes ($p = 0.0056$). Pairwise analysis showed, however, that observed temporal variation in the frequency of fragmented colonies of *A. palmata* was significantly higher after the hurricanes only at PTC ($p = 0.0377$) and at CON ($p < 0.0001$). These two locations suffered significant destruction of shallow coral assemblages by southeastern hurricane-driven wave action.

There was a non-significant increase in the proportion of *A. palmata* sexual recruits (crusts), either through time, regions, or sites (region) (Figure 7b, Table 4). However, the frequency of *A. palmata* crusts increased from a mean value of 0.016% to 0.037% (a net increase of 131%) following the hurricanes, but with very high spatial variability. No crusts were documented at ICA either before or after the hurricanes. The proportion of crusts at AUD increased from 2.2 to 2.9% after the hurricanes (a 31.8% increase). NO crusts were documented at RAT before the hurricanes. Its frequency increased to 3.2% after the hurricanes. The proportion of crusts at BTA increased from 2.8 to 3.0% after the hurricanes (a 31.8% increase). *Acropora palmata* crust proportion at BTA declined, however, from 4.3%

before hurricanes to 0% after hurricanes. In contrast, the proportion of *A. palmata* crusts at CON was 0% before the hurricanes and 11.1% after the hurricanes, showing an impressive burst of sexual recruitment between 2018 and 2019.

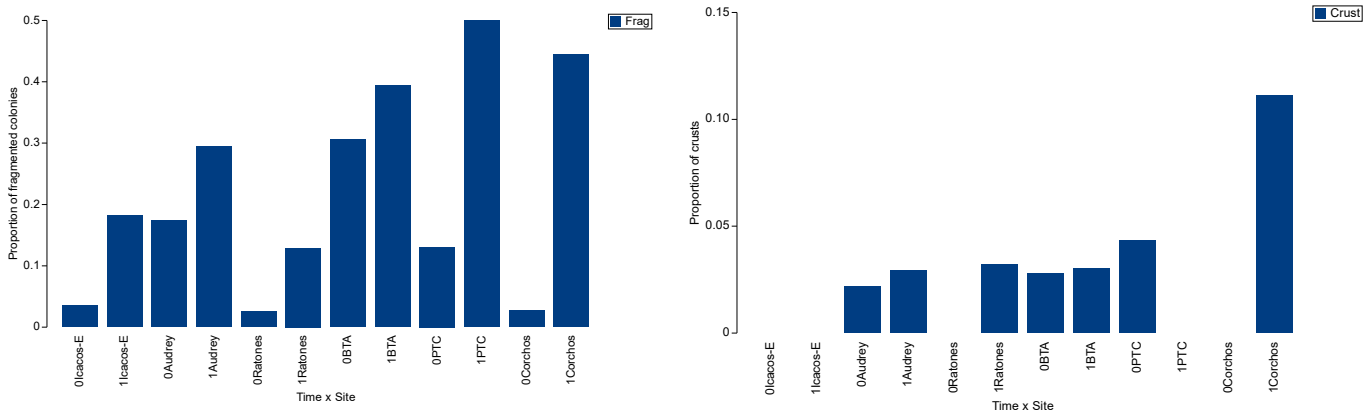


**Figure 7.** Spatio-temporal variation in *Acropora palmata* population parameters before and after Hurricanes: (**a**) Proportion of fragmented colonies; (**b**) Proportion of recruit crusts.

**Table 4.** Summary of a three-way nested PERMANOVA test of the spatio-temporal variation in the proportion of fragmented colonies and of recruits (crusts) of *Acropora palmata* before and after Hurricanes Irma and María.

| Source [1] | df | Proportion Fragmented Colonies | Proportion Recruits (Crusts) |
|---|---|---|---|
| Time | 1 | 10.5<br>0.0396 | 0.64<br>0.5049 |
| Region | 1 | 5.63<br>0.178 | 2.42<br>0.2303 |
| Site (region) | 4 | 3.09<br>0.0158 | 0.72<br>0.5698 |
| Time × Region | 1 | 1.73<br>0.287 | 0.05<br>0.8341 |
| Time × Site (region) | 4 | 2.76<br>0.0243 | 2.29<br>0.0604 |
| Residual | 544 | | |

[1] Based on 9999 permutations; data = Pseudo-F statistic, $p$ value.

### *3.3. Spatio-Temporal Variation in Endangered Corals Percent Live Cover*

Overall, there was a highly significant temporal (Pseudo F = 114.91; $p < 0.0001$), site (Pseudo F = 81.01; $p < 0.0001$), and depth-related decline (Pseudo F = 38.52; $p < 0.0001$) in percent live coral cover (Figure 8, Table 5). There were also significant time × site (Pseudo F = 9.65; $p < 0.0001$), time × depth (Pseudo F = 10.34; $p < 0.0001$), and site × depth (Pseudo F = 3.90; $p < 0.0001$) interactions. Time × site × depth interaction was also significant (Pseudo F = 1.73; $p = 0.0019$). Overall, hurricanes caused a generalized decline in percent coral cover that was site- and depth-related. For instance, percent coral cover showed important declines across sites, ranging from 10.2 to 68.1% in magnitude, with an overall loss from a mean of 14.2 to 9.3%, or a magnitude of 34.5%.

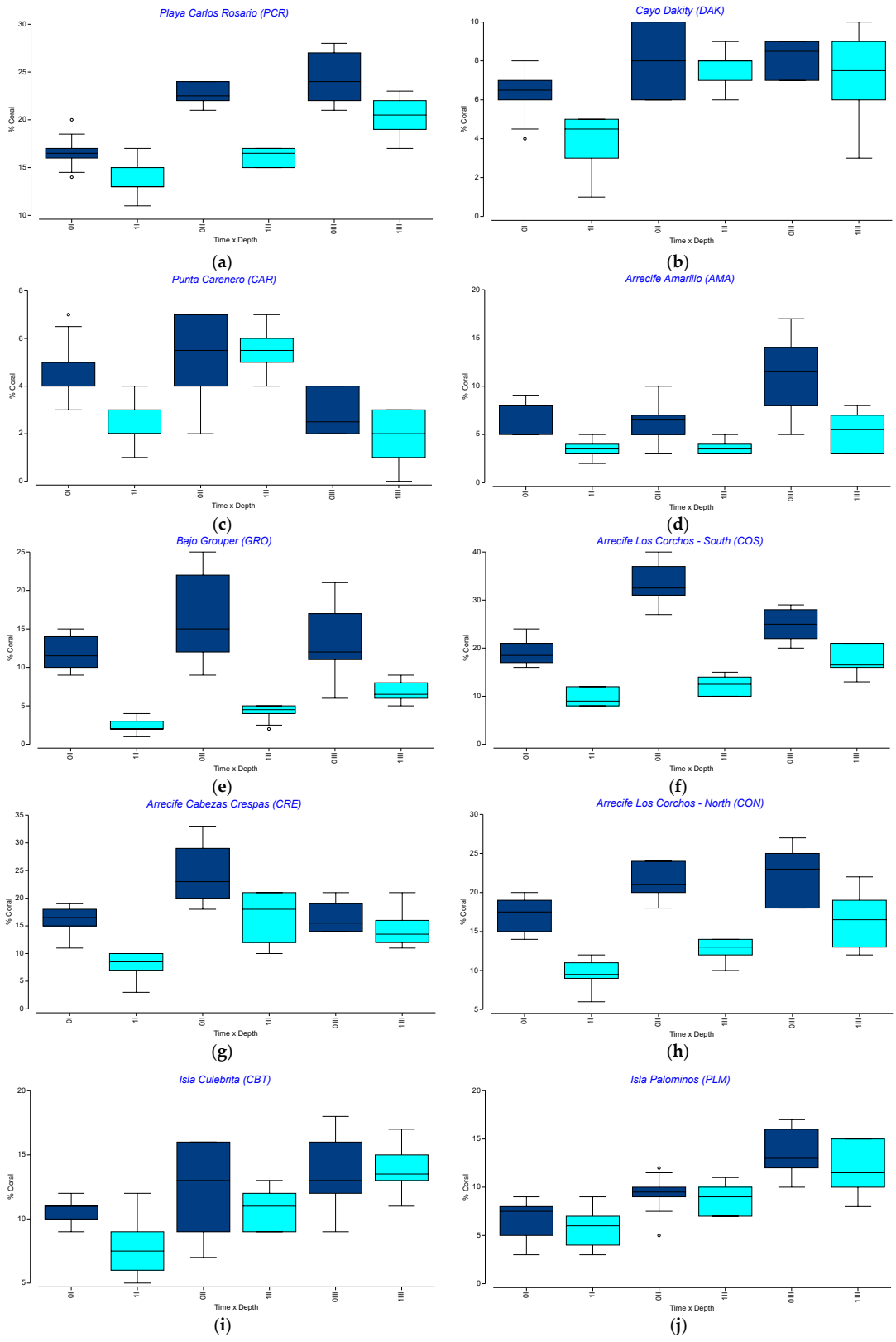


**Figure 8.** Box plot diagram of spatio-temporal variation in percent coral live cover before and after Hurricanes Irma and María: (**a**) PCR = Playa Carlos Rosario; (**b**) DAK = Cayo Dákity; (**c**) CAR = Punta Carenero; (**d**) AMA = Arrecife Amarillo; (**e**) GRO = Bajo Grouper; (**f**) COS= Arrecife Los Corchos-South; (**g**) CRE = Arrecife Cabezas Crespas; (**h**) CON = Arrecife Los Corchos-North; (**i**) CBT = Culebrita Island; (**j**) Palominos Island. 0 = Before hurricanes; 1 = After hurricanes; I = <5 m; II = 5–10 m; III = 10–15 m.

**Table 5.** Summary of a three-way crossed PERMANOVA test of the spatio-temporal variation in percent live coral cover before and after Hurricanes Irma and María.

| Source [1] | df | MS | Pseudo_F | P (Perm) | P (Perm) |
|---|---|---|---|---|---|
| Time | 1 | 8830.5 | 114.91 | <0.0001 | 9935 |
| Site | 9 | 6225.2 | 81.01 | <0.0001 | 9919 |
| Depth | 2 | 2960.2 | 38.52 | <0.0001 | 9955 |
| Time × Site | 9 | 741.84 | 9.65 | <0.0001 | 9891 |
| Time × Depth | 2 | 794.55 | 10.34 | <0.0001 | 9919 |
| Site × Depth | 18 | 299.50 | 3.90 | <0.0001 | 9850 |
| Time × Site × Depth | 18 | 133.11 | 1.73 | 0.0019 | 9844 |
| Residual | 300 | 76.849 | | | |

[1] Based on 9999 permutations.

Shallow-water reef zones were significantly affected by hurricane-driven waves and swells. Before the hurricanes, shallow reef zones (<5 m) had a global mean coral cover of 11.7%, intermediate depths (5–10 m) had a mean of 15.9%, and deeper zones (10–15 m) had a global mean of 15.0%. After the hurricanes, shallow reef zones had a global mean coral cover of 6.6% (a magnitude 43.1% decline), intermediate depths had a mean of 9.9% (a magnitude 38.1% decline), and deeper zones had a mean of 11.6% (a magnitude 23.2% decline).

Overall, hurricanes caused a generalized decline in percent coral cover that was site- and depth-related. For instance, percent coral cover showed important declines across sites, ranging from 10.2 to 68.1% in magnitude, with an overall loss from a global mean of 14.2 to 9.3%, or a magnitude of 34.5%. Hurricanes caused a widespread decline in the percent relative cover of *A. cervicornis* that was site- and depth-related. It showed a highly significant temporal (Pseudo F = 142.84; $p < 0.0001$), site (Pseudo F = 77.83; $p < 0.0001$), and depth-related decline (Pseudo F = 14.69; $p < 0.0001$) in percent live coral cover (Table 6 and Table S1). There was also significant time × site (Pseudo F = 12.67; $p < 0.0001$), time × depth (Pseudo F = 8.43; $p = 0.0002$), and site × depth (Pseudo F = 6.92; $p < 0.0001$) interactions. Time × site × depth interaction was also significant (Pseudo F = 3.65; $p < 0.0001$).

**Table 6.** Summary of a three-way crossed PERMANOVA test of the spatio-temporal variation in endangered coral percent live cover before and after Hurricanes Irma and María.

| Source [1] | df | *Acropora cervicornis* | *Orbicella annularis* | *Orbicella faveolata* | *Orbicella franksi* | *Dendrogyra cylindrus* |
|---|---|---|---|---|---|---|
| Time | 1 | 142.84<br><0.0001 | 1.39<br>0.2406 | 0.42<br>0.9072 | 0.88<br>0.3486 | 6.71<br>0.0063 |
| Site | 9 | 77.83<br><0.0001 | 50.87<br><0.0001 | 31.82<br><0.0001 | 4.55<br>0.0002 | 1.10<br>0.3535 |
| Depth | 2 | 14.69<br><0.0001 | 35.92<br><0.0001 | 30.68<br><0.0001 | 13.90<br><0.0001 | 2.74<br>0.0651 |
| Time × Site | 9 | 12.67<br><0.0001 | 0.87<br>0.5522 | 0.55<br>0.8495 | 0.84<br>0.5848 | 0.66<br>0.7522 |
| Time × Depth | 2 | 8.43<br>0.0002 | 0.16<br>0.8932 | 0.03<br>0.9908 | 0.01<br>0.9952 | 1.70<br>0.1852 |
| Site × Depth | 18 | 6.92<br><0.0001 | 3.55<br><0.0001 | 2.83<br><0.0001 | 0.78<br>0.7171 | 0.93<br>0.5502 |
| Time × Site × Depth | 18 | 3.65<br><0.0001 | 0.36<br>0.9967 | 0.28<br>0.9994 | 0.36<br>0.9930 | 0.84<br>0.6616 |
| Residual | 300 | | | | | |

[1] Based on 9999 permutations; data = Pseudo-F statistic and *p* value.

For instance, percent *A. cervicornis* cover showed important declines across sites, ranging from 0 to 100%, with an overall loss from a mean of 3.30 to 0.71%, or a magnitude

of 78.48% (Table S1). Shallow-water reef zones were significantly affected by hurricane-driven waves and swells. Before the hurricanes, shallow reef zones (<5 m) had a mean *A. cervicornis* cover of 2.12%, intermediate depths (5–10 m) had a mean of 5.25%, and deeper zones (10–15 m) had a mean of 2.53%. After the hurricanes, shallow reef zones had a global mean *A. cervicornis* cover of 0.05% (a magnitude 97.64% decline), intermediate depths had a mean of 1.07% (a magnitude 79.62% decline), and deeper zones had a mean of 1.0% (a magnitude 60.47% decline). These results point out the high vulnerability of *A. cervicornis* assemblages to strong hurricanes.

There was a non-significant temporal decline in the percent relative cover of the Columnar star coral, *Orbicella annularis* (Pseudo F = 1.39; $p = 0.2406$) (Tables 6 and S2). Site (Pseudo F = 50.87; $p < 0.0001$) and depth differences (Pseudo F = 35.92; $p < 0.0001$) were highly significant. There was also a significant site × depth interaction (Pseudo F = 6.92; $p < 0.0001$). Hurricanes caused a minimal decline in the percent relative cover of *O. annularis* that was site- and depth-related and was not exactly associated to direct mechanical destruction as in branching corals. In this case, most of the observed tissue loss in *O. annularis* was associated to sandblasting effects during localized sediment bedload (horizontal transport) effects, burial under hurricane-generated rubble fields, and due to post-hurricane mortality by a white plague-like condition. In addition, the results ranged from total loss to a gain in percent relative cover, which was most probably associated to spatial variation in transects positioning.

Percent relative cover in *O. annularis* showed important variation across sites, ranging from +19.53% to −100%, with an overall loss from a mean of 2.78 to 2.45%, or a magnitude of 11.87% (Table S2). Shallow-water reef zones were significantly affected by hurricane-driven waves and swells. Before the hurricanes, shallow reef zones (<5 m) had a mean *O. annularis* cover of 1.75%, intermediate depths (5–10 m) had a mean of 2.58%, and deeper zones (10–15 m) had a mean of 4.00%. After the hurricanes, shallow reef zones had a mean *O. annularis* cover of 1.38% (a magnitude 21.14% decline), intermediate depths had a mean of 2.45% (a magnitude 5.04% decline), and deeper zones had a mean of 3.52% (a magnitude 12.00% decline). These results point out that vulnerability of *O. annularis* assemblages to strong hurricanes was minimal in comparison to branching corals. However, impacts from sediment bedload, abrasion, and suffocation were locally important.

There was no significant temporal variation in percent relative cover of Laminar star coral, *O. faveolata*, (Pseudo F = 0.42; $p = 0.9072$) (Tables 6 and S3). However, site (Pseudo F = 31.82; $p < 0.0001$) and depth differences (Pseudo F = 30.68; $p < 0.0001$) were highly significant. Site × depth interaction was also highly significant (Pseudo F = 3.55; $p < 0.0001$). Hurricanes also caused a minimal decline in the percent relative cover of *O. faveolata* that was site- and depth-related and was largely associated to sandblasting effects during localized sediment bedload, burial under hurricane-generated rubble fields, and due to post-hurricane mortality by a white plague-like condition. The results ranged from total loss to a gain in percent relative cover, which was most probably associated to spatial variation in transects positioning. Percent *O. faveolata* cover showed important variation across sites, ranging from +43.82% to −71.79%, with an overall loss from a mean of 1.18 to 1.10%, or a magnitude of 6.78% (Table S3).

Shallow-water reef zones were significantly affected by hurricane-driven waves and swells. Before hurricanes, shallow reef zones (<5 m) had a mean *O. faveolata* cover of 0.70%, intermediate depths (5–10 m) had a global mean of 1.03%, and deeper zones (10–15 m) had a mean of 1.82%. After hurricanes, shallow reef zones had a mean *O. faveolata* cover of 0.60% (a magnitude 14.29% decline), intermediate depths had a mean of 0.97% (a magnitude 5.83% decline), and deeper zones had a mean of 1.73% (a magnitude 4.95% decline). These results point out that the vulnerability of *O. faveolata* assemblages to strong hurricanes was minimal in comparison to branching corals.

The results for spatio-temporal variation in percent relative cover of Boulder star coral, *O. franksi*, were nearly similar (Tables 6 and S4). There was no significant temporal variation in the percent relative cover of this species (Pseudo F = 0.88; $p = 0.3486$). However, site

(Pseudo F = 4.55; $p = 0.0002$) and depth differences (Pseudo F = 13.90; $p < 0.0001$) were highly significant. No significant interactions were documented. Hurricanes also caused a minimal decline in the percent relative cover of *O. franksi* that was site- and depth-related and was mostly associated to sandblasting effects, localized sediment bedload effects, burial under hurricane-generated rubble fields, and due to post-hurricane mortality by a white plague-like condition. The results ranged from total loss to a gain in percent relative cover, which was most probably associated to spatial variation in transects positioning. Percent *O. franksi* cover showed important variation across sites, ranging from +29.41% to −45.45%, with a loss from a mean of 0.19 to 0.17%, or a magnitude of 12.11% (Table S4).

Shallow-water reef zones were significantly affected by hurricane-driven waves and swells. Before hurricanes, shallow reef zones (<5 m) had a global mean *O. franksi* cover of 0.03%, intermediate depths (5–10 m) had a mean of 0.18%, and deeper zones (10–15 m) had a mean of 0.33%. After hurricanes, shallow reef zones had a mean *O. franksi* cover of 0.07% (a magnitude 103% increase), intermediate depths had a mean of 0.22% (a magnitude 18.58% increase), and deeper zones had a mean of 0.37% (a magnitude 10.21% increase).

Overall, there was a highly significant (Pseudo F = 6.71; $p = 0.0063$) post-hurricane decline in the percent relative cover of Pillar coral, *Dendrogyra cylindrus* (Tables 6 and S5). There was no significant variation among sites or depth zones, nor any significant interaction effect. Despite the severely depleted populations of *D. cylindrus* prior to both hurricanes, these caused a significant decline in the percent relative cover of this species that was site- and depth-related. Most of the observed tissue loss in *D. cylindrus* was associated to sandblasting effects during localized sediment bedload, burial under hurricane-generated rubble fields, and due to post-hurricane mortality by a white plague-like condition. The results ranged from a moderate to a total loss to a gain in percent relative cover. Percent *D. cylindrus* cover showed important variation across sites, ranging from 0 to −100%, with an overall loss from a global mean of 0.15 to 0.006%, or a magnitude of −96.00% (Table S5).

Before hurricanes, shallow reef zones (<5 m) had a mean *D. cylindrus* cover of 0%, intermediate depths (5–10 m) had a mean of 0.08%, and deeper zones (10–15 m) had a mean of 0.10%. After hurricanes, shallow reef zones remained at 0%, intermediate depths had a mean of 0.02% (a magnitude 79.52% decline), and deeper zones had a mean of 0% (a magnitude 100% decline). These results point out that high vulnerability of *D. cylindrus* assemblages to strong hurricanes was significant in comparison to other endangered coral species.

### *3.4. Spatio-Temporal Variation in the Percent Cover of Other Benthic Components*

There was a highly significant temporal (Pseudo F = 1102.3; $p < 0.0001$), site (Pseudo F = 45.75; $p < 0.0001$), and depth-related (Pseudo F = 396.33; $p < 0.0001$) post-hurricane increase in percent macroalgal cover (Figure 9, Tables 7 and S6). There was also significant time × site (Pseudo F = 25.50; $p < 0.0001$), time × depth (Pseudo F = 57.27; $p < 0.0001$), site × depth (Pseudo F = 9.97; $p < 0.0001$), and time × site × depth interactions (Pseudo F = 3.75; $p < 0.0001$). Hurricanes caused a major widespread increase in percent macroalgal cover across sites and depth gradients. Most of the immediate post-hurricane macroalgal growth response was associated to blooming red algae, mostly *Liagora* spp., *Acrosymphyton caribaeum*, and *Trichogloeopsis pedicellata*. These were still highly abundant in locations surveyed during early 2018. However, nuance brown macroalgae *Lobophora variegata* and *Dictyota* spp. became the dominant macroalgal component in locations surveyed during late 2018 and early 2019. Quantitative data analysis for the purpose of this study only categorized macroalgae as a general functional group and did not account for such taxonomic variation.

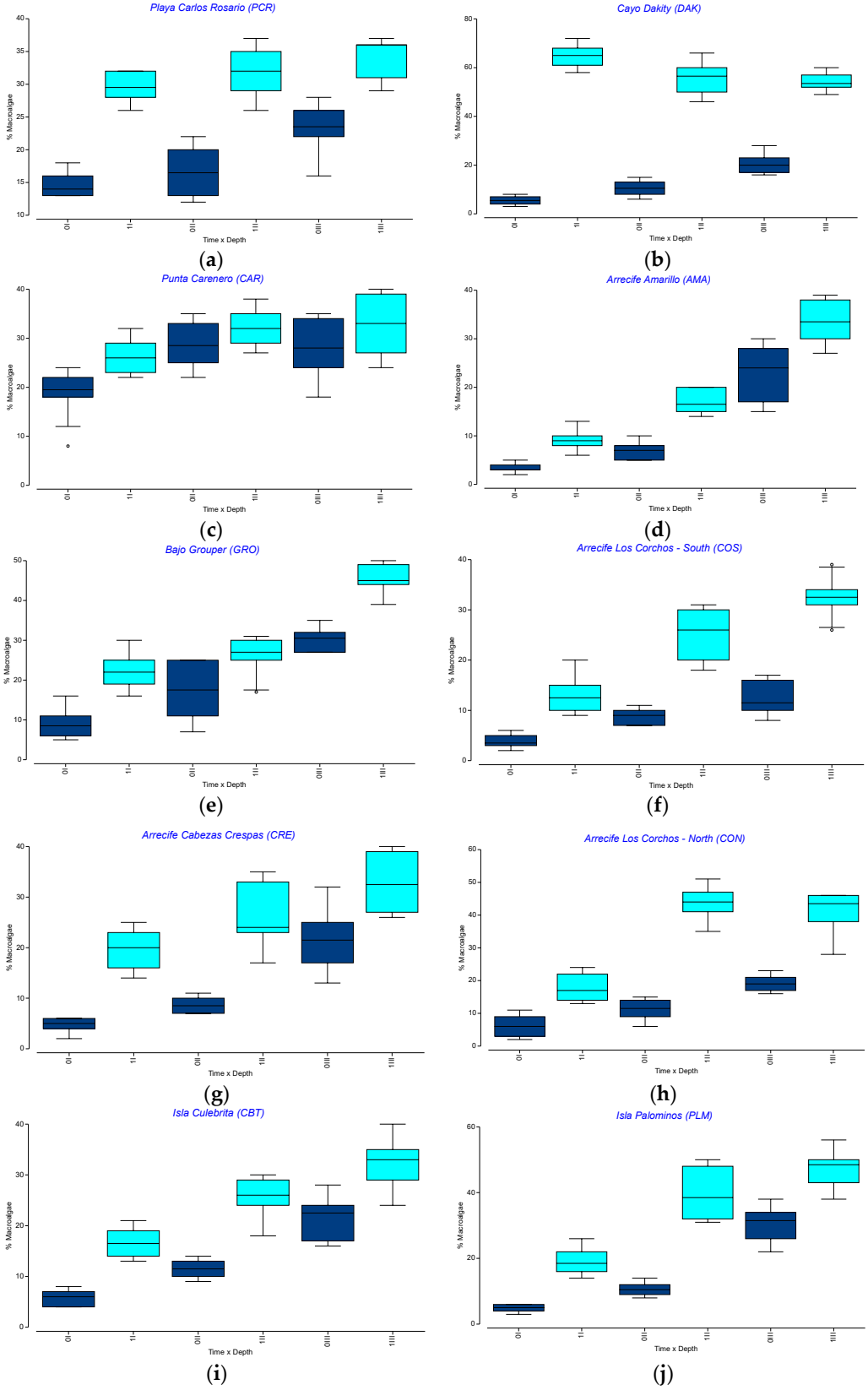


**Figure 9.** Box plot diagram of spatio-temporal variation in percent macroalgal cover before and after Hurricanes Irma and María: (**a**) PCR = Playa Carlos Rosario; (**b**) DAK = Cayo Dákity; (**c**) CAR = Punta Carenero; (**d**) AMA = Arrecife Amarillo; (**e**) GRO = Bajo Grouper; (**f**) Arrecife Los Corchos-South; (**g**) CRE = Arrecife Cabezas Crespas; (**h**) CON = Arrecife Los Corchos-North; (**i**) CBT = Culebrita Island; (**j**) Palominos Island. 0 = Before hurricanes; 1 = After hurricanes; I = <5 m; II = 5–10 m; III = 10–15 m.

**Table 7.** Summary of a three-way crossed PERMANOVA test of the spatio-temporal variation in percent cover of other benthic components before and after Hurricanes Irma and María.

| Source [1] | df | Macroalgae | Algal Turf | *Ramicrusta textilis* | Crustose Coralline Algae (Cca) | Cyanobacteria | Sand, Pavement, Rubble (SPR) | Sponge |
|---|---|---|---|---|---|---|---|---|
| Time | 1 | 1102.3<br><0.0001 | 120.55<br><0.0001 | 92.78<br><0.0001 | 70.90<br><0.0001 | 162.73<br><0.0001 | 51.21<br><0.0001 | 3.73<br>0.0512 |
| Site | 9 | 45.75<br><0.0001 | 52.71<br><0.0001 | 37.15<br><0.0001 | 9.55<br><0.0001 | 5.90<br><0.0001 | 28.42<br><0.0001 | 0.80<br>0.6119 |
| Depth | 2 | 396.33<br><0.0001 | 111.14<br><0.0001 | 33.01<br><0.0001 | 109.90<br><0.0001 | 64.85<br><0.0001 | 44.81<br><0.0001 | 11.52<br><0.0001 |
| Time × Site | 9 | 25.50<br><0.0001 | 9.53<br><0.0001 | 10.27<br><0.0001 | 4.24<br><0.0001 | 4.22<br>0.0002 | 18.71<br><0.0001 | 0.62<br>0.7869 |
| Time × Depth | 2 | 57.27<br><0.0001 | 1.83<br>0.1544 | 4.94<br>0.0014 | 2.74<br>0.0602 | 5.89<br>0.0020 | 15.47<br><0.0001 | 0.94<br>0.3966 |
| Site × Depth | 18 | 9.97<br><0.0001 | 20.53<br><0.0001 | 15.20<br><0.0001 | 4.32<br><0.0001 | 4.40<br><0.0001 | 9.20<br><0.0001 | 0.82<br>0.6710 |
| Time × Site × Depth | 18 | 3.75<br><0.0001 | 6.78<br><0.0001 | 4.15<br><0.0001 | 2.11<br>0.0026 | 1.65<br>0.0385 | 2.76<br><0.0001 | 0.74<br>0.7677 |
| Residual | 300 | | | | | | | |

[1] Based on 9999 permutations; data = Pseudo-F statistic and $p$ value.

The results ranged from a moderate to a major increase in percent macroalgal cover. For instance, percent macroalgal cover showed important increases across sites, ranging from +21.56 to +376.92%, with an overall increase from a global mean of 14.59 to 31.58%, or a magnitude of +116.45% (Table S6). Before hurricanes, shallow reef zones (<5 m) had a mean macroalgal cover of 7.65%, intermediate depths (5–10 m) had a mean of 13.08%, and deeper zones (10–15 m) had a mean of 23.03%. After hurricanes, shallow reef zones had a mean macroalgal cover of 23.87% (a magnitude 67.95% increase), intermediate depths had a mean of 32.30% (a magnitude 146.94% increase), and deeper zones had a mean of 38.57% (a magnitude 67.44% increase).

There was also a highly significant temporal (Pseudo F = 120.55; $p < 0.0001$), site (Pseudo F = 52.71; $p < 0.0001$), and depth-related (Pseudo F = 111.14; $p < 0.0001$) post-hurricane decline in percent algal turf cover (Table 7 and Table S7). There was also significant time × site (Pseudo F = 9.53; $p < 0.0001$), time × depth (Pseudo F = 1.83; $p < 0.0001$), site × depth (Pseudo F = 20.53; $p < 0.0001$), and time × site × depth interactions (Pseudo F = 6.78; $p < 0.0001$). Hurricanes caused a major widespread decline in percent algal turf cover across sites and depth gradients. Most of the immediate post-hurricane algal turf decline response was associated to displacement by blooming macroalgae. The results ranged from a moderate to a major decline in percent relative cover. Percent algal turf cover showed important declines across sites, ranging from −15.23 to −69.13%, with an overall decline from 25.22 to 16.91%, or a magnitude of 32.95% (Table S7).

Before hurricanes, shallow reef zones (<5 m) had a global mean algal turf cover of 34.03%, intermediate depths (5–10 m) had a global mean of 22.83%, and deeper zones (10–15 m) had a global mean of 18.78%. After hurricanes, shallow reef zones had a mean algal turf cover of 25.33% (a magnitude 25.57% decline), intermediate depths had a mean of mean of 13.22% (a magnitude 42.09% decline), and deeper zones had a mean of 12.18% (a magnitude 35.14% decline).

Significant temporal (Pseudo F = 92.78; $p < 0.0001$), site (Pseudo F = 37.15; $p < 0.0001$), and depth-related (Pseudo F = 33.01; $p < 0.0001$) post-hurricane decline in the percent cover of red encrusting algae *R. textilis* was also documented (Table 7 and Table S8). There was also significant time × site (Pseudo F = 10.27; $p < 0.0001$), time × depth (Pseudo F = 4.94; $p = 0.0014$), site × depth (Pseudo F = 15.20; $p < 0.0001$), and time × site × depth interactions (Pseudo F = 4.15; $p < 0.0001$). Hurricane-driven wave action resulted in a major widespread decline in percent *R. textilis* cover across sites and depth gradients. Most of the immediate post-hurricane decline was associated with mechanical disruption and fragmentation by

wave action and due to displacement by blooming macroalgae. The results ranged from a moderate to a major decline in percent relative cover. Percent *R. textilis* cover decline across sites ranged from +9.45 to −66.99%, with an overall decline from 17.28 to 11.67%, or a magnitude of 32.47% (Table S8).

Before hurricanes, shallow reef zones (<5 m) had a global mean *R. textilis* cover of 16.60%, intermediate depths (5–10 m) had a global mean of 17.58%, and deeper zones (10–15 m) had a mean of 17.65%. After hurricanes, shallow reef zones had a mean *R. textilis* cover of 9.77% (a magnitude 41.14% decline), intermediate depths had a mean of 10.97% (a magnitude 37.60% decline), and deeper zones had a mean of 14.28% (a magnitude 19.09% decline).

A significant temporal (Pseudo F = 70.90; $p < 0.0001$), site (Pseudo F = 9.55; $p < 0.0001$), and depth-related (Pseudo F = 109.90; $p < 0.0001$) post-hurricane decline in percent cover of crustose coralline algae (CCA) was also observed (Table 7 and Table S9). There was also significant time × site (Pseudo F = 4.24; $p < 0.0001$), site × depth (Pseudo F = 4.32; $p < 0.0001$), and time × site × depth interactions (Pseudo F = 2.11; $p = 0.0026$). Overall, there was a widespread decline in percent CCA cover across sites and depth gradients. Most of the immediate post-hurricane CCA decline response was associated with displacement by blooming macroalgae, and in some locations due to sediment bedload impacts and burial by hurricane-generated rubble. The results ranged from a moderate to a major decline in percent relative cover. For instance, percent CCA cover showed important declines across sites, ranging from +39.10 to −88.14%, with an overall decline from a mean of 4.77 to 2.50%, or a magnitude of 47.59% (Table S9).

Before hurricanes, shallow reef zones (<5 m) had a global mean CCA cover of 8.78%, intermediate depths (5–10 m) had a global mean of 4.25%, and deeper zones (10–15 m) had a mean of 1.28%. After hurricanes, shallow reef zones had a mean CCA cover of 5.17% (a magnitude 41.12% decline), intermediate depths had a mean of 1.77% (a magnitude 58.35% decline), and deeper zones had a mean of 0.57% (a magnitude 55.47% decline).

There was a significant temporal (Pseudo F = 162.93; $p < 0.0001$), site (Pseudo F = 5.90; $p < 0.0001$), and depth-related (Pseudo F = 64.85; $p < 0.0001$) post-hurricane increase in the percent cover of cyanobacteria (Table 7 and Table S10). There was also significant time × site (Pseudo F = 4.22; $p = 0.0002$), time × depth (Pseudo F = 5.89; $p = 0.0020$), site × depth (Pseudo F = 4.40; $p < 0.0001$), and time × site × depth interactions (Pseudo F = 1.65; $p = 0.0385$). A widespread burst in cyanobacterial growth across sites and depth gradients was observed following hurricanes. Percent cyanobacterial cover increased across sites, ranging from +98.21 to +1228.57%, with an overall increase from a global mean of 0.51 to 2.30%, or a magnitude of 350.98% (Table S10).

Before hurricanes, shallow reef zones (<5 m) had a mean cyanobacterial cover of 0.10%, intermediate depths (5–10 m) had a mean of 0.30%, and deeper zones (10–15 m) had a mean of 1.12%. After hurricanes, shallow reef zones had a mean cyanobacterial cover of 0.98% (a magnitude 880.00% increase), intermediate depths had a mean of 2.33% (a magnitude 676.67% increase), and deeper zones had a mean of 3.58% (a magnitude 219.64% increase).

A significant temporal (Pseudo F = 51.21; $p < 0.0001$), site (Pseudo F = 28.42; $p < 0.0001$), and depth-related (Pseudo F = 44.81; $p < 0.0001$) post-hurricane increase in the percent open substrate (sand, pavement, rubble) cover resulted from the strong hurricane mechanical impacts to reef substrate (Table 7 and Table S11). There were also significant time × site (Pseudo F = 18.71; $p < 0.0001$), time × depth (Pseudo F = 15.47; $p < 0.0001$), site × depth (Pseudo F = 9.20; $p < 0.0001$), and time × site × depth interactions (Pseudo F = 2.76; $p < 0.0001$). Observed variation in percent open substrate cover included both site-specific increases and declines, depending on site exposure to extreme wave action and swells and the destruction of the shallow reef's framework and the formation of extensive rubble fields. Percent open substrate cover shifted across sites, ranging from −55.33 to +343.29%, with an overall increase from a mean of 9.12 to 16.22%, or a magnitude of 77.85% (Table S11).

Before the hurricanes, shallow reef zones (<5 m) had a global mean percent open substrate cover of 9.68%, intermediate depths (5–10 m) had a global of 9.97%, and deeper

zones (10–15 m) had a mean of 7.70%. After the hurricanes, shallow reef zones had a mean open substrate cover of 21.58% (a magnitude 122.93% increase), intermediate depths had a mean of 19.58% (a magnitude 96.39% increase), and deeper zones had a mean of 7.48% (a magnitude 2.86% decline).

There was a marginally significant temporal decline in percent sponge cover from 0.19% to 0.11%, or a magnitude loss of 42% (Pseudo F = 3.72; $p = 0.0512$) (Table 7). Deeper zones sustained significantly higher percent sponge cover than middle or shallower zones (Pseudo F = 0.80; $p < 0.0001$). No significant location or interaction effects were documented.

### *3.5. Spatio-Temporal Variation in Benthic Community Structure*

There was a highly significant temporal (Pseudo F = 128.78; $p < 0.0001$), site (Pseudo F = 36.56; $p < 0.0001$), and depth-related (Pseudo F = 72.46; $p < 0.0001$) post-hurricane variation in benthic community structure (Table 8). There was also significant time × site (Pseudo F = 7.11; $p < 0.0001$), time × depth (Pseudo F = 10.37; $p < 0.0001$), site × depth (Pseudo F = 7.64; $p < 0.0001$), and time × site × depth interactions (Pseudo F = 1.96; $p < 0.0001$).

**Table 8.** Summary of a three-way crossed PERMANOVA test of the spatio-temporal variation in benthic community structure before and after Hurricanes Irma and María.

| Source [1] | df | MS | Pseudo_F | P (Perm) | P (Perm) |
|---|---|---|---|---|---|
| Time | 1 | 21019 | 128.78 | <0.0001 | 9950 |
| Site | 9 | 5966.5 | 36.56 | <0.0001 | 9850 |
| Depth | 2 | 11826 | 72.46 | <0.0001 | 9938 |
| Time × Site | 9 | 1161.2 | 7.11 | <0.0001 | 9871 |
| Time × Depth | 2 | 1682.7 | 10.37 | <0.0001 | 9943 |
| Site × Depth | 18 | 1246.9 | 7.64 | <0.0001 | 9824 |
| Time × Site × Depth | 18 | 319.78 | 1.96 | <0.0001 | 9834 |
| Residual | 300 | 163.22 | | | |

[1] Based on 9999 permutations.

Principal coordinates ordination (PCO) shows the spatio-temporal variation in benthic community structure across sites, before and after Hurricanes Irma and María (Figure 10). Vectors shown based on Spearman rank correlation >0.70 suggest that most of the observed variation across axis PCO 1 (37.8% of the total variation) were explained by pre-hurricane dominance by CCA, *Agaricia agaricites*, *A. cervicornis*, *Porites porites*, and *P. furcata*, and by an observed post-hurricane increase in dominance by blooming macroalgae and cyanobacteria. Axis PCO 2 explained 22.3% of the total variation mostly by variation in the dominance by Star coral species complex, *O. annularis*, *O. faveolata*, and *O. franksi*, and by *Diploria labyrinthiformis*. This solution explains 60.1% of the spatio-temporal variation.

Other coral decline, beyond endangered species, showed from modest to substantial populations declines following hurricane disturbances. Figure S3 shows bubble plots evidencing declining population trajectories of endangered coral species before and after Hurricanes Irma and María in *A. cervicornis*, *O. annularis*, *O. faveolata*, *O. franksi*, and *D. cylindrus*. Figure S4 shows population trajectories of branching coral species before and after the hurricanes for *P. porites*, *P. furcata*, *P. divaricata*, *A. agaricites*, and *A. humilis*. Figure S5 illustrates population trajectories in large and small massive coral species before and after the hurricanes for *Pseudodiploria strigosa*, *P. clivosa*, *D. labyrinthiformis*, *Siderastrea sidereal*, and *P. astreoides*. Observed coral decline was trait specific. Branching corals showed the highest post-hurricane mean decline (78%): *P. porites* (64%), *P. furcata* (70%), *P. divaricata* (100%). Mean decline in laminar corals was 77%: *A. agaricites* (72%), *A. humilis* (83%). The lowest mean decline (22%) was documented in small and large massive corals: *P. astreoides* (6%), *P. strigosa* (15%), *P. clivosa* (25%), *D. labyrinthiformis* (24%), *S. siderea* (42%).

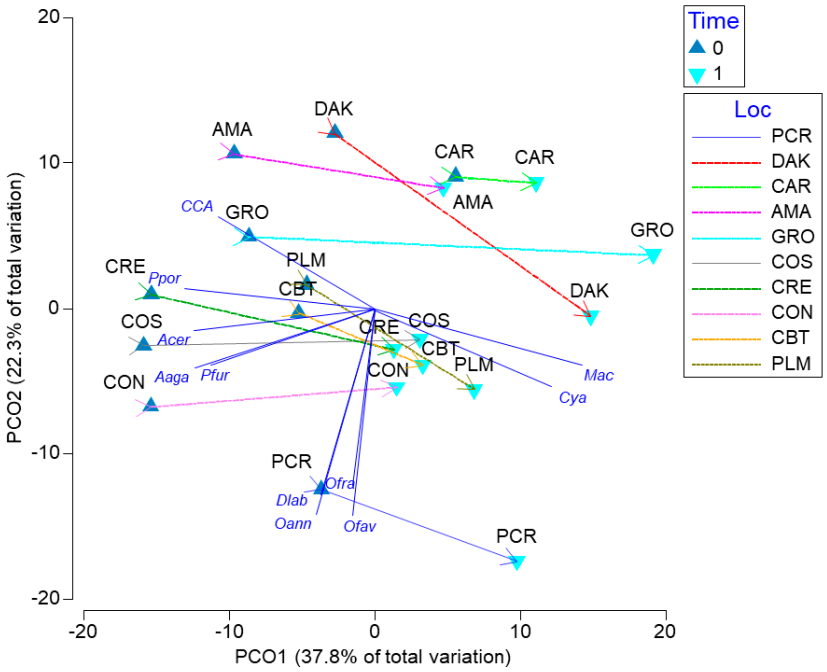


**Figure 10.** Principal coordinates ordination (PCO) showing trajectories of benthic community structure across sites, before and after Hurricanes Irma and María. 0 (dark blue) = before, 1 (aquamarine) = after. Vectors shown are based on a Spearman rank correlation > 0.70. This solution explains 60.1% of the observed spatio-temporal variation. *Acer* = *Acropora cervicornis*; *Ppor* = *Porites porites*; *Pfur* = *P. furcata*; *Aaga* = *Agaricia agaricites*; *Dlab* = *Diploria labyrinthiformis*; *Oann* = *Orbicella annularis*; *Ofav* = *O. faveolata*; *Ofra* = *O. franksi*; *Mac* = *Macrocalgae*; *CCA* = *Crustose coralline algae*; *Cya* = *Cyanobacteria*.

A similarity percentage (SIMPER) test of the temporal variation (before and after hurricanes) in coral reef benthic community structure across surveyed sites showed that turf was the dominant overall taxa (21.94%) before hurricanes, followed by *R. textilis* (18.95%), and macroalgae (16.71%), which explained 57.60% of the observed variation (Table S12). The most important coral species explaining the observed pre-hurricanes variation was *P. astreoides* (6.71%). Average pre-hurricane similarity was 68.40%. Macroalgae were the dominant overall taxa (27.92%) after hurricanes, followed by algal turf (17.64%), and open substrate (SPR) (15.78%), which explained 61.34% of the observed variation. The most important coral species explaining the observed variation was *P. astreoides* (6.31%). Average post-hurricane similarity was 70.13%. Endangered *A. cervicornis* percent contribution declined from 2.25 to 0.31%, *O. annularis* from 3.83 to 3.52%, and *D. cylindrus* from 0.1 to 0% after the hurricanes. *Orbicella faveolata* remained nearly stable from 1.24 to 1.25%, and *O. franksi* slightly increased from 0.12 to 0.19%. The observed variation suggests an important spatio-temporal phase shift in coral reef benthic community structure which favored macroalgae at some locations and filamentous algal turf at others. Macroalgae were the dominant taxa which explained before–after variation (12.33%), followed by algal turf (11.31%), and open substrate (SPR) (9.15%), which explained 32.80% of the observed before–after variation.

Additional SIMPER analyses showed that different taxa were dominant at different locations (Table S13). Non-reef building taxa were dominant across all sites, which could be an indicator of long-term decline. Macroalgae were dominant at PCR, DAK, GRO, and COS. Algal turf was dominant at CAR, CRE, CBT, and PLM. *Ramicrusta textilis* was dominant at AMA and CON. Table S13 also shows all the taxa that explained the observed spatial variation among all sites. Algal turf explained 35.5% of the observed variation among sites, while macroalgae explained 22.2%. Open substrate (SPR) and *A. cervicornis* explained 13.3% of the observed variation, respectively. CCA explained 8.9% of the observed variation,

while *O. annularis* explained 6.7% of the variation among sites. Algal turf explained 35.5% of the observed variation among sites, while macroalgae explained 22.2%. Open substrate (SPR) and *A. cervicornis* explained 13.3% of the observed variation, respectively. CCA explained 8.9% of the observed variation, while *O. annularis* explained 6.7% of the variation among sites.

SIMPER tests also showed temporal variation (before–after hurricanes) of coral reef benthic community structure across sites which suggests a widespread phase shift favoring macroalgae at some sites and filamentous algal turf at others (Table S14). Macroalgae were dominant at PCR before (18.96%) and after the hurricanes (25.88%). Turf was dominant at DAK before the hurricanes (32.68%), and then macroalgae was dominant after the hurricanes (41.21%). Turf dominated CAR before (30.84%) and after the hurricanes (28.41%). *Ramicrusta textilis* dominated AMA before the hurricanes (25.67%), and then open substrate (SPR) after the hurricanes (22.95%) because of extensive rubble fields formation. Similarly, *R. textilis* was dominant at GRO before the hurricanes (29.12%), and then open substrate after the hurricanes (30.13%) because of extensive rubble fields formation. Turf was dominant at COS before the hurricanes (16.85%), and then macroalgae after the hurricanes (21.80%). Similarly, turf was dominant at CRE before the hurricanes (19.31%), and then macroalgae after the hurricanes (23.73%). *Ramicrusta textilis* was dominant at CON before the hurricanes (23.45%), and then macroalgae after the hurricanes (25.46%). Turf was dominant at CBT before the hurricanes (23.91%), and then macroalgae after the hurricanes (21.97%). Turf was also dominant at PLM before the hurricanes (26.08%), and then macroalgae after the hurricanes (27.96%).

An increasing abundance of cyanobacteria explained most of the observed variation before and after the hurricanes at PCR (12.58%), while increasing abundance of macroalgae explained variation at DAK (26.65%) (Table S15). An increasing abundance of *Ramicrusta textilis* explained most of the observed variation before and after the hurricanes at CAR (14.02%), while an increasing abundance of open substrate (SPR) explained variations at AMA (14.99%). An increasing abundance of open substrate explained most of the observed variation before and after hurricanes at GRO (16.36%) and at COS (14.80%). An increasing abundance of macroalgae explained most of the observed variation before and after hurricanes at CRE (11.76%) and at CON (14.81%). An increasing abundance of turf explained most of the observed variation before and after hurricanes at CBT (15.26%) and at PLM (17.04%).

### *3.6. Spatio-Temporal Variation in Biodiversity*

There was a highly significant temporal (Pseudo F = 88.83; $p < 0.0001$), site (Pseudo F = 51.39; $p < 0.0001$), and depth-related (Pseudo F = 30.20; $p < 0.0001$) post-hurricane decline in coral species richness (Figure 11a, Table 9). There were also significant time × site (Pseudo F = 3.30; $p < 0.0001$), time × depth (Pseudo F = 5.86; $p < 0.0001$), and site × depth interactions (Pseudo F = 4.58; $p < 0.0001$).

A highly significant temporal (Pseudo F = 66.23; $p < 0.0001$), site (Pseudo F = 42.41; $p < 0.0001$), and depth-related (Pseudo F = 19.78; $p < 0.0001$) post-hurricane increase was documented in $H'_c$ (Figure 11b, Table 9). There were also significant time × site (Pseudo F = 4.01; $p < 0.0001$), time × depth (Pseudo F = 11.28; $p < 0.0001$), site × depth (Pseudo F = 4.58; $p < 0.0001$), and time × site × depth interactions (Pseudo F = 1.69; $p = 0.0378$).

$J'_c$ showed a highly significant temporal (Pseudo F = 5.57; $p = 0.0280$), site (Pseudo F = 11.86; $p < 0.0001$), and depth-related (Pseudo F = 6.02; $p = 0.0058$) post-hurricane increase (Figure 11c, Table 9). There were also significant time × site (Pseudo F = 7.91; $p < 0.0001$), time × depth (Pseudo F = 4.53; $p = 0.0195$), site × depth (Pseudo F = 5.34; $p < 0.0001$), and time × site × depth interactions (Pseudo F = 2.35; $p = 0.0055$).

A distance-based test for homogeneity of multivariate dispersions (PERMDISP) analysis of coral $\sqrt{}$-transformed β-diversity based on Euclidean distance showed highly significant overall temporal variation in multivariate dispersions following the hurricanes (F = 5.80; d.f. = 1;358; $p$ (perm) = 0.0005). There was also significant spatial variation in mul-

tivariate dispersions (F = 10.35; d.f. = 9;350; $p$ (perm) < 0.0001). No significant depth-related variation was observed (F = 2.07; d.f. = 2;357; $p$ (perm) = 0.3055). A highly significant spatio-temporal variation (F = 7.95; d.f. = 19;340; $p$ (perm) < 0.0001) in the homogeneity of multivariate dispersions was documented for time × site combinations. There was also a highly significant spatio-temporal variation (F = 6.05; d.f. = 5;354; $p$ (perm) = 0.0029) in the homogeneity of multivariate dispersions found for time × depth combinations. A highly significant spatio-temporal variation (F = 5.80; d.f. = 59;300; $p$ (perm) < 0.0001) in the homogeneity of multivariate dispersions was also found for time × site × depth combinations. Observed patterns reflect a combination of natural spatial variability in β-diversity, but also significant variation resulting from hurricane impacts. Declining species richness on multiple locations resulted in increased β-diversity by sampling unit.

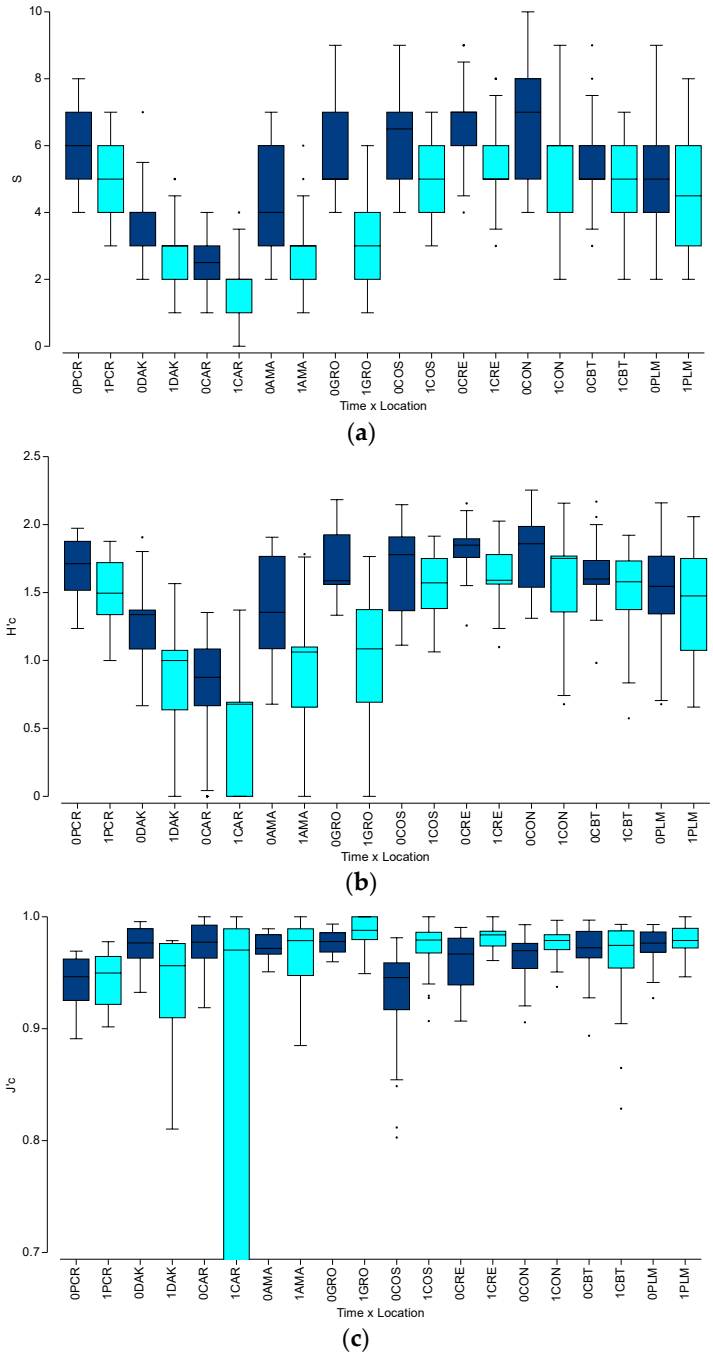


**Figure 11.** Spatio-temporal variation in coral biodiversity before and after Hurricanes Irma and María: (**a**) Species richness (S); (**b**) Species diversity index ($H'_c$); (**c**) Evenness ($J'_c$).

**Table 9.** Summary of a three-way crossed PERMANOVA test of the spatio-temporal variation in coral biodiversity before and after Hurricanes Irma and María: (a) Species richness (S); (b) Species diversity index ($H'_c$); (c) Evenness ($J'_c$).

| Source [1] | df | Species Richness (S) | Diversity Index ($H'_c$) | Evenness ($J'_c$) |
|---|---|---|---|---|
| Time | 1 | 88.83<br><0.0001 | 66.23<br><0.0001 | 5.57<br>0.028 |
| Site | 9 | 51.39<br><0.0001 | 42.41<br><0.0001 | 11.86<br><0.0001 |
| Depth | 2 | 30.2<br><0.0001 | 19.78<br><0.0001 | 6.02<br>0.0058 |
| Time × Site | 9 | 3.3<br>0.0006 | 4.01<br><0.0001 | 7.91<br><0.0001 |
| Time × Depth | 2 | 5.86<br>0.0026 | 11.28<br><0.0001 | 4.53<br>0.0195 |
| Site × Depth | 18 | 4.58<br><0.0001 | 4.58<br><0.0001 | 5.34<br><0.0001 |
| Time × Site × Depth | 18 | 1.04<br>0.4107 | 1.69<br>0.0378 | 2.35<br>0.0055 |
| Residual | 300 | | | |

[1] Based on 9999 permutations; data = Pseudo-F statistic, *p* value.

## 4. Discussion

### *4.1. Hurricane Impacts to Endangered Corals*

Hurricanes Irma and María, both category five hurricanes, had unprecedented impacts on coral reefs in the northeastern Caribbean, including PR. The degree of impact varied based on factors such as proximity to the hurricane's center, exposure to wave action, and coral morphological traits. Prior to these hurricanes, the last direct impact of a category five hurricane on PR was in 1928. According to the traditional ecological knowledge of many older fishers in PR, mechanical damage by that hurricane on shallow reefs never showed any recovery, implying persistent impacts lasting many decades. The observed mechanical impacts in 2017 primarily affected colonies of endangered coral species, raising concerns about the sustainability of coral reef ecological functions. The damage caused by the hurricanes can be categorized into four major types: (1) Mechanical destruction of reef framework leading to extensive rubble fields; (2) Colony fragmentation and dislodgment; (3) Abrasion by sediment bedload; and (4) Burial by displaced sediments and rubble. The mechanical destruction resulted from exposure to strong waves during the hurricanes, leading to the formation of rubble fields in shallow reef grounds, with further expansion into moderate to deeper reef zones depending on location and exposure to prevailing winds. Windward coral reefs facing east and southeast of Culebra Island and at ALCNR experienced more severe mechanical impacts.

These observations align with the existing literature on the profound impacts of major hurricanes. A comparable scenario occurred with category four Hurricane Hugo in 1989, which inflicted substantial physical damage to coral reefs in St. John, USVI [66,67]. Additionally, hurricanes have been found to increase species diversity in local scales due to the removal of dominant species [68]. Hurricane Allen in 1980, with 11.5 m waves, caused extensive mechanical damage to *A. palmata* assemblages in Discovery Bay, Jamaica, resulting in a significant loss of live coral cover [69–71]. The damage persisted for years [72] and was exacerbated by category five Hurricane Gilbert in 1988 [71,73]. The combined impact of Hurricane Allen in 1980 and post-hurricane coral diseases resulted in further loss of live coral cover in Jamaican reefs [74]. Similar losses occurred with Hurricane Iris in 2001 in Belize, emphasizing the persistent and severe consequences of strong hurricanes on coral ecosystems [75], and the high risks for already severely depleted endangered Acroporid coral stands.

This study revealed significant site-, depth-, and species-specific adverse effects on endangered coral species because of strong wave impacts on coral reefs. Branching or columnar species, including *A. palmata*, *A. cervicornis*, and *D. cylindrus*, experienced extensive damage at various locations, leading to nearly local population extirpation, especially in shallower windward reef zones. Larger size stages of Acroporid species witnessed remarkable declines, and pillar coral vanished from many locations. In contrast, endangered massive corals like *Orbicella* spp. were less affected by wave action but faced challenges from sediment bedload abrasion and burial by displaced sand or hurricane-generated rubble, regardless of its size stage. Notably, no signs of recovery were observed within a year of hurricane impacts, underscoring the importance of coral morphological traits in explaining the observed impacts on coral reef benthic assemblages.

A comprehensive study of 286 Caribbean coral reef locations reported an average 17% loss in percent live coral cover one year after the hurricanes [24]. The extent of this loss correlated with hurricane intensity and time since the last impact. In our investigation, there was a substantial 34.5% loss in percent live coral one year after being hit by two category five hurricanes, which is double the average annual loss following regional hurricanes from 1980 to 2001. The overall decline in coral cover at hurricane-impacted sites in the wider Caribbean during the same period was significantly faster (6% per annum) compared to non-impacted sites (2% per annum) [24]. However, the annual mean rate of percent live coral cover loss associated with the impacts of Hurricanes Irma and María in northeastern PR was an unprecedented 475% higher than the regional mean. Recovery to a pre-storm state was not evident in the Caribbean region for at least eight years after impact [24]. Similarly, our study showed no signs of recovery one year after the impacts, consistent with findings of a significant lack of natural coral community recovery in hurricane-affected locations in PR [23].

Hurricane impacts in this study exhibited differential vulnerability among coral species. Branching corals (*A. palmata*, *A. cervicornis*, *P. porites*, *P. furcata*, and *P. divaricata*) and pillar coral (*D. cylindrus*) were highly susceptible to mechanical fragmentation and dislodgment by hurricane-driven wave action and storm surge. Laminar and leaf corals (*A. agaricites*, *A. humilis*) showed moderate sensitivity to mechanical destruction by wave action. Small encrusting and massive colonies (*P. astreoides*, *P. strigosa*, *P. clivosa*, *D. labyrinthiformis*) had minimal vulnerability to wave action but were highly susceptible to sediment bedload and burial by displaced sand and rubble. Large-sized massive and boulder corals (*O. annularis*, *O. faveolata*, *O. franksi*, *S. siderea*) showed minimal vulnerability to dislodgment by wave action but were highly susceptible to sediment bedload and burial by displaced sand and rubble. Massive corals and *D. cylindrus* were also vulnerable to a post-hurricane white plague-like syndrome. Examples of these impacts are provided in Appendix A.

The study documented a substantial decline includen the colony surface area of the endangered *A. palmata*, revealing a 71% reduction in surface area, 78% in colony volume, 46% in colony height, and 23% in live tissue cover following both hurricanes. The frequency of colony fragments increased by 113%, and sexual recruits (crusts) exhibited a 131% increase, suggesting a fair level of population recovery in some of Culebra Island's sites. In contrast, the combined impacts of hurricanes Dennis, Katrina, Rita, and Wilma in 2005 in Florida resulted in only a 10% loss in *A. palmata* percent live tissue cover and a 20% reduction in colony surface area [76]. The noteworthy distinctions in impact include substantially higher maximum wind speeds exceeding 270 km/h in two consecutive hurricanes within two weeks in PR, compared to wind speeds ranging from 90 to 147 km/h in Florida during the 2005 hurricanes. Additionally, *A. palmata* colony sizes were generally larger in PR than in Florida. The findings of significant recovery of remnant fragments and high recruitment on some of the most impacted sites align with observations in St. John, USVI, following Hurricanes Hugo, Marilyn, and Louis [77], suggesting that recovery responses may vary depending on reef zone, degree of impact, and the environmental history of each location. Coral reefs under generally better environmental conditions, with adequate

water quality, higher biodiversity, live coral cover, and ecosystem resilience, promote a higher natural recovery potential following hurricane disturbance. Moreover, the observed higher abundance of *A. palmata* recruits on severely impacted locations may also reflect demographic impacts by hurricanes on potential space competitors (i.e., macroalgae, *R. textilis*, cyanobacteria) or the mechanical removal of corallivores.

The impacts of hurricanes on coral reefs are influenced by various factors, including temporal and spatial scales, life history characteristics, morphology of dominant species, reef zone depth, ecological history, and exposure to additional natural or human stresses [68]. Shallow reef assemblages with dominant species affected by hurricanes may exhibit higher recovery potential and increased species diversity. Coral size stage is also a crucial factor determining the outcome of major hurricane impacts. Large-sized hurricane-generated fragments of *A. palmata* showed higher survival rates than smaller fragments following Hurricane Gerta in Belize (1978), indicating the critical role of intermediate disturbances in promoting coral species redistribution and sustaining coral calcification [78]. Demographic evidence from *O. annularis* colonies affected by Hurricanes Irma and María in St. John, USVI suggests a significant decline in colonies of smaller size categories, indicating impacts on populations that have already undergone substantial loss in percent cover [79]. Similarly, combined impacts from Hurricane Mitch and a mass coral bleaching event in Belize resulted in an 80% loss in the abundance of coral recruits of numerous genera [80]. The long-term loss in percent live coral cover resulting from major disease outbreaks may lead to a permanent loss of large colonies in a population. Under such conditions, no net recovery following hurricane disturbances was documented in St. John, USVI, in coral reefs previously affected by mass coral mortalities due to disease outbreaks [77]. Therefore, a combination of direct factors (e.g., abrasion by dislodged colonies, fragments, burial by sand or rubble) and indirect factors (e.g., out-competition by macroalgae or cyanobacterial mats, corallivory, epizootic outbreaks) may play critical roles in determining the degree of impacts according to coral colony size stages, increasing the vulnerability of smaller colonies or hurricane-generated fragments. Therefore, coral demographic performance following hurricanes is critical to determine population persistence depending on life trait and size stage.

This study revealed that shallower reef zones experienced the most significant mechanical impacts, consistent with previous findings that documented substantial physical damage to reef flats and back reefs, particularly affecting species such as *A. palmata*, *Porites* spp., and small, massive species [81–83]. The observed impacts showed high persistence, with extensive mechanical damage and limited recovery [84,85]. Within a year of the impacts, the observed recovery of shallow coral assemblages in this study was mostly limited to modest natural reattachment of branching species, including *A. palmata*, *A. cervicornis*, and *Porites* spp. Endangered *A. cervicornis* experienced a decline of 79% following hurricanes Irma and María, comparable to the 65% reduction observed after category five Hurricane Allen (1980) in Jamaica [86]. However, there was a remarkable up to 98% loss in *A. cervicornis* stands within one year of the disturbance, primarily resulting from delayed mortality due to combined disease and predation impacts on remnant fragments [87]. The effects persisted for at least a decade following the disturbance [88]. In Jamaica, the mechanical destruction of reef frameworks significantly impacted the spatial distribution of fish habitats, reduced fish predator abundance, and altered the behavior of herbivores [89]. While fish assessments were not part of this study in PR, ongoing studies in Culebra Island have indicated that fish assemblages on hurricane-flattened reef frameworks, presently dominated by *R. textilis* and rubble, support significantly lower fish density, biomass, and species richness compared to adjacent locations with higher percent live coral cover and greater benthic spatial heterogeneity (Hernández-Delgado, unpublished data).

Post-hurricane declines in percent live coral cover for other endangered corals in this study varied from modest to substantial, with 7% in *O. faveolata*, 12% in *O. annularis* and *O. franksi*, and a significant 96% in *D. cylindrus*. As a comparison, the impacts of major hurricanes Emily and Wilma in 2005 in México resulted in a 2% loss in *O. annularis* and

a 66% loss in *O. faveolata* [90]. The observed coral decline in this study exhibited trait-specific patterns, with branching corals showing the highest post-hurricane mean decline (78%): *P. porites* (64%), *P. furcata* (70%), *P. divaricata* (100%). In México in 2005, there was a 93% loss in *P. porites* [90]. The mean decline in laminar corals in this study was 77%: *A. agaricites* (72%), *A. humilis* (83%). In comparison, there was a 36% loss in *A. agaricites*, a 100% loss in *A. lamarcki*, and a 96% loss in *A. tenuifolia* in México in 2005 [90]. The lowest mean decline in this study (22%) was documented in small and large massive corals: *P. astreoides* (6%), *P. strigosa* (15%), *D. labyrinthiformis* (24%), *P. clivosa* (25%), *S. siderea* (42%). In contrast, there was an 11% loss in *P. astreoides*, 88% loss in *P. strigosa*, 100% loss in *P. clivosa*, and a 4% loss in *S. siderea* in México following the 2005 hurricane impacts [90]. The observed loss in *D. cylindrus* in this study aligns with the documented mortality of large, fragmented columns in this species in San Andrés, Colombia [91]. However, hurricanes have been shown, at least in K-selected, low-recruiting *O. annularis*, to play a fundamental role in enhancing genetic diversity through mechanical fragmentation in locations exposed to a higher frequency of hurricanes [92]. Therefore, mechanical impacts on smaller and medium-sized columnar *O. annularis* colonies might be important for genotypic dispersion.

This study revealed a significant post-hurricane decline in coral reefs, posing a threat to the sustainability of their ecological functions. The loss in live coral cover was widespread across different geographic regions, locations, and depth zones, indicating a regime shift favoring the dominance of macroalgae, algal turf, and cyanobacteria. Hurricanes triggered a substantial and widespread macroalgal bloom, primarily led by red algae *Liagora* spp., *A. caribaeum*, and *T. pedicellata*, especially in windward locations exposed to strong wave action. A subsequent phase shift in macroalgal assemblages occurred, resulting in localized dominance by nuisance brown macroalgae *L. variegata* and *Dictyota* spp. The formation of hurricane-generated rubble fields, quickly colonized by macroalgae, was observed. These moving substrates can become projectiles during subsequent hurricanes, preventing natural coral recolonization and reef recovery due to a lack of bottom physical stability. This could further compromise the sustainability of reef ecological functions and services.

In Jamaica, the combined impacts of hurricane damage, overfishing, and coral diseases led to a staggering 90% loss in live coral cover within two decades, resulting in a major regime shift with macroalgal dominance [34]. Similarly, in Belize, three major hurricanes—Mitch (1998), Keith (2000), and Iris (2001)—caused a 67% loss in live coral cover, accompanied by a permanent increase in *L. variegata* cover [75]. Cozumel, México, experienced a 56% loss in live coral cover following the impacts of category five Hurricane Emily and category four Hurricane Wilma in 2005 [93]. These instances highlight how major hurricanes can severely undermine the resilience of natural coral reef ecosystems, triggering a significant regime shift favoring macroalgal dominance, compromising their ability to recover naturally and sustain ecological functions, services, and benefits.

In this study, a net loss of 42% in percent sponge cover was also observed, with considerable spatial variability. Most of the sponge mortality was attributed to sediment bedload, abrasion, and burial from hurricane-generated rubble. A comparison with the impacts of Hurricanes Irma and María in St. Thomas, USVI, revealed a 37% decline in upright sponges and a 24% increase in encrusting sponges, highlighting the trait-specific nature of damage inflicted by wave action in sponge communities [94].

Evidence from the southwestern Pacific highlights significant typhoon impacts on coral reef assemblages, many of which were similar to this study. Notable losses in percent coral cover were observed on windward reef slopes in Palau following super typhoon Bopha in 2012 and super typhoon Haiyan in 2013 [95,96]. These super typhoons generated a major bloom of red macroalgae *Lobophora* spp., leading to significant coral recruitment failure in Palau, like observations in this study. Super typhoon Yolanda (Haiyan) caused extensive mechanical destruction of shallower branching corals in the Philippines [97]. Super typhoon Wutip in 2013 in China resulted in a 46% loss of coral cover in shallow exposed forereef areas, with most impacts on branching forms [98]. Additionally, super typhoon Pamela (1976) caused substantial branching coral breakage on shallow reef zones

and significant sediment transport from adjacent beaches in Guam [99]. These observations support observations of this and other studies from the Atlantic that branching forms are the most vulnerable coral morphological trait. Catastrophic impacts were also observed on forereef slopes across other southwestern Pacific locations [100]. Interestingly, upper mesophotic (25–32 m) foliose coral assemblages were mechanically disrupted by typhoon Jelawat in Japan in 2012 [101]. Despite significant mechanical impacts by cyclone Erica (2003) in New Caledonia, coral reefs showed remarkable rapid recovery following the disturbance [102]. Moreover, despite a shift from dominance by foliose to bushy corals, upper mesophotic reefs in Japan exhibited rapid natural recovery following typhoon Jelawat [103]. Wave energy modeling has suggested that coral bleaching-related mortality in the Great Barrier Reef may lead to reduced wave energy attenuation during storm events [104]. Modeling has also projected that super typhoon impacts may significantly affect tabular and branching coral traits with increasing global warming impacts [105]. This aligns with potential expectations of future hurricane impacts across Atlantic reefs.

Combined extreme rainfall and wave action during both hurricanes also had a significant prolonged impact on water quality in PR, influencing post-hurricane algal and cyanobacterial blooming dynamics. Horizontal water transparency (Secchi disk) at various locations in Culebra declined significantly, affecting both outer Ensenada Honda Bay and the inner bay for an extended period after both hurricanes (Hernández-Delgado, unpub. data). In PR, up to 59% of coral reefs and 63% of seagrass communities were impacted by adverse water quality following Hurricanes Irma and María. Specifically, 48% of coral reefs exceeded chlorophyll-*a* thresholds in September, 38% in October, 60% in November, and 45% in December [106]. Additionally, 50% of coral reefs surpassed the light extinction coefficient (Kd490) threshold in September, 37% in October, 57% in November, and 47% in December, indicating a sustained decline in water quality over at least three months [106]. About 52% of coral reef habitats were moderately exposed to a high chlorophyll-*a* concentration, and 51% to Kd490 values beyond coral reef tolerance thresholds. These findings align with a temporal increase in turbidity for three months following both hurricanes in St. John, US Virgin Islands, resulting in a reduction in photosynthetically active radiation (PAR) at 19 m equivalent to <0.001% of surface irradiation [107]. Such a decline in PAR, coinciding with a low Kd490, may explain subsequent observations of blooming macroalgae and cyanobacteria. Large reductions in underwater irradiation have adverse implications for photosynthetic taxa, but through the turbidity that reduces underwater light, they promote population growth by suspension feeding invertebrates, including encrusting sponges, which might explain subsequent findings at St. Thomas [94]. Declining dissolved oxygen concentrations can also be deleterious for coral reef ecosystems [11]. Extreme rainfall during storm events can also be capable of producing significant coral mortality [108] and generate important sediment delivery to adjacent coral reefs [109–112]. The decline in dissolved oxygen concentration and sediment delivery to adjacent coral reefs during extreme rainfall events further underscores the need to address the impacts of strong hurricanes during the Anthropocene. Understanding the mechanisms of novel coral reef responses to disturbances and their recovery trajectories becomes increasingly important in this context.

Hurricane-driven waves represent the primary cause of physical damage to corals and coral reefs [113], often resulting in the breaking of coral branches and the overturning of colonies [114]. The dislodged coral pieces, combined with the destruction of a bioeroded reef framework, become projectiles that cause irreparable mechanical and abrasive damage to coral assemblages when propelled onto other parts of the reef. The wave action and strong winds from Hurricanes Irma and María also inflicted significant mechanical damage to associated seagrass communities in Puerto Rico and Florida [115,116]. These observations underscore the extensive nature of the impacts and highlight the permanent adverse effects of hurricanes on the sustainability of natural connectivity, ecological functions, benefits, and services within interconnected coastal ecosystems.

### *4.2. Can Coral Reefs Recover Rapidly from Major Hurricane Impacts?*

The level of mechanical damage caused by hurricanes is influenced by the degree of exposure to wave action and the wind field. This damage can lead to macroalgal blooms, as observed in Palau [117], and may impact long-term natural recovery, as documented in St. Croix, USVI, following Hurricane Hugo (1989) [77]. The combined impact of hurricanes Emily, Katrina, Rita, and Wilma (2005) scoured the reefs of the Florida Keys, resulting in limited coral loss [118]. However, Hurricane Rita caused an 11% decline in live coral cover on the deep reefs of the Flower Garden Banks in the Gulf of Mexico [119]. Studies have shown varying degrees of destruction by hurricanes to deeper banks, with significant live coral loss at different depths, both across Atlantic and Pacific reefs [100,120]. The nature and extent of wave action, wind strength, and duration of stronger conditions, as well as reef position, geomorphology, and biological composition, all play vital roles in determining the bathymetric extension of impacts, the degree of community modification, and their natural recovery ability.

Recovery from hurricane damage is variable in both time and space, and depending on coral life history traits. Branching corals, like *A. palmata*, have the potential for quick recovery due to their rapid growth, and broken branches can regrow in new areas [121–123]. However, recovery may face hindrances such as the accumulation of shifting sediments and movement of hurricane-generated rubble [83,100,111,124–128]. Additionally, an increased abundance of macroalgae and cyanobacteria, which compete for space within the reef, can impact coral recovery potential [75,79,129]. Terrestrial runoff resulting from heavy rainfall can further influence nearshore reef ecosystems by smothering corals with sediment and other debris, increasing turbidity and nutrient concentrations that influence macroalgal growth rates, and lowering salinity [106]. Current projections of reef decline due to compounding environmental degradation also suggest a significant decline in coral rubble ecological functions [130].

A recent study comparing coral reef fragility to hurricanes in Florida and PR found that coral reefs in PR are significantly more vulnerable to hurricanes [131]. Despite the previous devastation caused by major hurricanes in the wider Caribbean region, category five Hurricanes Irma and Maria (2017) resulted in only a 1–4% decline in coral cover in St. John, USVI, although there was a significant increase in macroalgal abundance [79]. These findings contrast with the results of the current study and with the previous literature. It has been suggested that decades of chronic coral mortality have changed the coral assemblages of St. John, resulting in degraded communities that are resistant to severe storms. Differences in coral reef fragility might have significantly changed following widespread impacts by the stony coral tissue loss disease (SCTLD) across the region [132–134]. The study argues that future major hurricanes could have limited impacts on coral biodiversity across the northeastern Caribbean due to the extensive nature of coral losses and habitat homogenization resulting from SCTLD since 2019 and from the 2023 widespread mass coral bleaching event. However, despite such conditions, limited natural recovery on multi-disturbance impacted coral reefs may promote higher fragility and vulnerability to future major hurricanes, potentially leading shallow Caribbean coral reefs to novel ecological states characterized by flattening and community homogenization, further minimizing natural recovery ability.

### *4.3. A Future of Stronger Hurricanes and Increasing Damage to Caribbean Coral Reefs?*

This study reveals a significant increase in the frequency of both weaker and stronger storms across the northeastern Caribbean over the last four decades, particularly during the period of 2011–2022. This pattern correlates strongly with ATM [$CO_2$] levels, ocean heat content, and thermosteric sea level changes from 1981 to 2022. Consistent with the recent literature, this pattern is associated with reduced wind-driven cold-water upwelling and weaker surface net heat loss, impacting SST anomalies and hurricane severity in 2017 [135]. Increased ocean heat content is linked to rapid intensification and extreme rainfall during hurricanes, as observed in Hurricane Harvey in 2017 in Texas [136], USA [137]. Global

records indicate rising rainfall rates in stronger hurricanes [138], aligning with increasing storm activity across the Atlantic over the past 150 years [139].

Numerous modeling studies support the expectation of heightened hurricane impacts under projected climate change scenarios, indicating increased intensification (though not necessarily frequency) [140–145]. Evidence suggests a five-fold increase in the formation of weak, short-lived storms across the Atlantic since the late 19th century [146]. Studies also indicate a notable rise in the proportions of both weaker and stronger hurricanes, with a 25–30% increase in the proportion of category 4 and 5 hurricanes per degree Celsius of global warming. This study's findings for the period of 2011–2022 align with the development of a bimodal intensity distribution, with a secondary maximum at category 4 hurricanes [147]. The consensus among researchers underscores expectations of mean stronger winds, lower pressure [148], increased environmental water vapor, higher hurricane rainfall rates with rising SST [144,149,150], and up to three-fold increases in landfalling hurricane damages by the end of the 21st century [151–153].

Atlantic hurricane models project additional changes, including an intensified convective potential [154], increased rates of rapid intensification [155–158], strengthened winds, and heightened rainfall potential [142]. The models also predict the poleward migration of the latitude of maximum intensity [159,160], a slowdown in the forward motion of major hurricanes [161,162], and these conditions have been observed in numerous storms, with expectations of increasing frequency in the future [145]. Some models also indicate an elevated risk of more intense rainfall events during hurricanes [135,163,164] and heightened risks of increased hurricane-related flooding events [165–167] and storm surge [168] under projected warming and SLR trends. These projections pose an enhanced risk to human coastal settlements and raise concerns about the persistence and sustainability of coral reefs and their associated ecosystems.

The potential effects associated with stronger hurricanes that could significantly impact coral reefs and their sustainability are numerous [169] and include the following: (1) enhanced sediment resuspension which can cause abrasion or burial of coral colonies as observed in this study; (2) significant strengthening of the surface wave spectrum which can lead to extensive coral colony fragmentation and dislodgment, as well as massive mechanical destruction of shallow to moderately deep reef frameworks, as observed in the study; (3) alteration in surface currents which can change in both directions and magnitude of surface currents leading to major sediment bedload and rubble field dispersal, resulting in the burial of extensive reef bottoms; (4) prolonged reduction in ambient light which can result in reduced PAR, impairing photosynthesis in coral's zooxanthellae [106,107]; (5) upwelling of cold, nutrient-rich, deeper ocean water which may trigger major macroalgal blooms, although blooming can also occur due to land-based runoff and sediment resuspension; (6) increase in runoff and water flow following heavy rainfall which can influence runoff, pollution, and lead to blooming macroalgae, cyanobacteria, and phytoplankton, creating a temporary state of high turbidity and low PAR; and (7) enhanced direct mechanical stress associated with degraded water quality, coral fragmentation and dislodgment, shifting sands, moving rubble, and macroalgal out-competition. These effects highlight the complex interplay between hurricanes and coral reef ecosystems, with multiple stressors influencing their health, resilience, and the sustainability of their ecological process, functions, and services.

## 5. Conclusions

The impacts of category five Hurricanes Irma and María in northeastern PR were significant, affecting all endangered coral species in a region-, site-, depth-, and life history trait-specific manner. The study revealed that shallower reefs, more exposed to wave action, were the most affected. Vulnerability to wave impacts varied among species, with those having branching forms being more susceptible. Species with foliose forms showed moderate to minimal vulnerability to wave action. Small-sized massive corals were more susceptible to sediment bedload and burial by displaced rubble fields. Large-sized massive

and boulder corals were more susceptible to sediment bedload, partial burial by displaced rubble fields, and a post-hurricane white plague-like syndrome.

Among the endangered species, *Acropora palmata*, *A. cervicornis*, and *D. cylindrus* were identified as the most vulnerable to hurricane-driven wave action. Acroporid species exhibited a low to moderate natural recovery ability through a combination of sexual recruitment and the natural reattachment of fragments to the bottom. The study highlighted a significant reattachment ability of hurricane-generated fragments for both Acroporid species. *Acropora palmata* also demonstrated important recovery through sexual recruitment in some offshore locations on Culebra Island. However, *D. cylindrus* showed very low short-term (decadal scale) recovery potential, and its post-hurricane survival was further compromised by the impacts of SCTLD, which decimated remnant populations.

The substantial decline in endangered coral assemblages poses a major threat to the sustainability of reef biodiversity, carbonate accretion, and various ecological processes. This emphasizes the need for conservation and restoration efforts, and management strategies to mitigate the impacts of extreme weather events on coral reefs and promote their recovery.

Projected climate change is expected to bring a higher frequency of stronger hurricanes to the tropical Atlantic, posing a severe threat to coral reef conservation, biodiversity, and the ecological balance of the region. Urgent conservation measures are essential, including safeguarding coral reefs, curbing greenhouse gas emissions, adopting sustainable practices in fishing and coastal development, and implementing ecological restoration programs at very large spatial scales. To support coral reef recovery, especially for vulnerable species like *A. palmata*, *A. cervicornis*, and *D. cylindrus*, sustained efforts in coral propagation and low-tech reef rehabilitation are crucial. The strategic recovery of local populations and the assisted reconstruction of damaged habitats are needed to enhance reproductive stocks and connectivity. This approach aims to revive fish assemblages, restore their trophic and geo-ecological functions, create nutrient hotspots through enhanced fish aggregation, and rebuild shallow nursery seascapes. In the long term, restoring shallow fringing reefs will not only support coral recovery but also enhance wave energy and runup attenuation, bolstering resilience against future hurricanes.

In the face of the increasing frequency of stronger hurricanes in the Atlantic and other Pacific regions, adaptive and robust sustainability management strategies are crucial for marine ecosystems, particularly coral reefs. Emergency responses following disturbances should be swift, with a focus on stabilizing rubble fields and incorporating artificial and semi-artificial restoration of benthic spatial relief as needed. Efforts should also be intensified in the propagation and restoration of rare, threatened, and endangered coral species. To understand survival and growth dynamics under various conditions, demographic performance quantification of out-planted corals is essential. Conservation initiatives must adapt and strengthen, encompassing the establishment of marine protected areas, robust enforcement and governance, co-management strategies involving local stakeholders, and measures to improve coastal water quality and land use at a watershed scale. Coral reef restoration, while critical for preventing ecological collapse and accelerating recovery post-disturbance, requires upscaling interventions by increasing the number of restored species and expanding spatio-temporal scales. Despite the significant damage inflicted by hurricanes on coral reefs, they also offer opportunities for successful ecological restoration, contributing to enhanced sustainability, resilience, connectivity, and the myriad benefits and services provided by these ecosystems.

**Supplementary Materials:** The following supporting information can be downloaded at https://www.mdpi.com/article/10.3390/su16041506/s1: Figure S1: Trajectory followed by Hurricane Irma between 6 and 7 September 2017 across Puerto Rico; Figure S2: Trajectory followed by Hurricane María during 20 September 2017 across Puerto Rico; Figure S3: Bubble plots showing species trajectories of endangered coral species before and after Hurricanes Irma and María: (a) *Acropora cervicornis*; (b) *Orbicella annularis*; (c) *O. faveolata*; (d) *O. franksi*; (e) *Dendrogyra cylindrus*; Figure S4: Bubble plots showing species trajectories of branching coral species before and after Hurricanes Irma and María: (a) *Porites porites*; (b) *P. furcata*; (c) *P. divaricata*; (d) *Agaricia agaricites*; (e) *A. humilis*;

Figure S5: Bubble plots showing large and small massive coral species trajectories before and after Hurricanes Irma and María: (a) *Pseudodiploria strigosa*; (b) *P. clivosa*; (c) *Diploria labyrinthiformis*; (d) *Siderastrea siderea*; (e) *Porites astreoides*; Table S1: Summary of spatio-temporal variation in percent relative cover of Staghorn coral, *Acropora cervicornis*, before and after Hurricanes Irma and María; Table S2: Summary of spatio-temporal variation in percent relative cover of Columnar star coral, *Orbicella annularis*, before and after Hurricanes Irma and María; Table S3: Summary of spatio-temporal variation in percent relative cover of Laminar star coral, *Orbicella faveolata*, before and after Hurricanes Irma and María; Table S4: Summary of spatio-temporal variation in percent relative cover of Massive star coral, *Orbicella franksi*, before and after Hurricanes Irma and María; Table S5: Summary of spatio-temporal variation in percent relative cover of Pillar coral, *Dendrogyra cylindrus*, before and after Hurricanes Irma and María; Table S6: Summary of spatio-temporal variation in percent relative cover of macroalgae before and after Hurricanes Irma and María; Table S7: Summary of spatio-temporal variation in percent relative cover of algal turf before and after Hurricanes Irma and María; Table S8: Summary of spatio-temporal variation in percent relative cover of red encrusting algae, *Ramicrusta textilis*, before and after Hurricanes Irma and María; Table S9: Summary of spatio-temporal variation in percent relative cover of crustose coralline algae (CCA) before and after Hurricanes Irma and María; Table S10: Summary of spatio-temporal variation in percent relative cover of cyanobacteria before and after Hurricanes Irma and María; Table S11: Summary of spatio-temporal variation in percent relative cover of open substrate (sand, pavement, rubble) before and after Hurricanes Irma and María; Table S12: Similarity percentage (SIMPER) test of temporal variation before and after Hurricanes Irma and María in coral reef benthic community structure across locations; Table S13: Similarity percentage (SIMPER) test of spatial variation in benthic community structure among locations; Table S14: Summary of similarity percentage (SIMPER) test of spatial variation in benthic community structure among locations; Table S15: Similarity percentage (SIMPER) test of spatio-temporal variation in benthic components within each location × time combination (before and after Hurricanes Irma and María).

**Author Contributions:** Conceptualization, E.A.H.-D.; methodology, E.A.H.-D. and S.E.S.-R.; data collection and processing, E.A.H.-D., P.A.-C., G.C.-B., J.S.F.-M., N.X.G.-A., P.G., R.G.-R., I.O.-M. and S.E.S.-R.; formal analysis, E.A.H.-D.; data curation, E.A.H.-D.; writing—original draft preparation, E.A.H.-D.; writing—review and editing, E.A.H.-D.; project administration, S.E.S.-R.; funding acquisition, E.A.H.-D. and S.E.S.-R. All authors have read and agreed to the published version of the manuscript.

**Funding:** This research was funded by the National Fish and Wildlife Foundation Coral Reef Conservation Program, grant number #0302.15.048715 to Sociedad Ambiente Marino (SAM).

**Institutional Review Board Statement:** Not applicable.

**Informed Consent Statement:** Not applicable.

**Data Availability Statement:** Data are contained within the article and supplementary materials.

**Acknowledgments:** Field work in this project was accomplished using R/V Caicu, and M/V Resu. We thank SAM for logistical support during field work. This publication is another contribution of the collaboration between SAM and the Center for Applied Tropical Ecology and Conservation (CATEC) of the University of Puerto Rico.

**Conflicts of Interest:** The authors declare no conflict of interest. The funders had no role in the design of the study; in the collection, analyses, or interpretation of data; in the writing of the manuscript; or in the decision to publish the results.

## Appendix A

Photographic record of the impacts by Hurricanes Irma and María in some of the surveyed coral reefs in Culebra Island, Puerto Rico (Figures A1–A41).

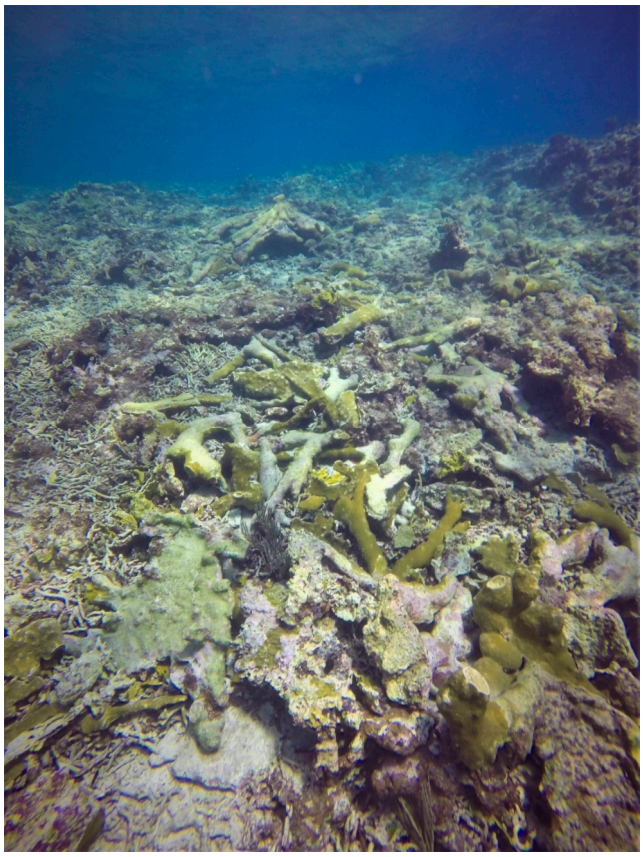

**Figure A1.** Example of a demolished shallow (<3 m) mixed stand of Elkhorn coral (*Acropora palmata*) and Staghorn coral (*Acropora cervicornis*) due to strong wave action during Hurricanes Irma and María. Note nearly total mortality of *A. cervicornis* and the substantial partial colony mortality in *A. palmata*. The end result of such massive reef destruction was a permanent flattening effect which severely decimated shallow reef's role as a fish nursery ground and as a natural buffer of wave energy and runup.

**Figure A2.** Example of a demolished deeper (8 m) patch of Staghorn coral (*Acropora cervicornis*) due to strong wave action during Hurricanes Irma and María. Note also the massive sand shift from shallow reef zones displaced to deeper reef sections and covering extensive areas of reef slopes. The end result of such massive reef destruction is a permanent flattening effect which severely decimated essential fish habitats, impairing natural reef recovery ability.

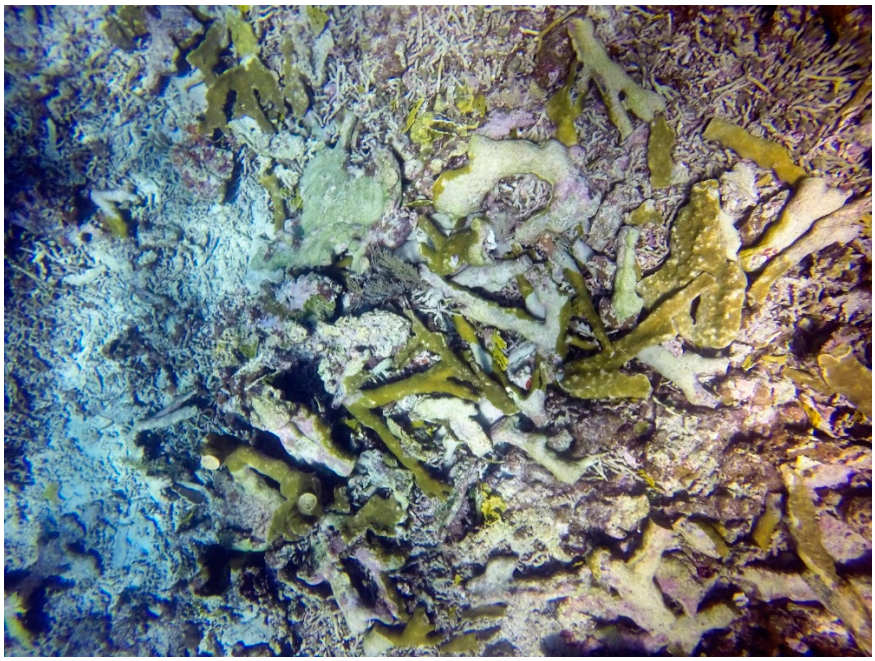

**Figure A3.** Example of a demolished shallow (<3 m) stand of Elkhorn coral (*Acropora palmata*) due to strong wave action during Hurricanes Irma and María. Pounding waves caused the massive destruction of *A. palmata*. Lose fragments piled up and suffocated numerous other fragments that remained below. Regular wave action also moved fragments causing further abrasion and fragment mortality.

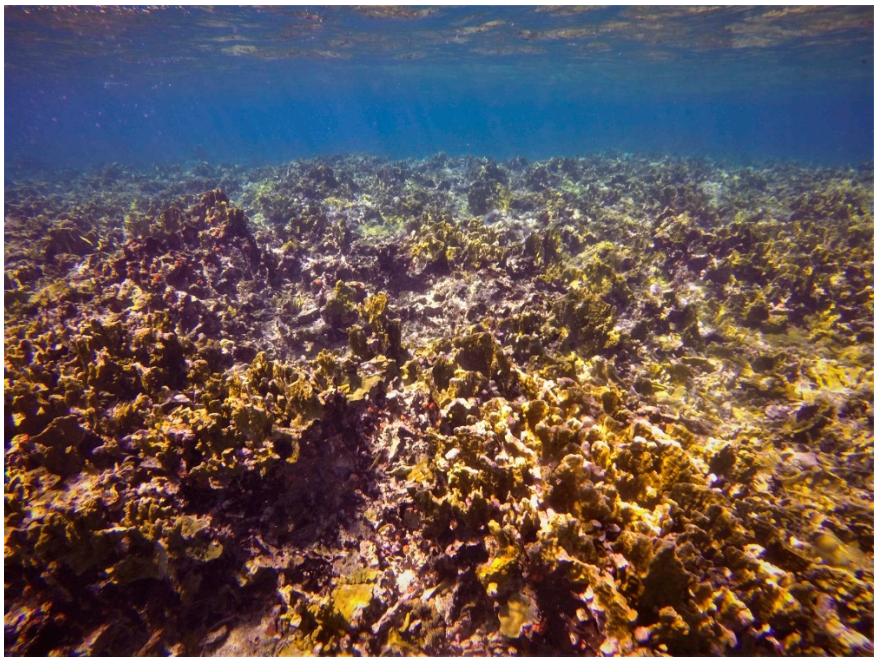

**Figure A4.** Example of a formerly demolished mixed stand of Finger coral (*Porites porites*) and Elkhorn coral (*Acropora palmata*) across a shallow reef front near Ensenada Honda Bay currently dominated by extensive stands of Fire coral (*Millepora complanata*). According to local older fishers, this shallow reef was mechanically impacted in 1979 by category 4 Hurricanes David and Frederick (1979). This is evidence of how much stochastic disturbances such as hurricanes can inflict major physical damage, shifting benthic community structure beyond natural recover, and permanently reshaping shallow reefs composition and ecological functions.

**Figure A5.** Example of the nearly total devastation of a Staghorn (*Acropora cervicornis*) thicket following Hurricanes Irma and Maria. Waves in excess of 10 m height caused extensive destruction of windward shallow reef's framework, resulting in a mechanical collapse and in permanent reef flattening.

**Figure A6.** The collapsed structure of Staghorn coral (*Acropora cervicornis*) patches resulted in major reef flattening, affecting reef fish and demersal invertebrate communities due to the immediate loss of diverse microhabitats.

**Figure A7.** Partial view of a rubble field formed following Hurricanes Irma and María that killed every coral colony across thousands of square meters of reef slope bottom at Grouper Reef (GRO). Rubble fields are formed after extensive mechanical destruction of shallower coral reef segments. Debris was deposited on backreefs and forereef slopes, causing immediate extensive coral mortality by burial and a permanent reef flattening effect. This image shows partially buried sea fan (*Gorgonia ventalina*) colonies.

**Figure A8.** Detailed view of a recently formed rubble field that suffocated thousands of coral colonies following Hurricanes Irma and Maria in Culebra Island. The major concern with such formations is that rubble fields are a novel, mobile substrate, capable of producing long-term extensive damage to adjacent reef bottoms during subsequent disturbances such as future winter swells, tropical storms, or hurricanes. Moving substrates can kill any potential sexual coral recruit by flipping over.

**Figure A9.** Example of a dislodged head of Columnar star coral (*Orbicella annularis*). This colony was temporarily overturned, which was already causing coral bleaching. The coral was also being subjected to significant macroalgal overgrowth by *Acrosymphyton caribaeum*.

**Figure A10.** Example of a partially buried and suffocated colony of Massive star coral (*Orbicella franksi*) under a recently formed rubble field during Hurricanes Irma and María. Note extensive bleaching and partial tissue mortality. Note also that most of the rubble was formed by demolished colonies of Finger corals (*Porites* spp.), which were rapidly dead by abrasion and suffocation.

**Figure A11.** Example of a partially dead colony of Massive star coral (*Orbicella franksi*) dislodged by wave action, and then suffocated under a recently formed rubble field during Hurricanes Irma and María.

**Figure A12.** Dislodged colony of Brain coral (*Pseudodiploria strigosa*). Dislodgment and overturning of coral heads under strong wave action often results in severe bleaching and eventual partial or total mortality.

**Figure A13.** Example of projectile impacts on soft corals. Massive impacts by dislodged rubble from adjacent reef areas can be devastating and lethal for octocorals. This is an example of such impacts. Note the nearly entire extirpation of the soft coral community from this reef following Hurricanes Irma and Maria.

**Figure A14.** Large colony of Elkhorn coral (*Acropora palmata*) showing blunt (and already healing) branches fragmented during Hurricanes Irma and Maria. Such blunt large coral colonies were commonly found across numerous shallow reefs across northeastern Puerto Rico.

**Figure A15.** Recently killed colony of the Mustard hill coral (*Porites astreoides*) due to severe abrasion and suffocation by projectiles from moving rubble.

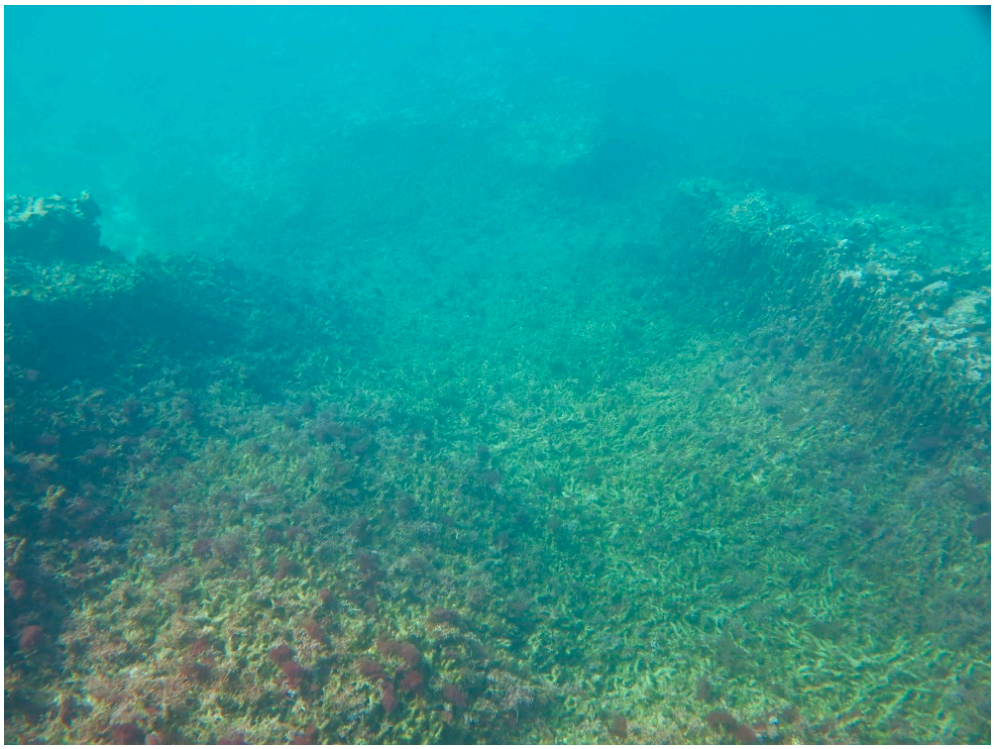

**Figure A16.** Unprecedented devastation from Hurricanes Irma and Maria. Extensive segments of spur and groove systems on offshore windward coral reefs were mechanically pulverized by wave action. Rubble produced by such massive destruction dispersed through adjacent grooves, clogging sand channels among spurs. These deposits may become future projectiles during strong storm events and heavy winter swells.

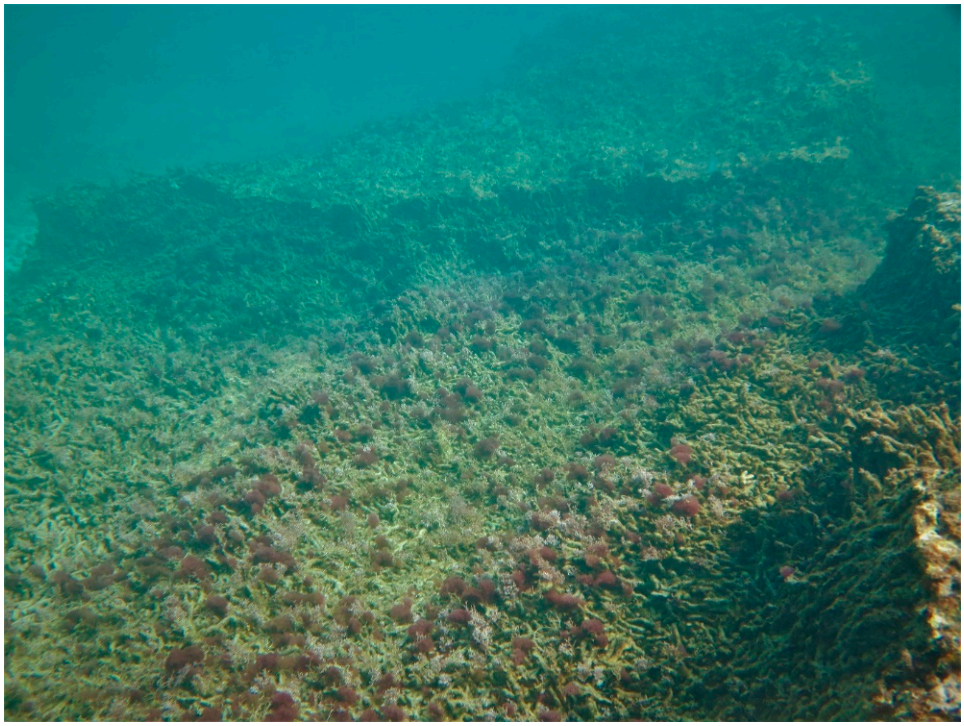

**Figure A17.** Unprecedented devastation from Hurricanes Irma and Maria. Extensive segments of spur and groove systems on offshore windward coral reefs dominated by Finger coral (*Porites porites*) were mechanically pulverized by wave action, resulting in the physical disintegration of the substrate and in extensive reef flattening. Rubble produced by such massive destruction dispersed through adjacent grooves.

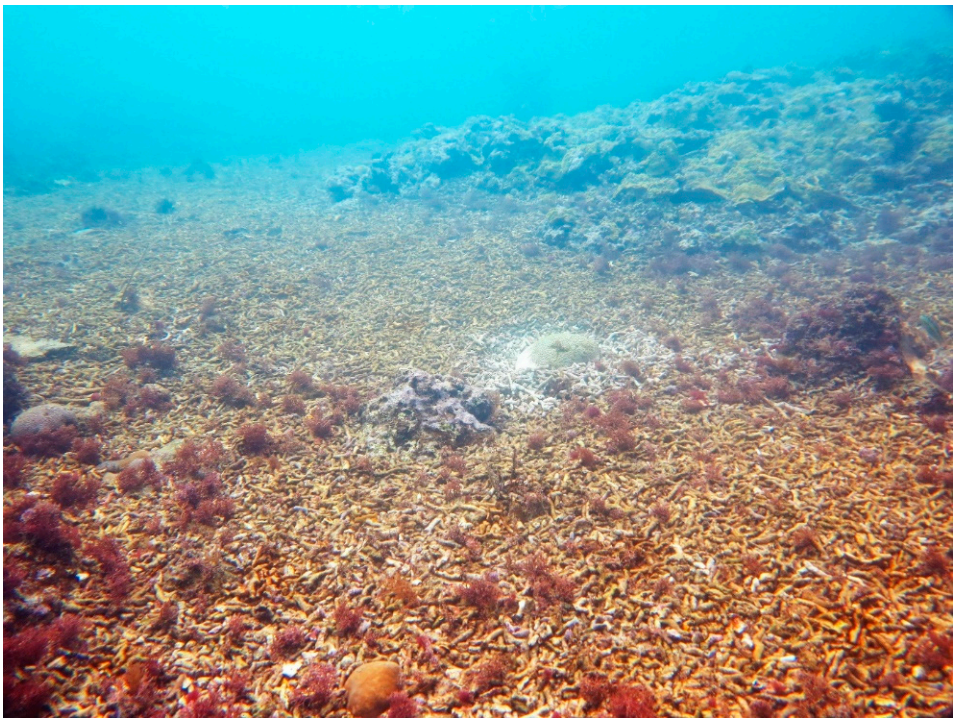

**Figure A18.** Rubble from the unprecedented destruction of adjacent reef spurs suffocated extensive zones of deeper reef terraces and slopes, sometimes at depths reaching 10–15 m after rubble spillover and burial.

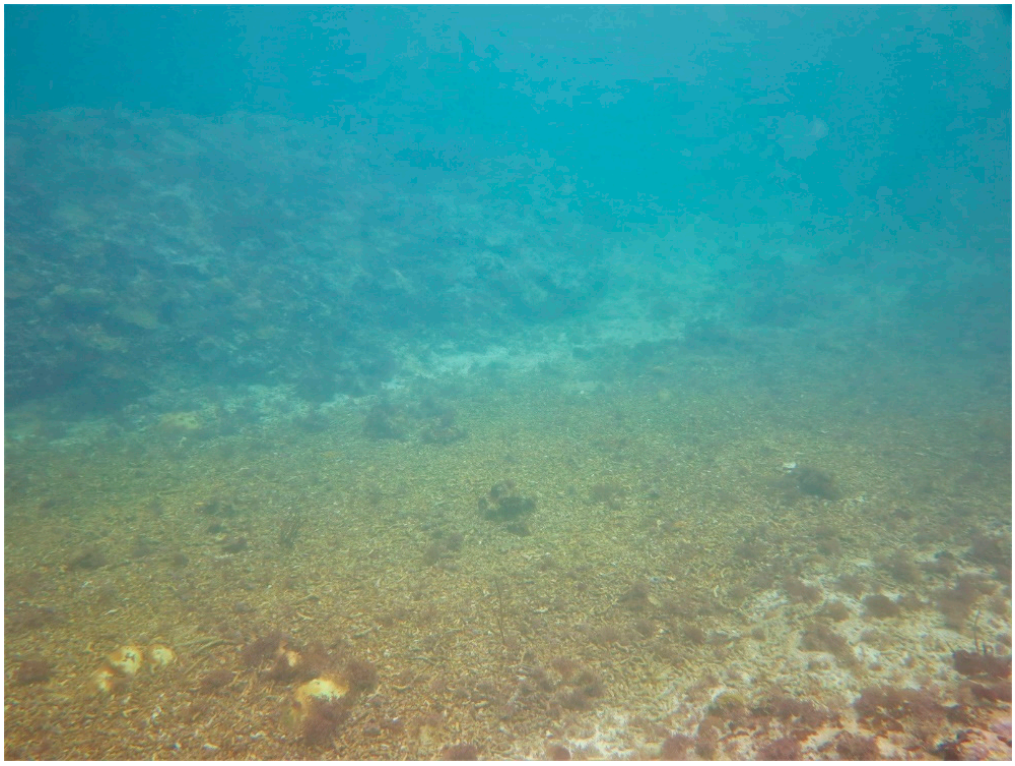

**Figure A19.** Example of a rubble field formed across a sandy reef groove system at a depth of 8–12 m. Deeper reef spur and grooves and forereef terraces were affected by spillover and burial by rubble displaced by wave action from shallower zones.

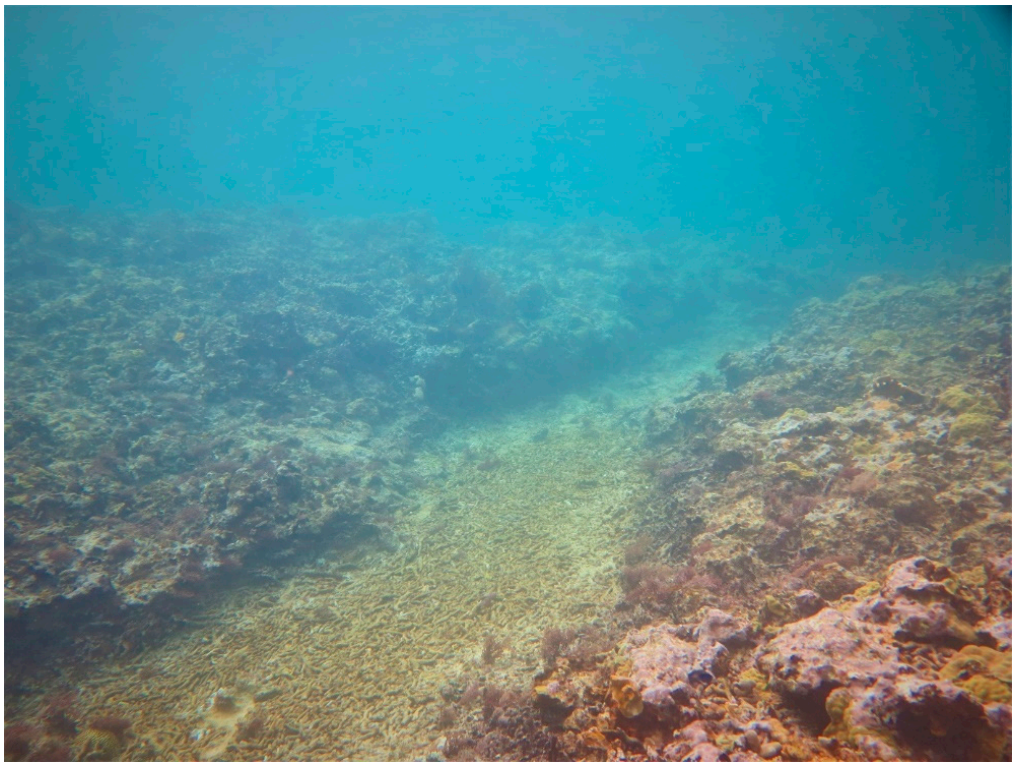

**Figure A20.** Example of a rubble field formed across a sandy reef groove system at a depth of 8–10 m. The substrate of some groove channels was elevated from 1 to 2 m due to the heavy sand shift and sediment or rubble deposition. This resulted in a stochastic reduction of benthic spatial heterogeneity.

**Figure A21.** Deeper reef slopes were also severely suffocated by moving hurricane-generated debris, causing further damage to corals, and a permanent loss of benthic spatial heterogeneity.

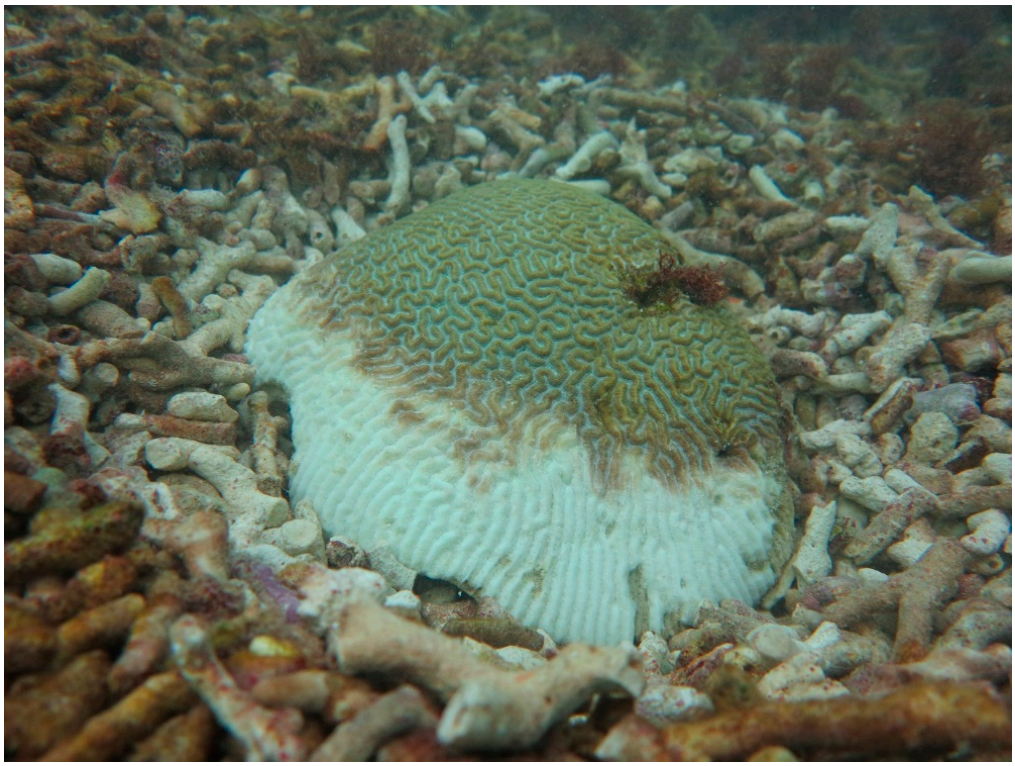

**Figure A22.** Partial suffocation and bleaching in a partially buried head of brain coral (*Colpophyllia natans*).

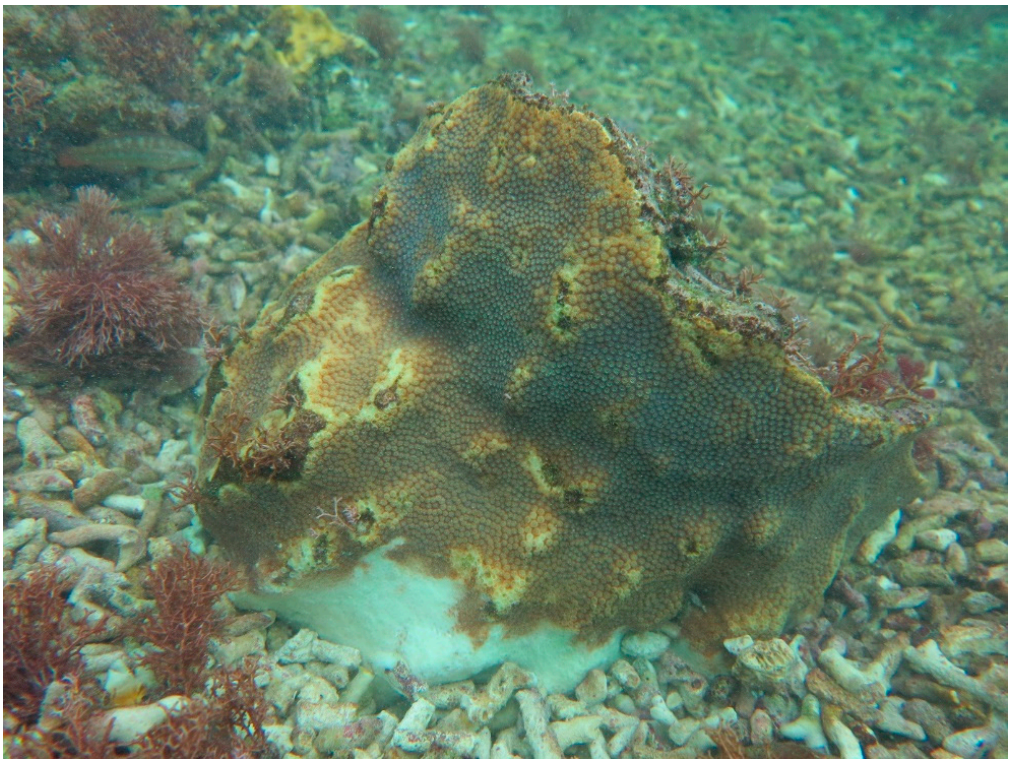

**Figure A23.** Partial bleaching and burial in a dislodged colony of Laminar star coral (*Orbicella faveolata*).

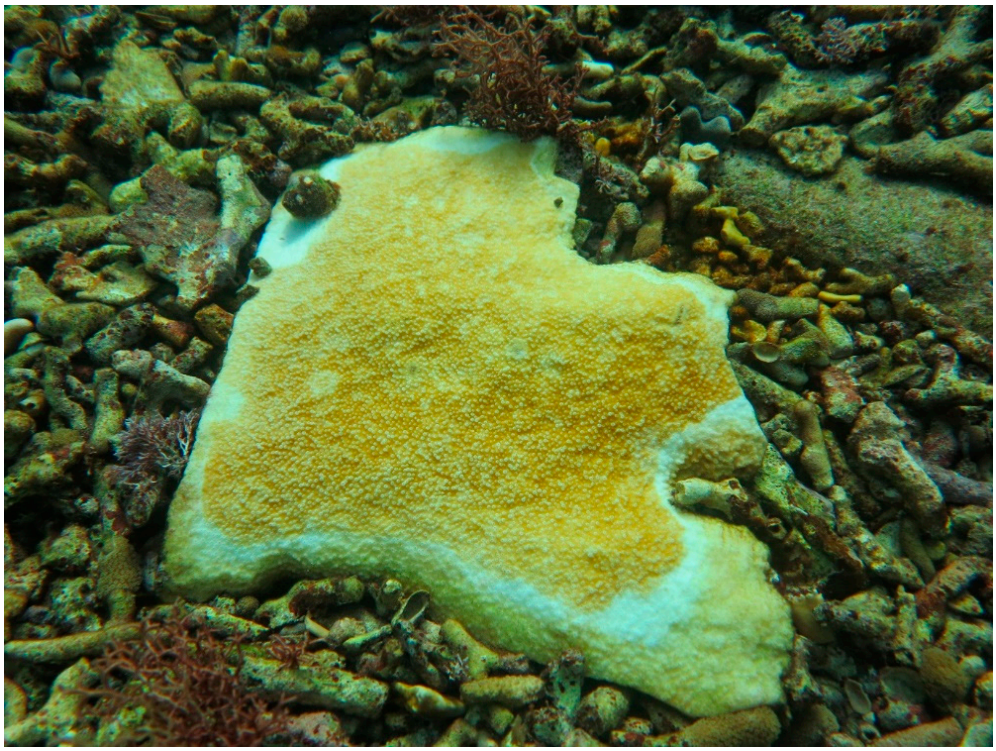

**Figure A24.** Partially bleached and killed fragment of Elkhorn coral (*Acropora palmata*). Numerous fragments of this species died by abrasive effects of projectiles during the hurricane or suffocation by moving debris.

**Figure A25.** Example of extremely turbid conditions of inner reefs at Ensenada Honda Bay, Culebra. Poor water transparency across coral reefs persisted for a period of more than two months after Hurricane María caused by blooming phytoplankton and resuspended silt following hurricanes and major turbid runoff impacts.

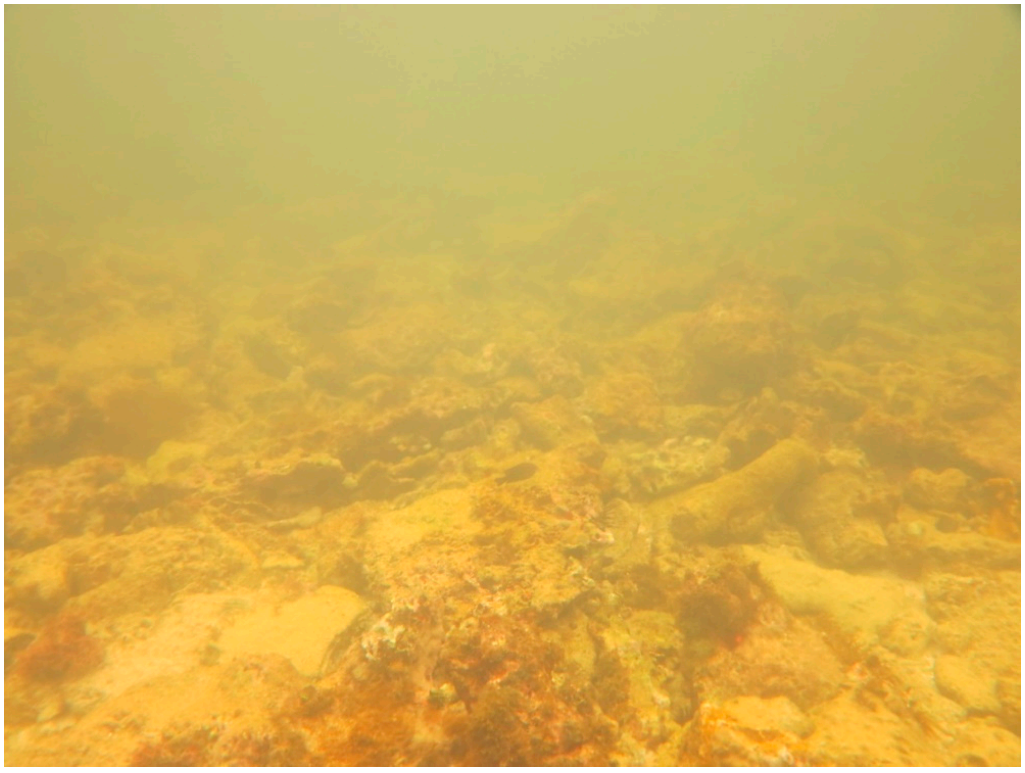

**Figure A26.** Example of massive reef destruction, in combination with very high turbidity across inner reefs at Ensenada Honda Bay, Culebra.

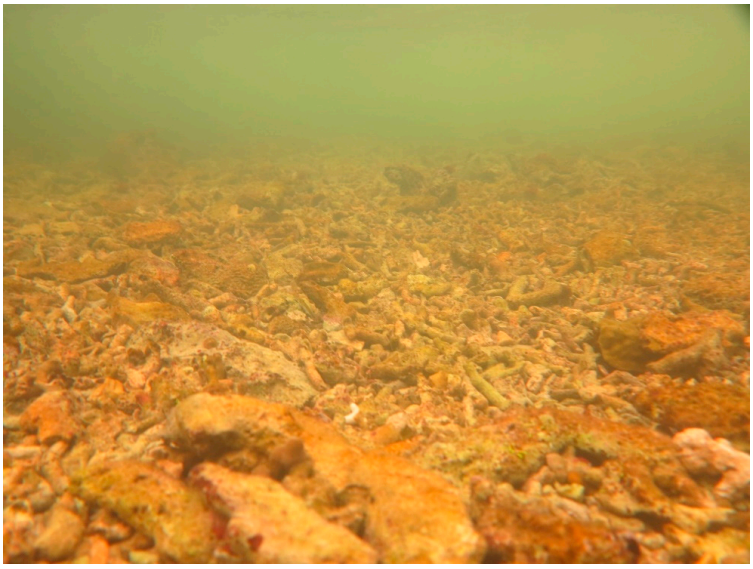

**Figure A27.** Example of massive reef destruction and rubble field formation, in combination with very high turbidity across inner reefs at Ensenada Honda Bay, Culebra.

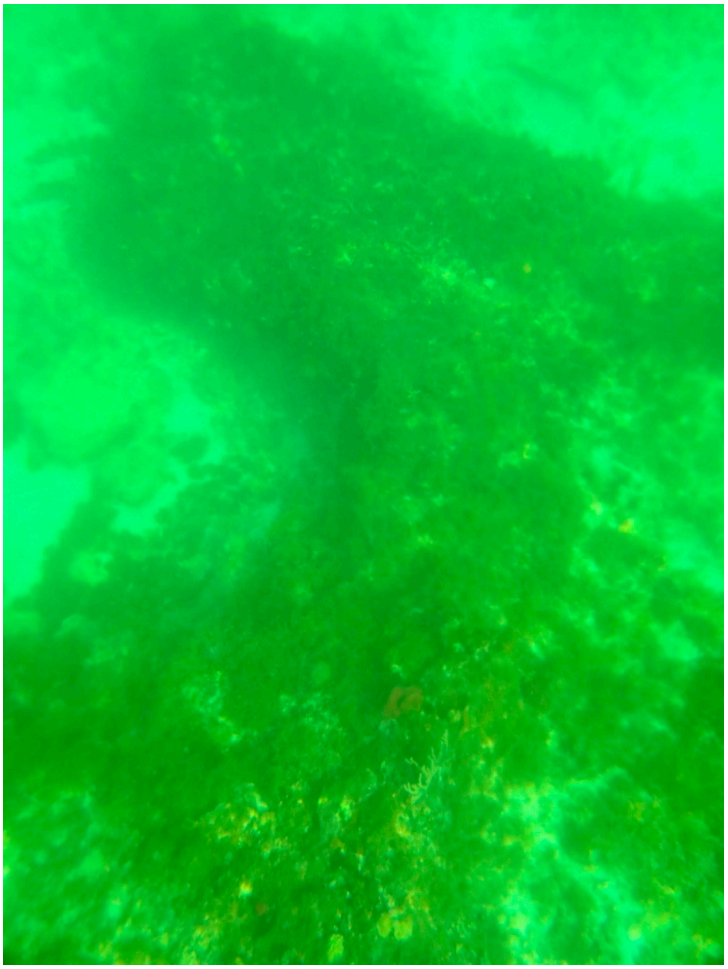

**Figure A28.** Example of a major macroalgal bloom and phytoplankton bloom across one of the outer reefs at Ensenada Honda Bay. Such blooms are common after major hurricanes, heavy rainfall, and sediment-laden, nutrient-loaded runoff events.

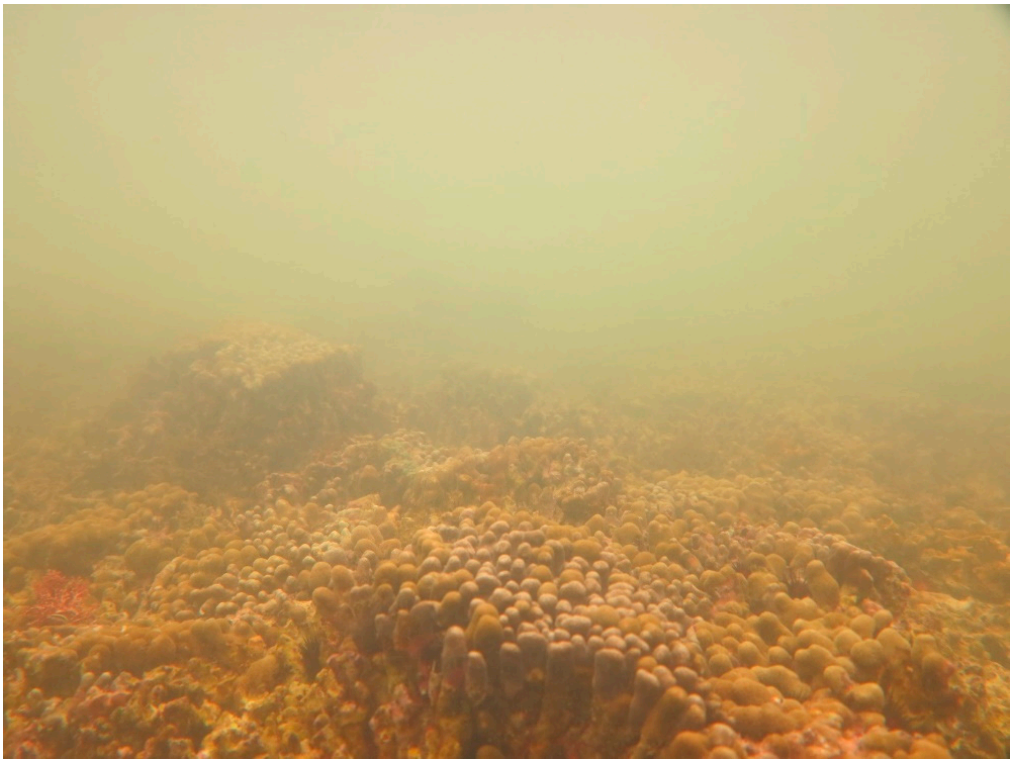

**Figure A29.** Example of a partially fragmented patch of Finger coral (*Porites porites*) in a coral reef at the entrance of Ensenada Honda Bay. Natural recovery ability of such moderate impacts can be significantly compromised due to chronic, extremely poor water quality.

**Figure A30.** Example of a major macroalgal bloom and phytoplankton bloom across one of the outer reefs at Ensenada Honda Bay. In this case, the reef is 100% covered by invasive Red encrusting algae (*Ramicrusta textilis*), intermingled with brown unpalatable macroalgae *Lobophora variegata* and *Dictyota* spp.

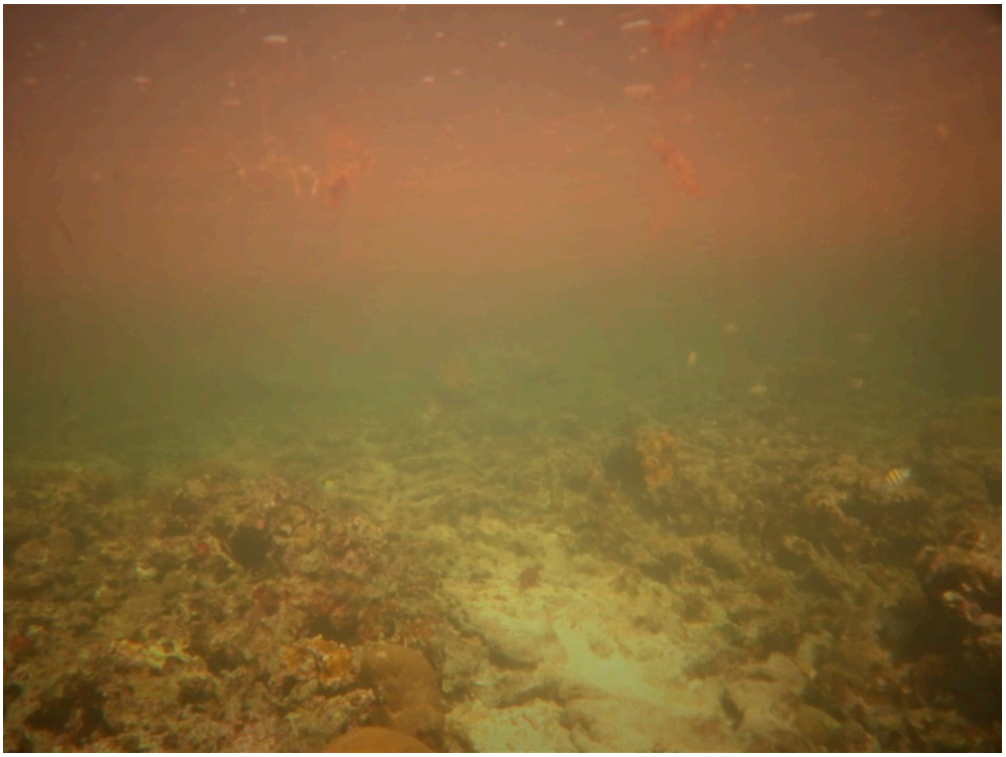

**Figure A31.** Example of a shallow reef segment at Cayo Quebrado being also impacted by a massive lens of turbid freshwater. Freshwater lenses following heavy rainfall, runoff, and groundwater seepage can be a significant source of stress and of partial coral colony mortality across shallow, semi-protected backreef zones.

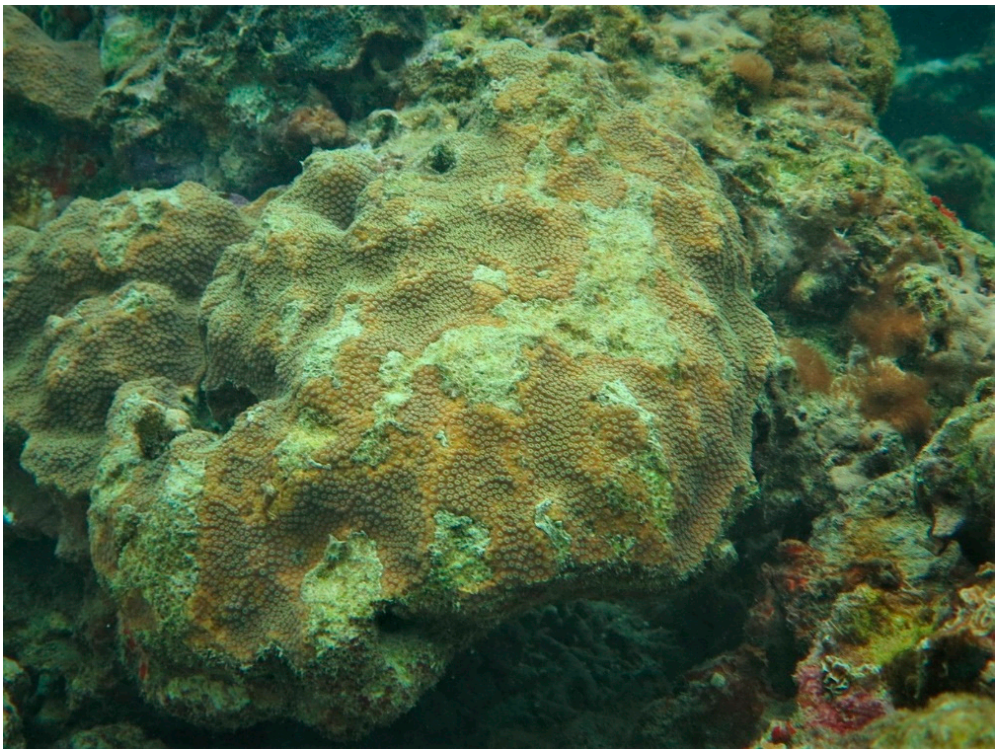

**Figure A32.** Example of a partially killed colony of Laminar star coral (*Orbicella faveolata*) after exposure to a freshwater lens following Hurricanes Irma and Maria.

**Figure A33.** Example of a partially killed colony of Brain coral (*Pseudodiploria strigosa*) impacted by Black band disease (BBD) after exposure to a freshwater lens following Hurricanes Irma and Maria.

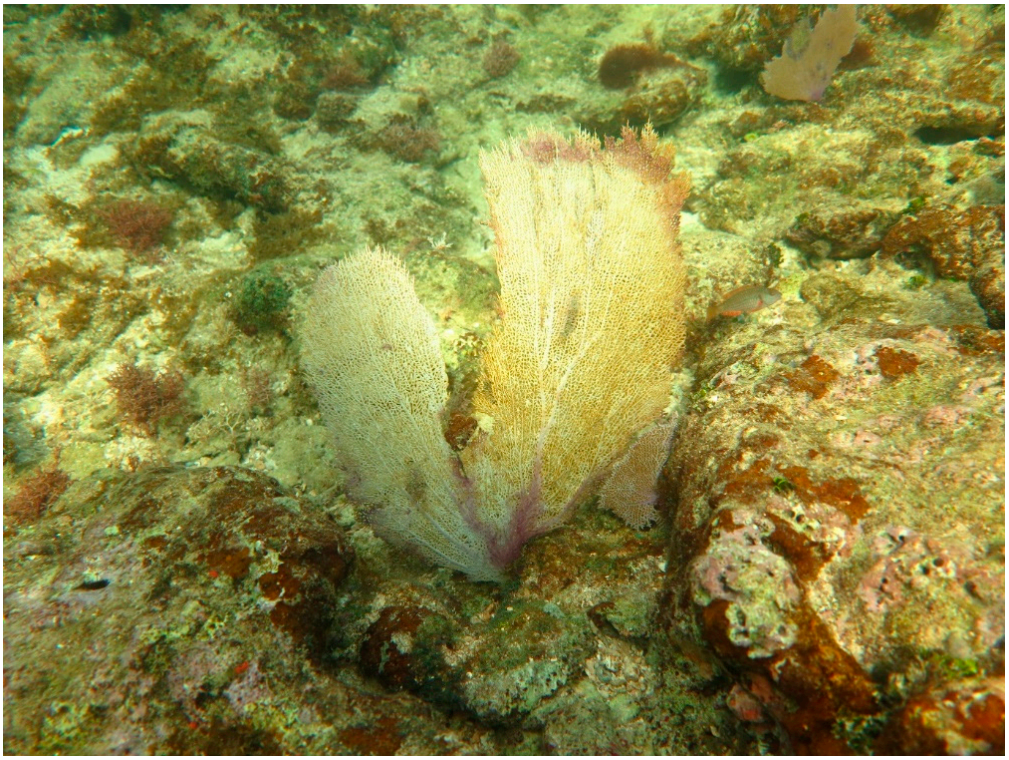

**Figure A34.** Example of a partially killed colony of a Sea fan (*Gorgonia flabellum*) after exposure to a freshwater lens following Hurricanes Irma and Maria.

**Figure A35.** Example of a partially bleached and killed colony of a mat zoanthid (*Palythoa caribbaorum*) after exposure to a freshwater lens following Hurricanes Irma and Maria.

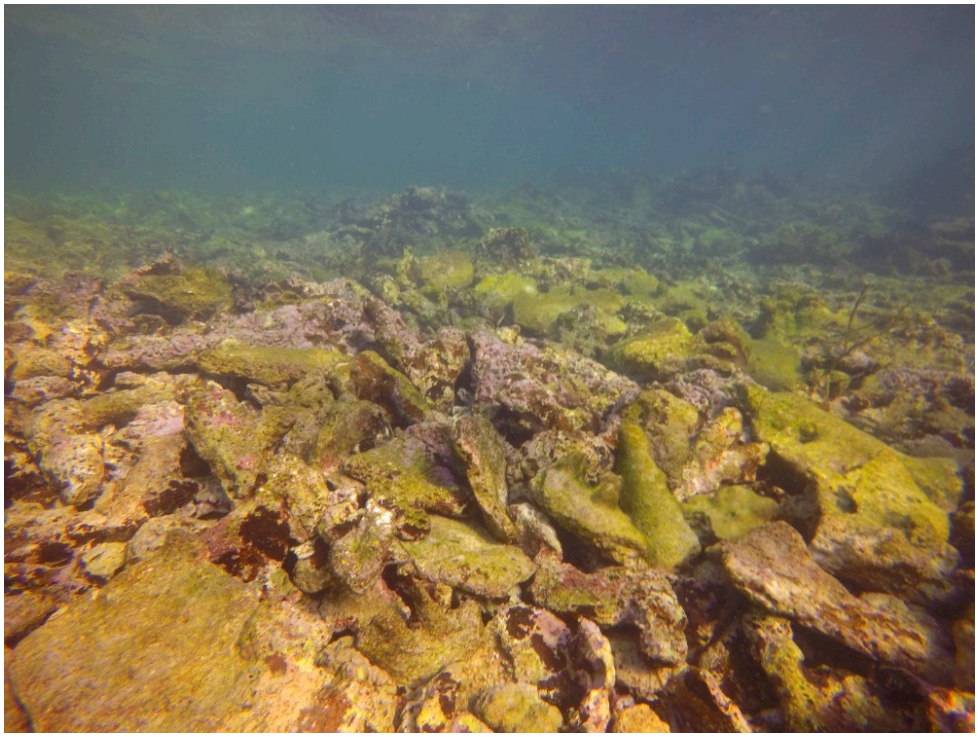

**Figure A36.** Example of a displaced pile of rubble from old hurricanes (e.g., David and Frederick, 1979) that was relocated in another segment of the Outer Bay Reef at the entrance of Ensenada Honda. Rubble pile displacement also impacted adjacent non-impacted reef segments by becoming lethal projectiles during hurricane-generated waves, resulting in burial of corals. Stabilizing such rubble fields is a paramount management priority to restore shallow reef zones.

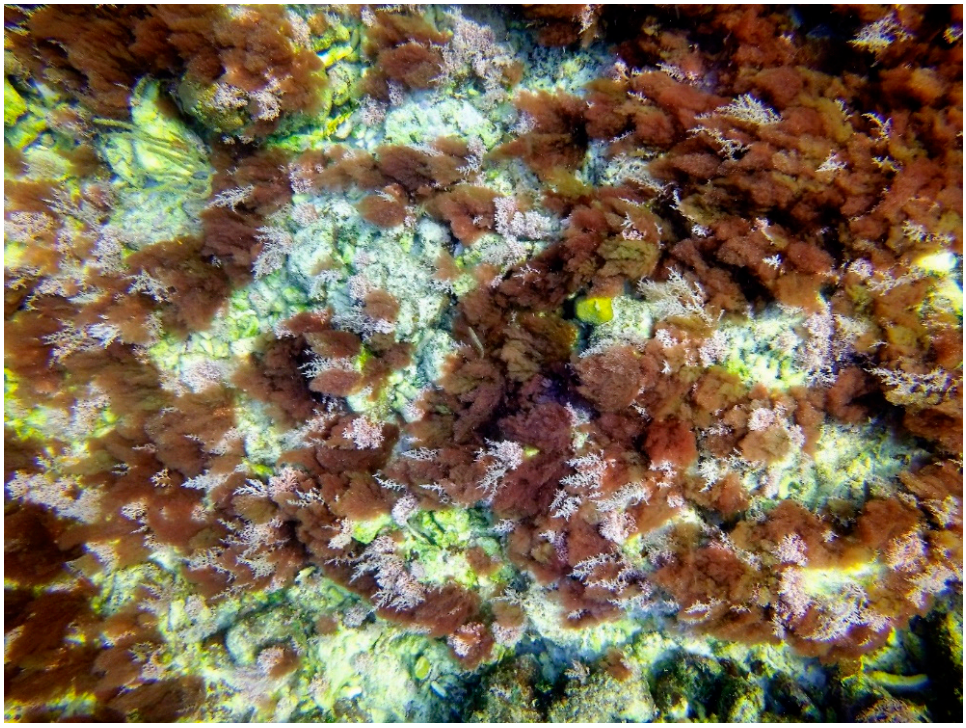

**Figure A37.** Example of a reef bottom largely impacted by a major macroalgal bloom following hurricane impacts, dominated by three red macroalgal species: *Liagora* spp., *Acrosymphyton caribaeum*, and *Trichogloeopsis pedicellata*. These species tend to occur in deeper habitats, but heavy algal and sediment resuspension due to strong wave action and bottom swells, in combination with heavy nutrient loading from major turbid runoff following heavy rainfall and flooding, resulted in major algal blooms, further impacting remnant surviving coral assemblages.

**Figure A38.** Example of mechanical impacts to reef framework: Dislodgement of a shallower head dominated by Columnar star coral (*Orbicella annularis*) at Cayo Dákity. This piece of the reef framework fell from an approximate depth of 5 m down to 12 m.

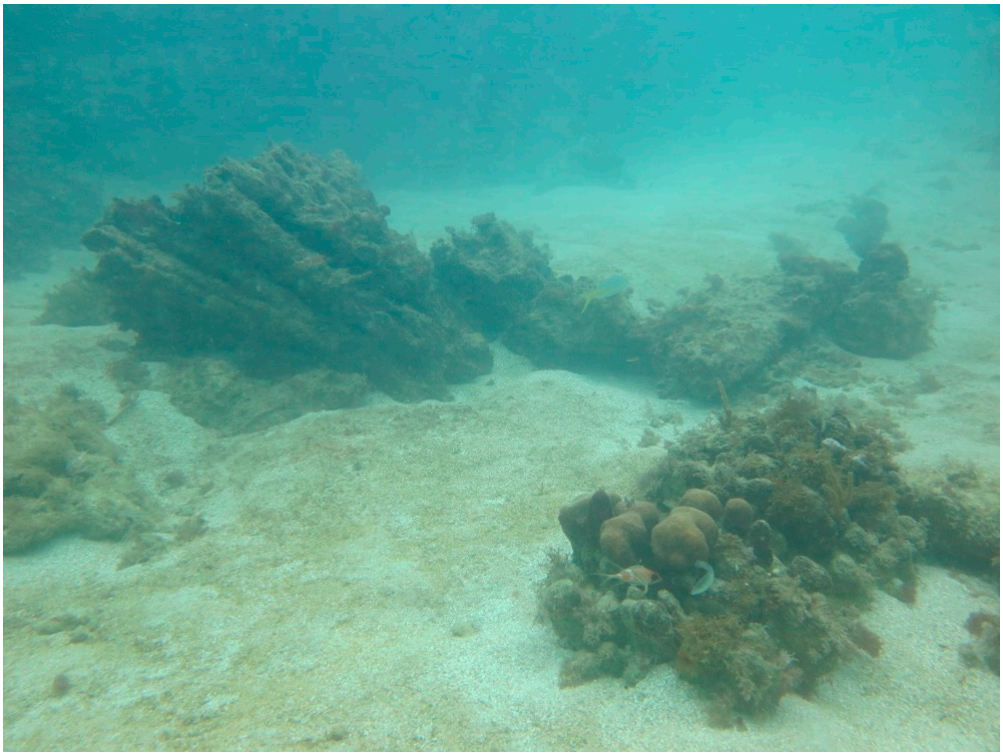

**Figure A39.** Example of mechanical impacts to reef framework: Dislodgement of another shallower head dominated by Columnar star coral (*Orbicella annularis*) at Cayo Dákity (background). This piece of the reef framework felt from an approximate depth of 6 m down to 12 m. Note the presence of another dislodged colony of *O. annularis* in the foreground that appears to have been also dislodged by a previous hurricane.

**Figure A40.** Example of mechanical impacts to reef framework: Dislodgement and overturning of a large head of Laminar star coral (*Orbicella faveolata*) and of Sea fan (*Gorgonia flabellum*) from 5 to 10 m.

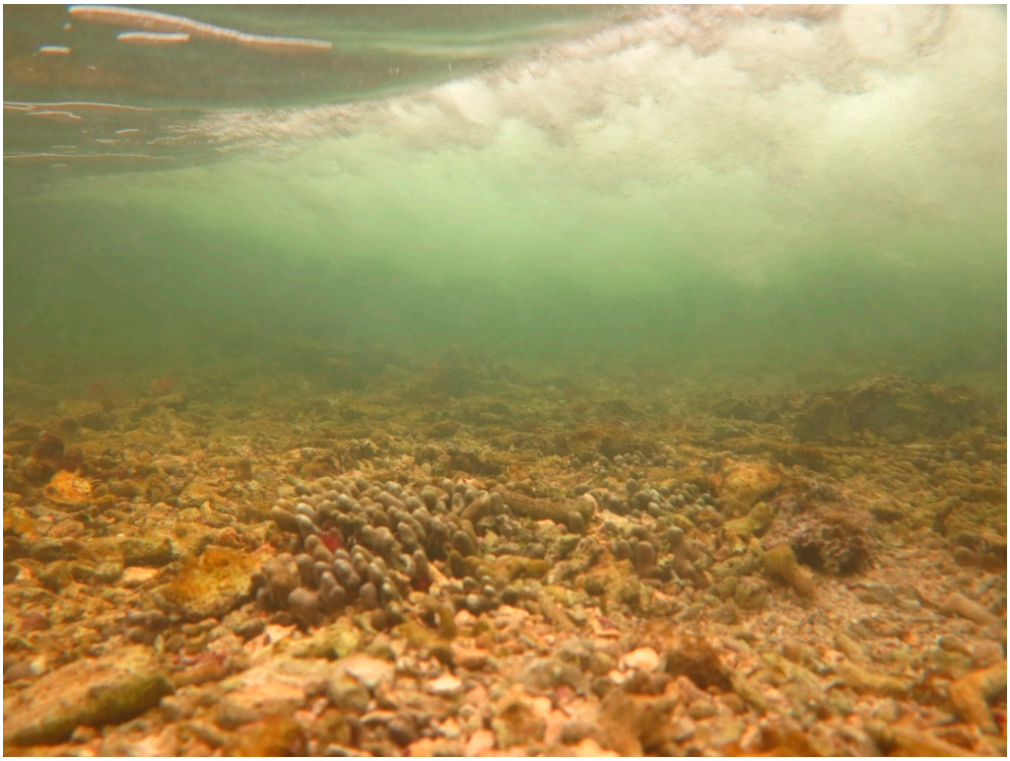

**Figure A41.** Impact by strong wave action over very shallow rubble fields: Waves rolling action may prevent cementation by crustose coralline algae and sponges, maintaining shifting rubble as moving projectiles. This can result into a continuing problem of abrasion and suffocation over adjacent remnant corals, also affecting successful coral's sexual larval recruitment, affecting reef's natural regeneration ability. It can also permanently impair shallow reef's role in wave energy and runup attenuation, and as fish nursery grounds. Therefore, this is a form of a carry-over hurricane impact effect which is still poorly understood, but which may extend to very long-term scales (years to decades, at least).

## References


1. Haas, A.F.; Fairoz, M.F.; Kelly, L.W.; Nelson, C.E.; Dinsdale, E.A.; Edwards, R.A.; Giles, S.; Hatay, M.; Hisakawa, N.; Knowles, B.; et al. Global microbialization of coral reefs. *Nat. Microbiol.* **2016**, *1*, 16042. [CrossRef] [PubMed]
2. Hoegh-Guldberg, O.; Poloczanska, E.S.; Skirving, W.; Dove, S. Coral reef ecosystems under climate change and ocean acidification. *Front. Mar. Sci.* **2017**, *4*, 158. [CrossRef]
3. Hoegh-Guldberg, O.; Jacob, D.; Taylor, M.; Guillén Bolaños, T.; Bindi, M.; Brown, S.; Camilloni, I.A.; Diedhiou, A.; Djalante, R.; Ebi, K.; et al. The human imperative of stabilizing global climate change at 1.5 C. *Science* **2019**, *365*, eaaw6974. [CrossRef] [PubMed]
4. Hughes, T.P.; Barnes, M.L.; Bellwood, D.R.; Cinner, J.E.; Cumming, G.S.; Jackson, J.B.; Kleypas, J.; Van De Leemput, I.A.; Lough, J.M.; Morrison, T.H.; et al. Coral reefs in the Anthropocene. *Nature* **2017**, *546*, 82–90. [CrossRef] [PubMed]
5. Hughes, T.P.; Kerry, J.T.; Álvarez-Noriega, M.; Álvarez-Romero, J.G.; Anderson, K.D.; Baird, A.H.; Babcock, R.C.; Beger, M.; Bellwood, D.R.; Berkelmans, R.; et al. Global warming and recurrent mass bleaching of corals. *Nature* **2017**, *543*, 373–377. [CrossRef] [PubMed]
6. Hughes, T.P.; Anderson, K.D.; Connolly, S.R.; Heron, S.F.; Kerry, J.T.; Lough, J.M.; Baird, A.H.; Baum, J.K.; Berumen, M.L.; Bridge, T.C.; et al. Spatial and temporal patterns of mass bleaching of corals in the Anthropocene. *Science* **2018**, *359*, 80–83. [CrossRef] [PubMed]
7. Hughes, T.P.; Kerry, J.T.; Baird, A.H.; Connolly, S.R.; Dietzel, A.; Eakin, C.M.; Heron, S.F.; Hoey, A.S.; Hoogenboom, M.O.; Liu, G.; et al. Global warming transforms coral reef assemblages. *Nature* **2018**, *556*, 492–496. [CrossRef]
8. Sutherland, K.P.; Griffin, A.; Park, A.; Porter, J.W.; Heron, S.F.; Eakin, C.M.; Berry, B.; Kemp, D.W.; Kemp, K.M.; Lipp, E.K.; et al. Twenty-year record of white pox disease in the Florida Keys: Importance of environmental risk factors as drivers of coral health. *Dis. Aquat. Orgs.* **2023**, *154*, 15–31. [CrossRef]
9. Hayes, N.K.; Walton, C.J.; Gilliam, D.S. Tissue loss disease outbreak significantly alters the Southeast Florida stony coral assemblage. *Front. Mar. Sci.* **2022**, *26*, 9. [CrossRef]

10. Toth, L.T.; Courtney, T.A.; Colella, M.A.; Ruzicka, R.R. Stony coral tissue loss disease accelerated shifts in coral composition and declines in reef accretion potential in the Florida Keys. *Front. Mar. Sci.* **2023**, *10*, 1276400. [CrossRef]
11. Nelson, H.R.; Altieri, A.H. Oxygen: The universal currency on coral reefs. *Coral Reefs* **2019**, *38*, 177–198. [CrossRef]
12. Hughes, D.J.; Alderdice, R.; Cooney, C.; Kühl, M.; Pernice, M.; Voolstra, C.R.; Suggett, D.J. Coral reef survival under accelerating ocean deoxygenation. *Nat. Clim. Change* **2020**, *10*, 296–307. [CrossRef]
13. Mann, M.E.; Emanuel, K.A. Atlantic hurricane trends linked to climate change. *Eos Trans. Am. Geophys. Union* **2006**, *87*, 233–241. [CrossRef]
14. Knutson, T.R.; Sirutis, J.J.; Garner, S.T.; Held, I.M.; Tuleya, R.E. Simulation of the recent multidecadal increase of Atlantic hurricane activity using an 18-km-grid regional model. *Bull. Am. Meteor. Soc.* **2007**, *88*, 1549–1565. [CrossRef]
15. Saunders, M.A.; Lea, A.S. Large contribution of sea surface warming to recent increase in Atlantic hurricane activity. *Nature* **2008**, *451*, 557–560. [CrossRef] [PubMed]
16. Grinsted, A.; Moore, J.C.; Jevrejeva, S. Projected Atlantic hurricane surge threat from rising temperatures. *Proc. Nat. Acad. Sci. USA* **2013**, *110*, 5369–5373. [CrossRef] [PubMed]
17. Zimmerman, J.K.; Willig, M.R.; Hernández-Delgado, E.A. Resistance, resilience, and vulnerability of social-ecological systems to hurricanes in Puerto Rico. *Ecosphere* **2020**, *11*, e03159. [CrossRef]
18. Smith, T.B.; Brandt, M.E.; Calnan, J.M.; Nemeth, R.S.; Blondeau, J.; Kadison, E.; Taylor, M.; Rothenberger, P. Convergent mortality responses of Caribbean coral species to seawater warming. *Ecosphere* **2013**, *4*, 1–40. [CrossRef]
19. De Bakker, D.M.; Van Duyl, F.C.; Bak, R.P.; Nugues, M.M.; Nieuwland, G.; Meesters, E.H. 40 Years of benthic community change on the Caribbean reefs of Curaçao and Bonaire: The rise of slimy cyanobacterial mats. *Coral Reefs* **2017**, *36*, 355–367. [CrossRef]
20. Perry, C.T.; Murphy, G.N.; Kench, P.S.; Smithers, S.G.; Edinger, E.N.; Steneck, R.S.; Mumby, P.J. Caribbean-wide decline in carbonate production threatens coral reef growth. *Nature Comm.* **2013**, *4*, 1402. [CrossRef]
21. Jackson, J.; Donovan, M.; Cramer, K.; Lam, V. *Status and Trends of Caribbean Coral Reefs: 1970–2012*; Global Coral Reef Monitoring Network; International Union for the Conservation of Nature (IUCN): Gland, Switzerland, 2014; Volume 1–304.
22. González-Figueroa, M.C.; Hernández-Delgado, E.A. Variación espacial en los patrones de recuperación natural de los arrecifes de coral someros urbanos en Puerto Rico. *Persp. Asuntos Amb.* **2021**, *9*, 90–111.
23. Hernández-Delgado, E.A.; Ortiz-Flores, M.F. The long and winding road of coral reef recovery in the Anthropocene: A case study from Puerto Rico. *Diversity* **2022**, *14*, 804. [CrossRef]
24. Gardner, T.A.; Côté, I.M.; Gill, J.A.; Grant, A.; Watkinson, A.R. Hurricanes and Caribbean coral reefs: Impacts, recovery patterns, and role in long-term decline. *Ecology* **2005**, *86*, 174–184. [CrossRef]
25. Roth, F.; Saalmann, F.; Thomson, T.; Coker, D.J.; Villalobos, R.; Jones, B.H.; Wild, C.; Carvalho, S. Coral reef degradation affects the potential for reef recovery after disturbance. *Mar. Environ. Res.* **2018**, *142*, 48–58. [CrossRef]
26. Speare, K.E.; Adam, T.C.; Winslow, E.M.; Lenihan, H.S.; Burkepile, D.E. Size-dependent mortality of corals during marine heatwave erodes recovery capacity of a coral reef. *Glob. Change Biol.* **2022**, *28*, 1342–1358. [CrossRef] [PubMed]
27. Rogers, C.S.; Miller, J. Permanent 'phase shifts' or reversible declines in coral cover? Lack of recovery of two coral reefs in St. John, US Virgin Islands. *Mar. Ecol. Progr. Ser.* **2006**, *306*, 103–114. [CrossRef]
28. Miller, J.; Waara, R.; Muller, E.; Rogers, C. Coral bleaching and disease combine to cause extensive mortality on reefs in US Virgin Islands. *Coral Reefs* **2006**, *25*, 418. [CrossRef]
29. Rogers, C. Coral bleaching and disease should not be underestimated as causes of Caribbean coral reef decline. *Proc. R. Soc. B Biol. Sci.* **2009**, *276*, 197–198. [CrossRef] [PubMed]
30. Hernández-Delgado, E.A.; González-Ramos, C.M.; Alejandro-Camis, P.J. Large-scale coral recruitment patterns on Mona Island, Puerto Rico: Evidence of a transitional community trajectory after massive coral bleaching and mortality. *Rev. Biol. Trop.* **2014**, *62*, 283–298.
31. Edmunds, P.J.; Elahi, R. The demographics of a 15-year decline in cover of the Caribbean reef coral *Montastraea annularis*. *Ecol. Monogr.* **2007**, *77*, 3–18. [CrossRef]
32. Miller, J.; Muller, E.; Rogers, C.; Waara, R.; Atkinson, A.; Whelan, K.R.; Patterson, M.; Witcher, B. Coral disease following massive bleaching in 2005 causes 60% decline in coral cover on reefs in the US Virgin Islands. *Coral Reefs* **2009**, *28*, 925–937. [CrossRef]
33. Hernández-Pacheco, R.; Hernández-Delgado, E.A.; Sabat, A.M. Demographics of bleaching in a major Caribbean reef-building coral: *Montastraea annularis*. *Ecosphere* **2011**, *2*, art9. [CrossRef]
34. Hughes, T.P. Catastrophes, phase shifts, and large-scale degradation of a Caribbean coral reef. *Science* **1994**, *265*, 1547–1551. [CrossRef] [PubMed]
35. Anthony, K.R.; Maynard, J.A.; Díaz-Pulido, G.; Mumby, P.J.; Marshall, P.A.; Cao, L.; Hoegh-Guldberg, O. Ocean acidification and warming will lower coral reef resilience. *Global Change Biol.* **2011**, *17*, 1798–1808. [CrossRef]
36. Mumby, P.J. Embracing a world of subtlety and nuance on coral reefs. *Coral Reefs* **2017**, *36*, 1003–1011. [CrossRef]
37. Hobbs, R.J.; Arico, S.; Aronson, J.; Baron, J.S.; Bridgewater, P.; Cramer, V.A.; Epstein, P.R.; Ewel, J.J.; Klink, C.A.; Lugo, A.E.; et al. Novel ecosystems: Theoretical and management aspects of the new ecological world order. *Glob. Ecol. Biogeogr.* **2006**, *15*, 1–7. [CrossRef]
38. Hobbs, R.J.; Higgs, E.; Harris, J.A. Novel ecosystems: Implications for conservation and restoration. *Trends Ecol. Evol.* **2009**, *24*, 599–605. [CrossRef]

39. Graham, N.A.; Cinner, J.E.; Norström, A.V.; Nyström, M. Coral reefs as novel ecosystems: Embracing new futures. *Curr. Opinion Environ. Sust.* **2014**, *7*, 9–14. [CrossRef]
40. Perry, C.T.; Alvarez-Filip, L. Changing geo-ecological functions of coral reefs in the Anthropocene. *Funct. Ecol.* **2019**, *33*, 976–988. [CrossRef]
41. Williams, G.J.; Graham, N.A. Rethinking coral reef functional futures. *Funct. Ecol.* **2019**, *33*, 942–947. [CrossRef]
42. Norström, A.V.; Nyström, M.; Jouffray, J.B.; Folke, C.; Graham, N.A.; Moberg, F.; Olsson, P.; Williams, G.J. Guiding coral reef futures in the Anthropocene. *Front. Ecol. Environ.* **2016**, *14*, 490–498. [CrossRef]
43. Bellwood, D.R.; Pratchett, M.S.; Morrison, T.H.; Gurney, G.G.; Hughes, T.P.; Álvarez-Romero, J.G.; Day, J.C.; Grantham, R.; Grech, A.; Hoey, A.S.; et al. Coral reef conservation in the Anthropocene: Confronting spatial mismatches and prioritizing functions. *Biol. Conserv.* **2019**, *236*, 604–615. [CrossRef]
44. Mcleod, E.; Anthony, K.R.; Mumby, P.J.; Maynard, J.; Beeden, R.; Graham, N.A.; Heron, S.F.; Hoegh-Guldberg, O.; Jupiter, S.; MacGowan, P.; et al. The future of resilience-based management in coral reef ecosystems. *J. Environ. Mgmt.* **2019**, *233*, 291–301. [CrossRef]
45. Williams, S.M.; García-Sais, J.R. A potential new threat on the coral reefs of Puerto Rico: The recent emergence of *Ramicrusta* spp. *Mar. Ecol.* **2020**, *41*, e12592. [CrossRef]
46. Souter, D.W.; Linden, O. The health and future of coral reef systems. *Ocean Coast. Mgmt.* **2000**, *43*, 657–688. [CrossRef]
47. Hernández-Delgado, E.A. The emerging threats of climate change on tropical coastal ecosystem services, public health, local economies and livelihood sustainability of small islands: Cumulative impacts and synergies. *Mar. Poll. Bull.* **2015**, *101*, 5–28. [CrossRef] [PubMed]
48. National Marine Fisheries Service. *Final Endangered Species Act 4 (d) Regulations for Threatened Elkhorn and Staghorn Corals*; National Oceanic and Atmospheric Administration, Southeast Regional Center: St. Petersburg, FL, USA, 2008; pp. 1–24.
49. Hernández-Delgado, E.A. Effects of Anthropogenic Stress Gradients in the Structure of Coral Reef Epibenthic and Fish Communities. Ph.D. Thesis, Department Biology, University of Puerto Rico, San Juan, Puerto Rico, 2000; pp. 1–330.
50. Hernández-Delgado, E.A. Historia natural, caracterización, distribución y estado actual de los arrecifes de coral Puerto Rico. In *Biodiversidad de Puerto Rico: Vertebrados Terrestres y Ecosistemas. Serie Historia Natural*; Joglar, R.L., Ed.; Editorial Instituto de Cultura Puertorriqueña: San Juan, Puerto Rico, 2005; pp. 281–356.
51. García, J.R.; Morelock, J.; Castro, R.; Goenaga, C.; Hernández, E. Puerto Rican reefs: Research synthesis, present threats and management perspectives. In *Latin American Coral Reefs*; Cortés, J., Ed.; Elsevier: Amsterdam, The Netherlands, 2003; pp. 111–130.
52. García-Sais, J.R.; Appeldoorn, R.; Batista, T.; Bauer, L.; Bruckner, A.; Caldow, C.; Carruba, L.M.; Corredor, J.; Díaz, E.; Lyliestrom, C.; et al. The state of coral reef ecosystems in Puerto Rico. In *The State of Coral Reef Ecosystems of the United States and Pacific Freely Associated States*; Waddell, E.E., Clarke, A.M., Eds.; National Oceanic and Atmospheric Administration Technical Memorandum National Ocean Service, National Centers for Coastal Ocean Science 73. National Oceanic and Atmospheric Administration/National Centers for Coastal Ocean Science; Center for Coastal Monitoring and Assessment's Biogeography Team: Silver Spring, MD, USA, 2008; pp. 75–116.
53. Ballantine, D.L.; Appeldoorn, R.S.; Yoshioka, P.; Weil, E.; Armstrong, R.; García, J.R.; Otero, E.; Pagán, F.; Sherman, C.; Hernández-Delgado, E.A.; et al. Biology and ecology of Puerto Rican coral reefs. In *Coral Reefs of the World, Vol. I. Coral Reefs of the USA*; Riegl, B.M., Dodge, R.E., Eds.; Springer-Science + Business Media B.V.: Berlin/Heidelberg, Germany, 2008; pp. 375–406.
54. Ramos-Scharrón, C.E.; Arima, E. Hurricane María's precipitation signature in Puerto Rico: A conceivable presage of rains to come. *Sci. Rep.* **2019**, *9*, 15612. [CrossRef] [PubMed]
55. Cangialosi, J.P.; Latto, A.S.; Berg, R. *National Hurricane Center Tropical Cyclone Report—Hurricane Irma (AL112017)*; National Hurricane Center: Miami, FL, USA, 2021; pp. 1–111.
56. Pasch, R.J.; Penny, A.B.; Berg, R. *National Hurricane Center Tropical Cyclone Report—Hurricane María (AL152017)*; National Hurricane Center: Miami, FL, USA, 2023; pp. 1–48.
57. NOAA. *Status of Puerto Rico's Coral Reefs in the aftermath of Hurricanes Irma and María*; Assessment Report Submitted by NOAA to the FEMA Natural and Cultural Resources Recovery Support Function; National Oceanic and Atmospheric Administration: Washington, DC, USA, 2018; pp. 1–37.
58. Toledo-Hernández, C.; Ruiz-Diaz, C.P.; Hernández-Delgado, E.A.; Suleimán-Ramos, S.E. Devastation of 15-year old community-based coral farming and reef-restoration sites in Puerto Rico by major hurricanes Irma and María. *Caribb. Nat.* **2018**, *53*, 1–6.
59. Wachnicka, A.; Armitage, A.R.; Zink, I.; Browder, J.; Fourqurean, J.W. Major 2017 hurricanes and their cumulative impacts on coastal waters of the USA and the Caribbean. *Estuaries Coasts* **2020**, *43*, 941–942. [CrossRef]
60. Clarke, K.R.; Gorley, R.N.; Somerfield, P.J.; Warwick, R.M. *Change in Marine Communities: An Approach to Statistical Analysis and Interpretation*, 3rd ed.; PRIMER-E: Plymouth, UK, 2014.
61. Williams, D.E.; Miller, M.W.; Kramer, K.L. *Demographic Monitoring Protocols for Threatened Caribbean Acropora spp. Corals*; National Oceanic and Atmospheric Administration Technical Memorandum National Marine Fisheries Service-Southeast Fisheries Science Center-543; National Oceanic and Atmospheric Administration: Washington, DC, USA, 2006; pp. 1–91.
62. Anderson, M.J. *Permutational Multivariate Analysis of Variance*; Department of Statistics, University of Auckland: Auckland, New Zealand, 2005; Volume 26, pp. 32–46.

63. Bray, J.R.; Curtis, J.T. An Ordination of the Upland Forest Communities of Southern Wisconsin. *Ecol. Monogr.* **1957**, *27*, 325–349. [CrossRef]
64. Anderson, M.J.; Gorley, R.N.; Clarke, K.R. *PERMANOVA+ for PRIMER: Guide to Software and Statistical Methods*; Massey University, Auckland and PRIMER-e Ltd.: Plymouth, UK, 2008.
65. Anderson, M.J.; Ellingsen, K.E.; McArdle, B.H. Multivariate Dispersion as a Measure of Beta Diversity. *Ecol. Lett.* **2006**, *9*, 683–693. [CrossRef]
66. Rogers, C.S.; Suchanek, T.H.; Pecora, F.A. Effects of hurricanes David and Frederic (1979) on shallow *Acropora palmata* reef communities: St. Croix, US Virgin Islands. *Bull. Mar. Sci.* **1982**, *32*, 532–548.
67. Rogers, C.S.; McLain, L.N.; Tobias, C.R. Effects of Hurricane Hugo (1989) on a coral reef in St. John, USVI. *Mar. Ecol. Progr. Ser.* **1991**, *78*, 189–199. [CrossRef]
68. Rogers, C.S. Hurricanes and coral reefs: The intermediate disturbance hypothesis revisited. *Coral Reefs* **1993**, *12*, 127–137. [CrossRef]
69. Kjerfve, B.; Magill, K.E.; Porter, J.W.; Woodley, J.D. Hindcasting of hurricane characteristics and observed storm damage on a fringing reef, Jamaica, West Indies. *J. Mar. Res.* **1986**, *44*, 119–148. [CrossRef]
70. Woodley, J.D.; Chornesky, E.A.; Clifford, P.A.; Jackson, J.B.; Kaufman, L.S.; Knowlton, N.; Lang, J.C.; Pearson, M.P.; Porter, J.W.; Rooney, M.C.; et al. Hurricane Allen's impact on Jamaican coral reefs. *Science* **1981**, *214*, 749–755. [CrossRef] [PubMed]
71. Woodley, J.D. The incidence of hurricanes on the north coast of Jamaica since 1870: Are the classic reef descriptions atypical? *Hydrobiologia* **1992**, *247*, 133–138. [CrossRef]
72. Liddell, W.D.; Ohlhorst, S.L. Patterns of reef community structure, North Jamaica. *Bull. Mar. Sci.* **1987**, *40*, 311–329.
73. Aronson, R.B.; Precht, W.F. Evolutionary paleoecology of Caribbean coral reefs. In *Evolutionary Paleoecology: The Ecological Context of Macroevolutionary Change*; Columbia University Press: New York, NY, USA, 2001; pp. 171–234.
74. Mumby, P.J.; Hastings, A.; Edwards, H.J. Thresholds and the resilience of Caribbean coral reefs. *Nature* **2007**, *450*, 98–101. [CrossRef] [PubMed]
75. Mumby, P.J.; Foster, N.L.; Fahy, E.A. Patch dynamics of coral reef macroalgae under chronic and acute disturbance. *Coral Reefs* **2005**, *24*, 681–692. [CrossRef]
76. Gleason, A.C.; Lirman, D.; Williams, D.; Gracias, N.R.; Gintert, B.E.; Madjidi, H.; Reid, R.P.; Boynton, C.G.; Negahdaripour, S.; Miller, M.; et al. Documenting hurricane impacts on coral reefs using two-dimensional video-mosaic technology. *Mar. Ecol.* **2007**, *28*, 254–258. [CrossRef]
77. Bythell, J.C.; Hillis-Starr, Z.M.; Rogers, C.S. Local variability but landscape stability in coral reef communities following repeated hurricane impacts. *Mar. Ecol. Progr. Ser.* **2000**, *204*, 93–100. [CrossRef]
78. Highsmith, R.C.; Riggs, A.C.; D'Antonio, C.M. Survival of hurricane-generated coral fragments and a disturbance model of reef calcification/growth rates. *Oecologia* **1980**, *46*, 322–329. [CrossRef]
79. Edmunds, P.J. The demography of hurricane effects on two coral populations differing in dynamics. *Ecosphere* **2019**, *10*, e02836. [CrossRef]
80. Mumby, P.J. Bleaching and hurricane disturbances to populations of coral recruits in Belize. *Mar. Ecol. Progr. Ser.* **1999**, *190*, 27–35. [CrossRef]
81. Stoddart, D.R. Catastrophic storm effects on the British Honduras reefs and cays. *Nature* **1962**, *196*, 512–515. [CrossRef]
82. Stoddart, D.R. Effects of Hurricane Hattie on the British Honduras reefs and cays, 30–31 October 1961. *Atoll Res. Bull.* **1963**, *95*, 1–142. [CrossRef]
83. Lirman, D.; Fong, P. Sequential storms cause zone-specific damage on a reef in the northern Florida reef tract: Evidence from Hurricane Andrew and the 1993 Storm of the Century. *Fla. Sci.* **1996**, *59*, 50–64.
84. Stoddart, D.R. Post-hurricane changes on the British Honduras reefs and cays: Re-survey of 1965. *Atoll Res. Bull.* **1969**, *131*, 50–64. [CrossRef]
85. Stoddart, D.R. Coral reefs and islands and catastrophic storms. In *Applied Coastal Geomorphology*; Palgrave Macmillan: London, UK, 1971; pp. 155–197.
86. Williams, A.H. The effects of Hurricane Allen on back reef populations of Discovery Bay, Jamaica. *J. Exp. Mar. Biol. Ecol.* **1984**, *75*, 233–243. [CrossRef]
87. Knowlton, N.; Lang, J.C.; Rooney, C.M.; Clifford, P. Evidence for delayed mortality in hurricane-damaged Jamaican staghorn corals. *Nature* **1981**, *294*, 251–252. [CrossRef]
88. Knowlton, N.; Lang, J.C.; Keller, B.D. Case study of natural population collapse: Post-hurricane predation on Jamaican staghorn corals. *Smith. Contrib. Mar. Sci.* **1990**, *31*, 1–125. [CrossRef]
89. Kaufman, L.S. Effects of Hurricane Allen on reef fish assemblages near Discovery Bay, Jamaica. *Coral Reefs* **1983**, *2*, 43–47. [CrossRef]
90. Álvarez-Filip, L.; Millet-Encalada, M.; Reyes-Bonilla, H. Impact of Hurricanes Emily and Wilma on the coral community of Cozumel Island, Mexico. *Bull. Mar. Sci.* **2009**, *84*, 295–306.
91. Bernal-Sotelo, K.; Acosta, A.; Cortés, J. Decadal change in the population of *Dendrogyra cylindrus* (*Scleractinia*: *Meandrinidae*) in old providence and St. Catalina Islands, Colombian Caribbean. *Front. Mar. Sci.* **2019**, *5*, 513. [CrossRef]

92. Foster, N.L.; Baums, I.B.; Sanchez, J.A.; Paris, C.B.; Chollett, I.; Agudelo, C.L.; Vermeij, M.J.; Mumby, P.J. Hurricane-driven patterns of clonality in an ecosystem engineer: The Caribbean coral *Montastraea annularis*. *PLoS ONE* **2013**, *8*, e53283. [CrossRef] [PubMed]
93. Álvarez-Filip, L.; Dulvy, N.K.; Gill, J.A.; Côté, I.M.; Watkinson, A.R. Flattening of Caribbean coral reefs: Region-wide declines in architectural complexity. *Proc. R. Soc. B Biol. Sci.* **2009**, *276*, 3019–3025. [CrossRef] [PubMed]
94. Gochfeld, D.J.; Olson, J.B.; Chaves-Fonnegra, A.; Smith, T.B.; Ennis, R.S.; Brandt, M.E. Impacts of hurricanes Irma and Maria on coral reef sponge communities in St. Thomas, US Virgin Islands. *Estuaries Coasts* **2020**, *43*, 1235–1247. [CrossRef]
95. Doropoulos, C.; Roff, G.; Zupan, M.; Nestor, V.; Isechal, A.L.; Mumby, P.J. Reef-scale failure of coral settlement following typhoon disturbance and macroalgal bloom in Palau, Western Pacific. *Coral Reefs* **2014**, *33*, 613–623. [CrossRef]
96. Gouezo, M.; Golbuu, Y.; Van Woesik, R.; Rehm, L.; Koshiba, S.; Doropoulos, C. Impact of two sequential super typhoons on coral reef communities in Palau. *Mar. Ecol. Progr. Ser.* **2015**, *540*, 73–85. [CrossRef]
97. Anticamara, J.A.; Go, K.T.B. Impacts of super-typhoon Yolanda on Philippine reefs and communities. *Reg. Environ. Change* **2017**, *17*, 703–713. [CrossRef]
98. Yang, H.; Yu, K.; Zhao, M.; Shi, Q.; Tao, S.; Yan, H.; Chen, T.; Liu, G. Impact on the coral reefs at Yongle Atoll, Xisha Islands, South China Sea from a strong typhoon direct sweep: Wutip, September 2013. *J. Asian Earth Sci.* **2015**, *114*, 457–466. [CrossRef]
99. Ogg, J.G.; Koslow, J.A. The impact of typhoon Pamela (1976) on Guam's coral reefs and beaches. *Pac. Sci.* **1978**, *32*, 105–118.
100. Harmelin-Vivien, M.L.; Laboute, P. Catastrophic impact of hurricanes on atoll outer reef slopes in the Tuamotu (French Polynesia). *Coral Reefs* **1986**, *5*, 55–62. [CrossRef]
101. White, K.N.; Ohara, T.; Fujii, T.; Kawamura, I.; Mizuyama, M.; Montenegro, J.; Shikiba, H.; Naruse, T.; McClelland, T.; Denis, V.; et al. Typhoon damage on a shallow mesophotic reef in Okinawa, Japan. *PeerJ* **2013**, *1*, e151. [CrossRef] [PubMed]
102. Guillemot, N.; Chabanet, P.; Le Pape, O. Cyclone effects on coral reef habitats in New Caledonia (South Pacific). *Coral Reefs* **2010**, *29*, 445–453. [CrossRef]
103. White, K.N.; Weinstein, D.K.; Ohara, T.; Denis, V.; Montenegro, J.; Reimer, J.D. Shifting communities after typhoon damage on an upper mesophotic reef in Okinawa, Japan. *PeerJ* **2017**, *5*, e3573. [CrossRef] [PubMed]
104. Vila-Concejo, A.; Duce, S.; Nagao, M.; Nakashima, Y.; Ito, M.; Fujita, K.; Kan, H. Typhoon waves on coral reefs. *Coast. Dyn.* **2017**, *263*, 697–701.
105. Hongo, C.; Kawamata, H.; Goto, K. Catastrophic impact of typhoon waves on coral communities in the Ryukyu Islands under global warming. *J. Geophys. Res. Biogeosci.* **2012**, *117*, G02029. [CrossRef]
106. Hernández, W. *Quantifying the Effects of Hurricanes Irma and Maria on Coastal Water Quality, Habitats, and Resources in Puerto Rico Using Moderate and High Resolution Satellite Sensors*; Technical Report; National Oceanic and Atmospheric Administration Restoration Center and Coral Reef Conservation Program: Silver Spring, MD, USA, 2018; pp. 1–40.
107. Edmunds, P.J.; Tsounis, G.; Boulon, R.; Bramanti, L. Acute effects of back-to-back hurricanes on the underwater light regime of a coral reef. *Mar. Biol.* **2019**, *166*, 20. [CrossRef]
108. Hernández-Delgado, E.A.; Mercado-Molina, A.E.; Alejandro-Camis, P.J.; Candelas-Sánchez, F.; Fonseca-Miranda, J.S.; González-Ramos, C.M.; Guzmán-Rodríguez, R.; Mège, P.; Montañez-Acuña, A.A.; Olivo-Maldonado, I.; et al. Community-based coral reef rehabilitation in a changing climate: Lessons learned from hurricanes, extreme rainfall, and changing land use impacts. *Open J. Ecol.* **2014**, *4*, 918–944. [CrossRef]
109. Ramos-Scharrón, C.E.; Amador, J.M.; Hernández-Delgado, E.A. An interdisciplinary erosion mitigation approach for coral reef protection—A case study from the eastern Caribbean. In *Marine Ecosystems*; Cruzado, A., Ed.; Intech Publications: Rijeka, Croatia, 2012; pp. 127–160.
110. Ramos-Scharrón, C.; Torres-Pulliza, D.; Hernández-Delgado, E.A. 2015. Watershed- and island-scale land cover changes in Puerto Rico (1930s-2004) and their potential effects on coral reef ecosystems. *Sci. Total Environ.* **2015**, *506–507*, 241–251. [CrossRef]
111. Otaño-Cruz, A.; Montañez-Acuña, A.A.; Torres-López, V.I.; Hernández-Figueroa, E.M.; Hernández-Delgado, E.A. Effects of changing weather, oceanographic conditions, and land uses on spatio-temporal variation of sedimentation dynamics along near-shore coral reefs. *Front. Mar. Sci.* **2017**, *4*, 249. [CrossRef]
112. Otaño-Cruz, A.; Montañez-Acuña, A.A.; Benson, E.; Cuevas, E.P.; Ortiz, J.; Hernández-Delgado, E.A. Response of near-shore coral reefs benthic communities to changes of sedimentation dynamics and environmental conditions. *Front. Mar. Sci.* **2019**, *6*, 551. [CrossRef]
113. Lugo, A.E. Effects and outcomes of Caribbean hurricanes in a climate change scenario. *Sci. Total Environ.* **2000**, *262*, 243–251. [CrossRef]
114. Heron, S.; Morgan, J.; Eakin, M.A.; Skirving, W. Hurricanes and their effects on coral reefs. In *Status of Caribbean Coral Reefs After Bleaching and Hurricanes in 2005*; Wilkinson, C., Souter, D., Eds.; Global Coral Reef Monitoring Network, and Reef and Rainforest Research Centre: Townsville, AU, USA, 2008; pp. 31–36.
115. Hernández-Delgado, E.A.; Toledo-Hernández, C.; Ruíz-Díaz, C.P.; Gómez-Andújar, N.; Medina-Muñiz, J.L.; Canals-Silander, M.F.; Suleimán-Ramos, S.E. Hurricane impacts and the resilience of the invasive sea vine, *Halophila stipulacea*: A case study from Puerto Rico. *Estuaries Coasts* **2020**, *43*, 1263–1283. [CrossRef]
116. Wilson, S.S.; Furman, B.T.; Hall, M.O.; Fourqurean, J.W. Assessment of Hurricane Irma impacts on South Florida seagrass communities using long-term monitoring programs. *Estuaries Coasts* **2020**, *43*, 1119–1132. [CrossRef]

117. Roff, G.; Chollett, I.; Doropoulos, C.; Golbuu, Y.; Steneck, R.S.; Isechal, A.L.; van Woesik, R.; Mumby, P.J. Exposure-driven macroalgal phase shift following catastrophic disturbance on coral reefs. *Coral Reefs* **2015**, *34*, 715–725. [CrossRef]
118. Donahue, S.; Acosta, A.; Akins, L.; Ault, J.; Bohnsack, J.; Boyer, J.; Callahan, M.; Causey, B.; Cox, C.; Delaney, J.; et al. The state of coral reef ecosystems of the Florida Keys. In *The State of Coral Reef Ecosystems of the United States and Pacific Freely Associated States*; NOAA Technical Mem. NOS NCCOS 73; NOAA/NCCOS Center for Coastal Monitoring and Assessment's Biogeography Team: Silver Spring, MD, USA, 2008; pp. 161–187.
119. Lugo-Fernández, A.; Gravois, M. Understanding impacts of tropical storms and hurricanes on submerged bank reefs and coral communities in the northwestern Gulf of Mexico. *Cont. Shelf Res.* **2010**, *30*, 1226–1240. [CrossRef]
120. Zimmer, B.; Duncan, L.; Deis, D.R.; Robbart, M.L.; Aronson, R.B.; Deslarzes, K.J.; Precht, W.F.; Sinclair, J.; Hickerson, E.L.; Schmah, G.P.; et al. Post-hurricane assessment of reefs and banks in the NW Gulf of Mexico. In Proceedings of the 11th International Coral Reef Symposium, Fort Lauderdale, FL, USA, 7–11 July 2008; Session 23. pp. 1–5.
121. Fong, P.; Lirman, D. Hurricanes cause population expansion of the branching coral *Acropora palmata* (*Scleractinia*): Wound healing and growth patterns of asexual recruits. *Mar. Ecol.* **1995**, *16*, 317–335. [CrossRef]
122. Lirman, D.; Fong, P. Patterns of damage to the branching coral *Acropora palmata* following Hurricane Andrew: Damage and survivorship of hurricane-generated asexual recruits. *J. Coast. Res.* **1997**, *1*, 67–72.
123. Lirman, D. Fragmentation in the branching coral *Acropora palmata* (Lamarck): Growth, survivorship, and reproduction of colonies and fragments. *J. Exp. Mar. Biol. Ecol.* **2000**, *251*, 41–57. [CrossRef]
124. Rasser, M.; Riegl, B. Holocene coral reef rubble and its binding agents. *Coral Reefs* **2002**, *21*, 57–72. [CrossRef]
125. Shannon, A.M.; Power, H.E.; Webster, J.M.; Vila-Concejo, A. Evolution of coral rubble deposits on a reef platform as detected by remote sensing. *Remote Sens.* **2013**, *5*, 1–18. [CrossRef]
126. Cameron, C.M.; Pausch, R.E.; Miller, M.W. Coral recruitment dynamics and substrate mobility in a rubble-dominated back reef habitat. *Bull. Mar. Sci.* **2016**, *92*, 123–136. [CrossRef]
127. Kenyon, T.M.; Doropoulos, C.; Dove, S.; Webb, G.E.; Newman, S.P.; Sim, C.W.; Arzan, M.; Mumby, P.J. The effects of rubble mobilisation on coral fragment survival, partial mortality and growth. *J. Exp. Mar. Biol. Ecol.* **2020**, *533*, 151467. [CrossRef]
128. Kenyon, T.M.; Doropoulos, C.; Wolfe, K.; Webb, G.E.; Dove, S.; Harris, D.; Mumby, P.J. Coral rubble dynamics in the Anthropocene and implications for reef recovery. *Limnol. Oceanogr.* **2023**, *68*, 110–147. [CrossRef]
129. Vroom, P.; Walters, L.; Beach, K.; Coyer, J.; Smith, J.; Abgrall, M.J.; Byron, D.; DeAngelis, K.; Konar, B.; Liss, J.; et al. Hurricane-induced propagation and rapid regrowth of the weedy brown alga *Dictyota* in the Florida Keys. *Fla. Sci.* **2005**, *1*, 161–174.
130. Wolfe, K.; Kenyon, T.M.; Mumby, P.J. The biology and ecology of coral rubble and implications for the future of coral reefs. *Coral Reefs* **2021**, *40*, 1769–1806. [CrossRef]
131. Madden, I.A.; Mariwala, A.; Lindhart, M.; Narayan, S.; Arkema, K.K.; Beck, M.W.; Baker, J.W.; Suckale, J. Quantifying the fragility of coral reefs to hurricane impacts: A case study of the Florida Keys and Puerto Rico. *Environ. Res. Lett.* **2023**, *18*, 024034. [CrossRef]
132. Weil, E.; Hernández-Delgado, E.A.; González, M.; Williams, S.; Suleimán-Ramos, S.E.; Figuerola, M.; Metz-Estrella, T. Spread of the new coral disease "SCTLD" into the Caribbean: Implications for Puerto Rico. *Reef Enc.* **2019**, *34*, 38–43.
133. Brandt, M.E.; Ennis, R.S.; Meiling, S.S.; Townsend, J.; Cobleigh, K.; Glahn, A.; Quetel, J.; Brandtneris, V.; Henderson, L.M.; Smith, T.B. The emergence and initial impact of stony coral tissue loss disease (SCTLD) in the United States Virgin Islands. *Front. Mar. Sci.* **2021**, *8*, 715329. [CrossRef]
134. Williams, S.M.; García-Sais, J.; Sabater-Clavell, J. Prevalence of stony coral tissue loss disease at el seco, a mesophotic reef system off Vieques Island, Puerto Rico. *Front. Mar. Sci.* **2021**, *8*, 668669. [CrossRef]
135. Hallam, S.; Marsh, R.; Josey, S.A.; Hyder, P.; Moat, B.; Hirschi, J.J. Ocean precursors to the extreme Atlantic 2017 hurricane season. *Nat. Comm.* **2019**, *10*, 896. [CrossRef] [PubMed]
136. Emanuel, K. Assessing the present and future probability of Hurricane Harvey's rainfall. *Proc. Nat. Acad. Sci. USA* **2017**, *114*, 12681–12684. [CrossRef]
137. Trenberth, K.E.; Cheng, L.; Jacobs, P.; Zhang, Y.; Fasullo, J. Hurricane Harvey links to ocean heat content and climate change adaptation. *Earth's Future* **2018**, *6*, 730–744. [CrossRef]
138. Guzmán, O.; Jiang, H. Heavier inner-core rainfall of major hurricanes in the North Atlantic Basin than in other global basins. *J. Clim.* **2021**, *34*, 5707–5721. [CrossRef]
139. Emanuel, K. Atlantic tropical cyclones downscaled from climate reanalyses show increasing activity over past 150 years. *Nat. Comm.* **2021**, *12*, 7027. [CrossRef]
140. Bender, M.A.; Knutson, T.R.; Tuleya, R.E.; Sirutis, J.J.; Vecchi, G.A.; Garner, S.T.; Held, I.M. Modeled impact of anthropogenic warming on the frequency of intense Atlantic hurricanes. *Science* **2010**, *327*, 454–458. [CrossRef] [PubMed]
141. Bengtsson, L.; Hodges, K.I.; Esch, M.; Keenlyside, N.; Kornblueh, L.; Luo, J.J.; Yamagata, T. How may tropical cyclones change in a warmer climate? *Tellus A* **2007**, *59*, 539–561. [CrossRef]
142. Hill, K.A.; Lackmann, G.M. The impact of future climate change on TC intensity and structure: A downscaling approach. *J. Clim.* **2011**, *24*, 4644–4661. [CrossRef]
143. Staid, A.; Guikema, S.D.; Nateghi, R.; Quiring, S.M.; Gao, M.Z. Simulation of tropical cyclone impacts to the US power system under climate change scenarios. *Clim. Change* **2014**, *127*, 535–546. [CrossRef]

144. Walsh, K.J.; McBride, J.L.; Klotzbach, P.J.; Balachandran, S.; Camargo, S.J.; Holland, G.; Knutson, T.R.; Kossin, J.P.; Lee, T.C.; Sobel, A.; et al. Tropical cyclones and climate change. *Wiley Int. Rev. Clim. Change* **2016**, *7*, 65–89. [CrossRef]
145. Knutson, T.R.; Chung, M.V.; Vecchi, G.; Sun, J.; Hsieh, T.L.; Smith, A.J. Climate change is probably increasing the intensity of tropical cyclones. In *Critical Issues in Climate Change Science, Science Brief Review*; No. 4570334; Tyndall Centre, University of East Anglia: Norwich, UK, 2021. [CrossRef]
146. Landsea, C.W.; Vecchi, G.A.; Bengtsson, L.; Knutson, T.R. Impact of duration thresholds on Atlantic tropical cyclone counts. *J. Clim.* **2010**, *23*, 2508–2519. [CrossRef]
147. Holland, G.; Bruyère, C.L. Recent intense hurricane response to global climate change. *Clim. Dyn.* **2014**, *42*, 617–627. [CrossRef]
148. Tsuboki, K.; Yoshioka, M.K.; Shinoda, T.; Kato, M.; Kanada, S.; Kitoh, A. Future increase of supertyphoon intensity associated with climate change. *Geophys. Res. Lett.* **2015**, *42*, 646–652. [CrossRef]
149. Liu, M.; Vecchi, G.A.; Smith, J.A.; Knutson, T.R. Causes of large projected increases in hurricane precipitation rates with global warming. *NPJ Clim. Atmos. Sci.* **2019**, *2*, 38. [CrossRef]
150. Huprikar, A.; Stansfield, A.; Reed, K. A storyline analysis of Hurricane Irma's precipitation under various levels of climate warming. *Environ. Res. Lett.* **2023**, *19*, 014004. [CrossRef]
151. Ranson, M.; Kousky, C.; Ruth, M.; Jantarasami, L.; Crimmins, A.; Tarquinio, L. Tropical and extratropical cyclone damages under climate change. *Clim. Change* **2014**, *127*, 227–241. [CrossRef]
152. Gettelman, A.; Bresch, D.N.; Chen, C.C.; Truesdale, J.E.; Bacmeister, J.T. Projections of future tropical cyclone damage with a high-resolution global climate model. *Clim. Change* **2018**, *146*, 575–585. [CrossRef]
153. Bjarnadottir, S.; Li, Y.; Stewart, M.G. A probabilistic-based framework for impact and adaptation assessment of climate change on hurricane damage risks and costs. *Struct. Saf.* **2011**, *33*, 173–185. [CrossRef]
154. Knutson, T.R.; Tuleya, R.E. Impact of CO 2-induced warming on simulated hurricane intensity and precipitation: Sensitivity to the choice of climate model and convective parameterization. *J. Clim.* **2004**, *17*, 3477–3495. [CrossRef]
155. Balaguru, K.; Foltz, G.R.; Leung, L.R. Increasing magnitude of hurricane rapid intensification in the central and eastern tropical Atlantic. *Geophys. Res. Lett.* **2018**, *45*, 4238–4247. [CrossRef]
156. Balaguru, K.; Foltz, G.R.; Leung, L.R.; Xu, W.; Kim, D.; López, H.; West, R. Increasing hurricane intensification rate near the US Atlantic coast. *Geophys. Res. Lett.* **2022**, *49*, e2022GL099793. [CrossRef]
157. Bhatia, K.T.; Vecchi, G.A.; Knutson, T.R.; Murakami, H.; Kossin, J.; Dixon, K.W.; Whitlock, C.E. Recent increases in tropical cyclone intensification rates. *Nat. Comm.* **2019**, *10*, 635. [CrossRef]
158. Bhatia, K.; Baker, A.; Yang, W.; Vecchi, G.; Knutson, T.; Murakami, H.; Kossin, J.; Hodges, K.; Dixon, K.; Bronselaer, B.; et al. A potential explanation for the global increase in tropical cyclone rapid intensification. *Nat. Comm.* **2022**, *13*, 6626. [CrossRef] [PubMed]
159. Haarsma, R.J.; Hazeleger, W.; Severijns, C.; De Vries, H.; Sterl, A.; Bintanja, R.; Van Oldenborgh, G.J.; Van Den Brink, H.W. More hurricanes to hit western Europe due to global warming. *Geophys. Res. Lett.* **2013**, *40*, 1783–1788. [CrossRef]
160. Studholme, J.; Fedorov, A.V.; Gulev, S.K.; Emanuel, K.; Hodges, K. Poleward expansion of tropical cyclone latitudes in warming climates. *Nat. Geosci.* **2022**, *15*, 14–28. [CrossRef]
161. Mei, W.; Primeau, F.; McWilliams, J.C.; Pasquero, C. Sea surface height evidence for long-term warming effects of tropical cyclones on the ocean. *Proc. Nat. Acad. Sci. USA* **2013**, *110*, 15207–15210. [CrossRef]
162. Kossin, J.P. A global slowdown of tropical-cyclone translation speed. *Nature* **2018**, *558*, 104–107. [CrossRef]
163. Gründemann, G.J.; van de Giesen, N.; Brunner, L.; van der Ent, R. Rarest rainfall events will see the greatest relative increase in magnitude under future climate change. *Commun. Earth Environ.* **2022**, *3*, 235. [CrossRef]
164. Reed, K.A.; Wehner, M.F.; Zarzycki, C.M. Attribution of 2020 hurricane season extreme rainfall to human-induced climate change. *Nat. Commun.* **2022**, *13*, 1905. [CrossRef] [PubMed]
165. Lin, N.; Smith, J.A.; Villarini, G.; Marchok, T.P.; Baeck, M.L. Modeling extreme rainfall, winds, and surge from Hurricane Isabel (2003). *Weather Forecast.* **2010**, *25*, 1342–1361. [CrossRef]
166. Lin, N.; Goni, G.J.; Knaff, J.A.; Forbes, C.; Ali, M.M. Ocean heat content for tropical cyclone intensity forecasting and its impact on storm surge. *Nat. Hazards* **2013**, *66*, 1481–1500. [CrossRef]
167. Lin, N.; Kopp, R.E.; Horton, B.P.; Donnelly, J.P. Hurricane Sandy's flood frequency increasing from year 1800 to 2100. *Proc. Nat. Acad. Sci. USA* **2016**, *113*, 12071–12075. [CrossRef]
168. Lin, N.; Lane, P.; Emanuel, K.A.; Sullivan, R.M.; Donnelly, J.P. Heightened hurricane surge risk in northwest Florida revealed from climatological-hydrodynamic modeling and paleorecord reconstruction. *J. Geophys. Res. Atmos.* **2014**, *119*, 8606–8623. [CrossRef]
169. Collier, C.; Ruzicka, R.; Banks, K.; Barbieri, L.; Beal, J.; Bingham, D.; Bohnsack, J.A.; Brooke, S.; Craig, N.; Fisher, L.E.; et al. The state of coral reef ecosystems of southeast Florida. In *The State of Coral Reef Ecosystems of the United States and Pacific Freely Associated States*; NOAA Technical Mem. NOS NCCOS 73; NOAA/NCCOS Center for Coastal Monitoring and Assessment's Biogeography Team: Silver Spring, MD, USA, 2008; pp. 131–159.